2009-09

Numerical study of effects of fluid-structure interaction on dynamic responses of composite plates

Kendall, Peter K.

Monterey, California. Naval Postgraduate School

NAVAL POSTGRADUATE SCHOOL

MONTEREY, CALIFORNIA

THESIS

NUMERICAL STUDY OF EFFECTS OF FLUID-STRUCTURE INTERACTION ON DYNAMIC RESPONSES OF COMPOSITE PLATES

by

Peter K. Kendall

September 2009

Thesis Advisor:	Young W. Kwon
Second Reader:	Jarema M. Didoszak

Approved for public release; distribution is unlimited.

THIS PAGE INTENTIONALLY LEFT BLANK

REPORT DOCUMENTATION PAGE			Form Approved OMB No. 0704-0188
Public reporting burden for this collection of information is estimated to average 1 hour per response, including the time for reviewing instruction, searching existing data sources, gathering and maintaining the data needed, and completing and reviewing the collection of information. Send comments regarding this burden estimate or any other aspect of this collection of information, including suggestions for reducing this burden, to Washington headquarters Services, Directorate for Information Operations and Reports, 1215 Jefferson Davis Highway, Suite 1204, Arlington, VA 22202-4302, and to the Office of Management and Budget, Paperwork Reduction Project (0704-0188) Washington DC 20503.			
1. AGENCY USE ONLY *(Leave blank)*	**2. REPORT DATE** September 2009	**3. REPORT TYPE AND DATES COVERED** Master's Thesis	
4. TITLE AND SUBTITLE Numerical Study of Effects of Fluid-Structure Interaction on Dynamic Responses of Composite Plates			**5. FUNDING NUMBERS**
6. AUTHOR(S) Peter K. Kendall			
7. PERFORMING ORGANIZATION NAME(S) AND ADDRESS(ES) Naval Postgraduate School Monterey, CA 93943-5000			**8. PERFORMING ORGANIZATION REPORT NUMBER**
9. SPONSORING /MONITORING AGENCY NAME(S) AND ADDRESS(ES) N/A			**10. SPONSORING/MONITORING AGENCY REPORT NUMBER**
11. SUPPLEMENTARY NOTES The views expressed in this thesis are those of the author and do not reflect the official policy or position of the Department of Defense or the U.S. Government.			
12a. DISTRIBUTION / AVAILABILITY STATEMENT Approved for public release; distribution is unlimited.			**12b. DISTRIBUTION CODE**

13. ABSTRACT (maximum 200 words)

Composite materials are seeing increased use in structural applications because of their various benefits. When composite structures are employed in a water environment, their dynamic responses are greatly affected by the fluid medium. Water density is comparable to many composite materials and the effects of fluid-structure interaction on dynamic behaviors of composite structures are significant. The effects of fluid-structure interaction include changes of frequency, magnitude, energy dissipation, etc., of structural characteristics. Hence, it is critical to understand the fluid-structure interaction of composite structures subjected to dynamic loading in water environments. This work focuses on finding parameters affecting the transient dynamic responses of composite structures. Coupled fluid-structure interaction analyses of composite plates are conducted numerically, using finite element models, including various parametric studies. The results are compared to those of dry structures to identify the role of each parameter.

14. SUBJECT TERMS Fluid-Structure Interaction, Composite, Carbon Fiber Composite, Dynamic Response, Finite Element			**15. NUMBER OF PAGES** 115
			16. PRICE CODE
17. SECURITY CLASSIFICATION OF REPORT Unclassified	**18. SECURITY CLASSIFICATION OF THIS PAGE** Unclassified	**19. SECURITY CLASSIFICATION OF ABSTRACT** Unclassified	**20. LIMITATION OF ABSTRACT** UU

NSN 7540-01-280-5500

Standard Form 298 (Rev. 2-89)
Prescribed by ANSI Std. 239-18

THIS PAGE INTENTIONALLY LEFT BLANK

Approved for public release; distribution is unlimited.

NUMERICAL STUDY OF EFFECTS OF FLUID-STRUCTURE INTERACTION ON DYNAMIC RESPONSES OF COMPOSITE PLATES

Peter K. Kendall
Lieutenant Commander, United States Navy
B.S., North Carolina State University, 1994
M.E., North Carolina State University, 1997

Submitted in partial fulfillment of the
requirements for the degree of

MASTER OF SCIENCE IN MECHANICAL ENGINEERING

from the

NAVAL POSTGRADUATE SCHOOL
September 2009

Author: Peter K. Kendall

Approved by: Young W. Kwon
Thesis Advisor

Jarema M. Didoszak
Second Reader

Knox T. Millsaps
Chairman, Department of Mechanical and Astronautical Engineering

THIS PAGE INTENTIONALLY LEFT BLANK

ABSTRACT

Composite materials are seeing increased use in structural applications because of their various benefits. When composite structures are employed in a water environment, their dynamic responses are greatly affected by the fluid medium. Water density is comparable to many composite materials and the effects of fluid-structure interaction on dynamic behaviors of composite structures are significant. The effects of fluid-structure interaction include changes of frequency, magnitude, energy dissipation, etc., of structural characteristics. Hence, it is critical to understand the fluid-structure interaction of composite structures subjected to dynamic loading in water environments. This work focuses on finding parameters affecting the transient dynamic responses of composite structures. Coupled fluid-structure interaction analyses of composite plates are conducted numerically, using finite element models, including various parametric studies. The results are compared to those of dry structures to identify the role of each parameter.

THIS PAGE INTENTIONALLY LEFT BLANK

TABLE OF CONTENTS

LIST OF FIGURES

THIS PAGE INTENTIONALLY LEFT BLANK

ACKNOWLEDGMENTS

First and foremost, I would like to thank my wife, Cheryl; son, Talon; and daughter, Aspen, for their steadfast love and support; to my parents, Bob and Nancy, for instilling my drive, determination and thirst for knowledge, which has made me successful. Finally, I would like to thank Dr. Young Kwon for his mentorship throughout my graduate studies and course of this research at the Naval Postgraduate School.

THIS PAGE INTENTIONALLY LEFT BLANK

I. INTRODUCTION

A. BACKGROUND

Composites are seeing increased use in maritime, aerospace and automotive structures used in both civil and military applications. Early uses of composites were limited to secondary structures; however, as knowledge and understanding of mechanical characteristics of composites has grown, more primary load-bearing structures have been fabricated. In recent years, large composite structures have been incorporated into naval vessels to increase operational performance while lowering ownership costs [1]. For example, carbon-fiber composite material provides high strength and stiffness while maintaining low weight, which in turn translates to increased fuel economy or increased payload. A further advantage of composites over metals is lower maintenance and resistance to corrosion, making composites very desirable for maritime applications. The use of composites in engineering components has initiated numerous studies to analyze structural components fabricated from various composites rather than traditional metals. While composites provide advantages over metals, they also come with complex and challenging engineering problems for analysts and designers [2]. Because the structural behavior is impacted by Fluid Structure Interaction (FSI), this work focuses on the implications of utilizing composite structures in maritime applications below the waterline.

B. LITERATURE SURVEY

It is critical to assess the structural behavior of composite structures used in marine applications beneath the waterline where FSI plays an important role on the dynamic response and failure of the submerged composite structure. Because composite structures are much lighter than metallic structures, the effect of FSI is much greater. Many polymer composite materials are only a few times heavier than water; therefore, the added mass effect of the fluid becomes critical.

Numerous studies have examined the effect of FSI for metallic structures, especially for underwater explosive loading [3]–[10]. Some works are experimental

studies, while others are numerical work. A few studies examined FSI for composite structures subjected to underwater explosion [11]–[17].

C. OBJECTIVES

This work investigates the effects of the surrounding fluid on dynamic responses of composite structures subjected to a mechanical loading via applied concentrated force, uniform pressure and impact. The research examines several parameters affecting transient dynamic responses of submerged composite structures to identify major controlling parameters of FSI. This research focuses on computational modeling of coupled fluid-structure interaction analyses of composite structures—specifically plates—under water for various parametric studies. Results are normalized to those of completely dry structures to illustrate the role of each parameter on FSI.

II. COMPUTATIONAL MODEL

A. MATERIAL SPECIFICATIONS

The composite material used in this study is an e-glass woven fabric with a plain weave fiber architecture and vinyl-ester resin. The composite has elastic modulus 17 GPa, Poisson's ratio 0.3, and density of 2020 kg/m^3. To make a fair comparison between dry and wet structures, any potential change of composite material properties associated with moisture absorption from water is not considered. The steel used for impact study has elastic modulus 200 GPa, Poisson's ratio 0.3, and density 8000 kg/m^3. For a dry structure, i.e., in air, there is no specific modeling of the air medium. For models that examine FSI, the water is modeled with a density of 1000 kg/m^3, and bulk modulus of 2.2 GPa, while water viscosity is neglected.

B. FINITE ELEMENT MODEL DEVELOPEMENT

As an initial step in studying Fluid Structure Interaction effects, only linear elastic behavior is considered in this study. Solid materials are modeled using the Lagrangian-based finite element method, while fluid is solved using the Eulerian-based finite element method [18]. The composite plate used in the study is thin (0.002 m thickness), having an aspect ratio of at least 150 (length to thickness), and necessitates modeling through shell elements.

Due to the thin composite plate requiring to be modeled with shell elements, coupling between the fluid/composite interfaces presented a challenge, as the interface between them needs to be uniquely defined by a volume or solid elements. To have a uniquely-defined volume, a stiffened composite plate is used to create a unique volume of composite. The stiffened composite shell structure is composed of top and bottom skin plates, coupled through vertical stiffeners. Each skin plate is 0.3 m x 0.3 m and 0.002 m thick and is modeled with e-glass composite. The stiffeners are modeled of the same composite material with the same thickness of the skin plates. Their sizes are 0.3 m long and 0.01 m tall, and spaced every 0.05 m apart. The spacing between nodes of composite model was 1 cm, such that the 0.3 m skin plates have a 30 by 30 mesh. The stiffened

composite plate is depicted in Figure 1, with the lines denoting the locations of stiffeners. With this stiffened composite plate, FSI can be investigated by comparing three different cases: 1) completely dry, 2) two-sides wet, and 3) one-side wet.

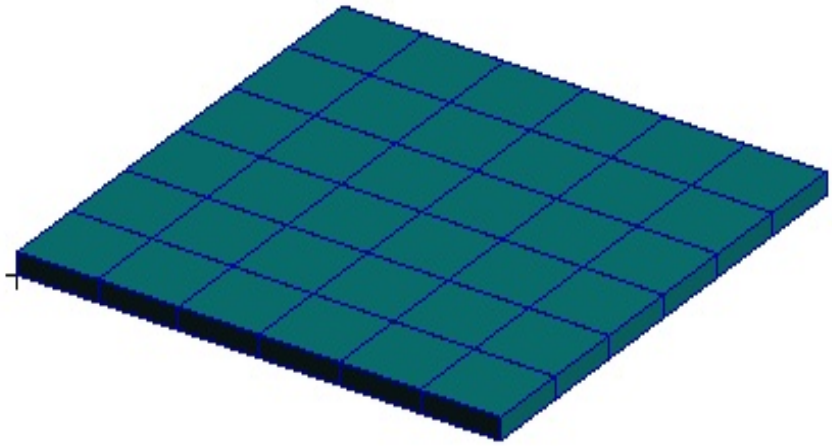

Figure 1. Stiffened Composite Plate Structure

Various parametric studies, including boundary conditions and loading types, are examined to investigate FSI effects. The edges of the stiffened composite plate use either a clamped or simply-supported boundary condition. The plate is subjected to constant applied force at the center of the top skin plate, equivalent pressure loading over the surface of the top plate, or impact loading at center of the top plate from a steel projectile at various initial velocities.

The Finite Element Models (FEM) were constructed in PATRAN and solved numerically using DYTRAN. The computations were run using a HPC cluster system. The computational time required to perform 0.05 second transient solutions varied from approximately 5 minutes for the dry structure to as much as 40 hours for the one-side wet structural model. The dry case structural model has 2,220 elements and the wet models have up to 30,000 elements. The geometry used to define the composite material uses a Lagrangian-based quadrilateral shape for defining the shell elements. The geometry used to define the Eulerian-based fluid is composed of hexagonal solid elements.

1. Dry Structure

The reference case throughout the study is a completely dry structure using only the composite plate constructed as described previously. No specific modeling of air surrounding, and within, the void spaces of the stiffened composite plate structure is accounted for, due to its negligible effects. The dry structure dynamic response is used for normalization with other cases to show the effects of FSI.

2. Two-Sides Wet Structure

A two-sides wet structure is used to examine the influence of fluid (water) on the response. It is modeled with the stiffened composite plate embedded within a cube of water. The surrounding fluid domain is much greater than the composite plate structure with a two to one ratio of largest dimension. Additionally, the non-reflective boundary condition is applied to the outside fluid boundary. Although there may be some reflected waves from the non-reflective boundary due to imperfect boundary condition, the time period of interest for structural response is too short to include the effects of reflected waves.

3. One-Side Wet Structure

A one-side wet structure is used to simulate a condition in which fluid is on one side of the plate while air is on the other, such as would be encountered in construction of a ship hull with composite plates. To create an air space on one side of the stiffened plate, five additional rigid composite sides are added below the stiffened plate. The sides are rigid shells composed of the same composite material and form the volume to be coupled with the surrounding fluid. The one-side wet structure is depicted in Figure 2. The air volume between the bottom of the stiffened plate and the bottom of the rigid box is 0.01m in height.

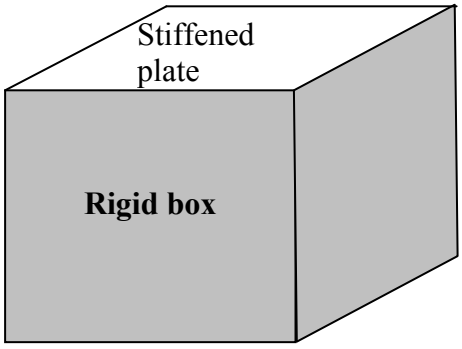

(a) Box made of a stiffened composite plate and five rigid sides

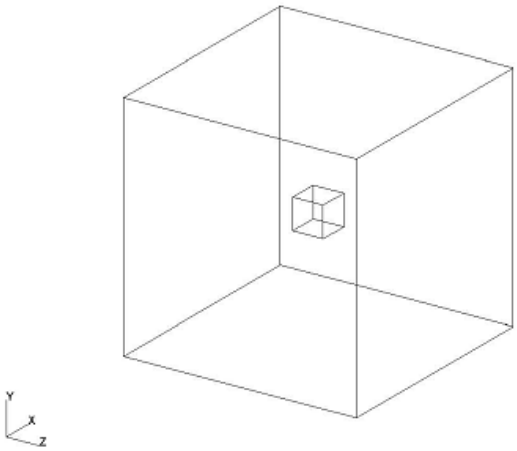

(b) Composite box inside water

Figure 2. Stiffened Composite Plate Supported by Rigid Box used in One-Side Wet Case

III. PARAMETRIC STUDIES USING COMPUTATIONAL MODEL

A. TYPE OF BOUNDARY CONDITION

Two different boundary conditions are applied to the stiffened composite plate, clamped or simply supported. In reality it is difficult at best to achieve a perfectly clamped boundary condition, and thus actual boundaries are a mixture of clamped and simply supported. To bound the dynamic response of composite plate, both boundaries are applied individually to determine any difference between FSI effects. Any experimental work done in conjunction with this study will have imperfectly clamped boundaries, and thus the behavior will be a mixture of both boundary conditions. These numerical models can be used to understand the differences.

B. APPLIED LOADING TYPE

The basis for this study uses an applied concentrated force of 1000N at the center of the top skin plate to observe the dynamic response and determine the FSI. Additionally, an equivalent pressure to the concentrated force is also examined to reveal any differences in response from loading methods. Finally, impulse type loads are imparted to the composite plate using steel projectiles. The steel projectiles are 0.3 m long, and have either a circular or square impact face with area of $1.6129e^{-4}$ m^2 (0.25 in^2). The steel projectiles start 2 mm above the top skin plate, and are given an initial velocity of 1 m/s, 5 m/s or 10 m/s.

C. PLATE SIZE

The basic stiffened composite plate used in this numerical study consists of a 0.3 m by 0.3 m skin plate. A larger 0.5 m by 0.5 m skin plate model is also examined, so the differences in FSI can be examined from increased spacing between supports.

D. PLATE SHAPE

The basis for this study is the standard 0.3 m by 0.3 m square stiffened plate. To examine the impact of plate shape on the dynamic response and FSI, an equivalent area rectangular shaped plate is also modeled with dimensions of 0.2 m by 0.45 m.

E. COMPOSITE MATERIAL PROPERTIES

Parametric studies are conducted using the basic 0.3 m by 0.3 m stiffened plate to examine the effect of composite material properties on FSI and dynamic response. The composite material is modeled with a nominal density of 2020 kg/m^3 and nominal elastic modulus of 1.7e^{10} Pa. Two different densities, approximately a 50% reduction and 100% increase from the nominal, are used to investigate the change in response; specifically, the composite densities are 1020 kg/m^3 and 4020 kg/m^3. Two different elastic moduli, approximately a 50% reduction and 50% increase from the nominal, are used to investigate the change in response; specifically, the composite elastic moduli are 0.7e^{10} Pa and 2.7e^{10} Pa.

IV. NUMERICAL STUDY RESULTS AND DISCUSSION

A. METHODOLOGY

The basic methodology used to determine the difference in dynamic behavior of a stiffened composite plate is to normalize the two-sides and one-side wet cases with the completely dry case. In this manner, the dry case is the base response and tends to differentiate the particular changes due to the FSI. In general, the base case used for normalization is the completely dry plate with composite properties of 2020 kg/m3 for density, $1.7e^{10}$ Pa for elastic modulus with clamped edges, and a 1000 N concentrated force applied at the center of the top skin plate. When strains are examined the normalization is accomplished with respect to the normal x-axis strain.

This method of normalization shows the transient variation of various response variables; such as displacement of the central node of top skin plate, strain energy and/or kinetic energy of the stiffened composite plate, and stress or strain at one of three locations on the bottom skin plate. The numerical solutions from DYTRAN using shell elements only permit stress to be determined. Strains are calculated using the standard stress/strain transformation equations. In the computational model, stress (and hence strain through transformation equations) is calculated at the element in center of plate of one quadrant (this location is termed 'center'), at an element half way between the center and edge of one quadrant (this location is termed 'side'), and at an element half-way between the center and the corner along a diagonal of one quadrant (this location is termed 'quarter'). An example of this scheme of specific elements used to calculate stress/strain is shown in Figure 3 for a 10 by 10 element mesh, although actual composite plate mesh is finer.

The normalized transient responses of displacement and strain energy typically show the same shape and frequency, with only minor differences in relative amplitudes, and thus can be used interchangeably to demonstrate the behavior of the composite plate.

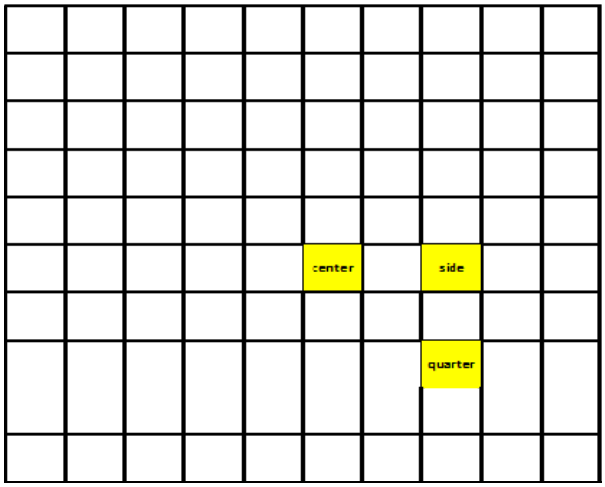

Figure 3. Sample of Element Locations used to Calculate Stress/Strain

B. DYNAMIC RESPONSE OF COMPOSITE PLATE SUBJECTED TO CONCENTRATED FORCE AND CLAMPED BOUNDARY

The baseline stiffened composite plate of density 2020 kg/m3 and elastic modulus of 1.7e ^{10} P a with clamped edges and centrally applied concen trated force w ill be discussed first. Follo w on sectio ns will exam ine variations in boundary condition , loading, size, shape and im pact. Figures 4, 5 and 6 show the response of the displacement, strain energy and kinetic energy of the plate respectivel y (the dry case is used for normalization).

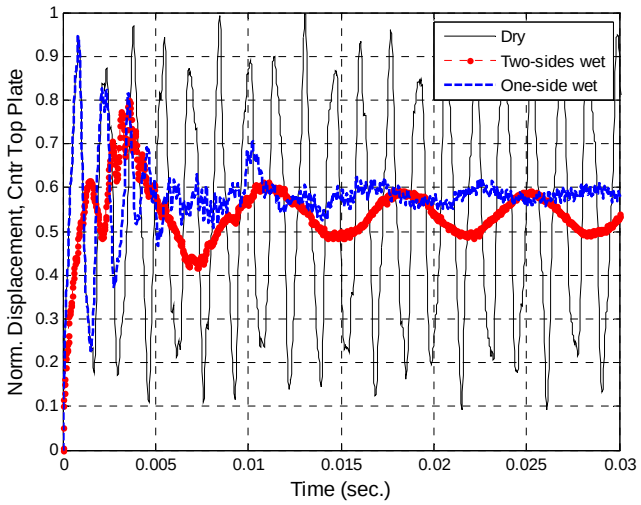

Figure 4. Normalized Displacement at Center of Top Skin Plate

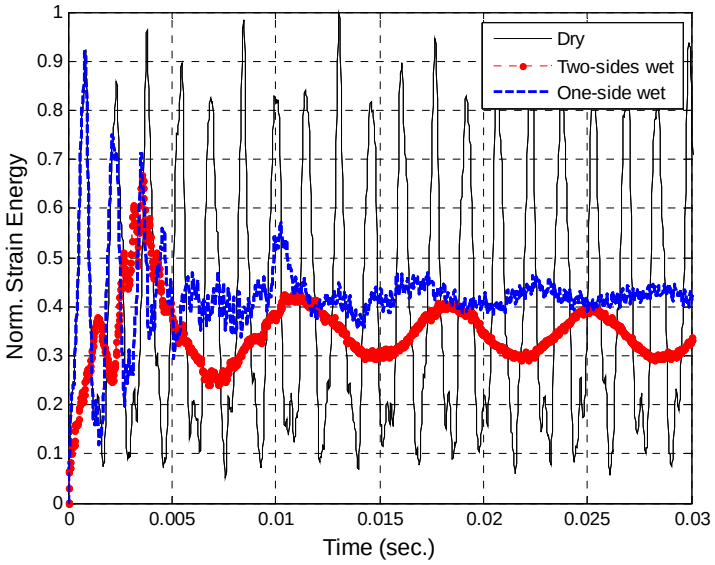

Figure 5. Normalized Strain Energy of Composite Plate

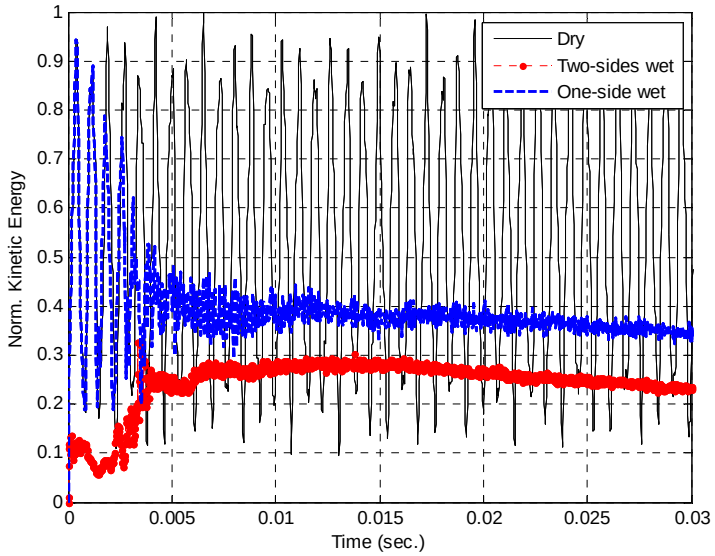

Figure 6. Normalized Kinetic Energy of Composite Plate

These figures show the com parison be tween one-side wet and two-sides wet structural responses. The FSI with either one-side or tw o-sides wet of the com posite structure significantly influences both the m agnitude and frequency of the strain energy plot. The oscillating m agnitude and the fr equency are drastically reduced by the FSI effect. Two-sides wet FSI results in the lowe st peak energy values and their frequency

among the three cases. However, the magnitude of oscillatory behavior is the least for the one-side wet structure. The figures show the effects of FSI, with average displacement and energy being reduced through the fluid interaction. Additionally, FSI causes a decrease in frequency and magnitude of structural responses, with significantly more rapid damping effects than the dry case.

The transverse displacement plot at the node of the applied force is compared in Figure 4 for three different cases. The displacement response is very similar to that of strain energy of Figure 5. The two-sides wet structure has the lowest peak displacement and frequency, and the one-side wet structure has the least vibratory motion. It is interesting to note that even though the displacement characteristics are quite different among the three conditions; their respective average values are comparable.

When average values of the three strain energy variations are compared (Figure 5), the dry structure has the greatest average value and the two-sides wet structure has the smallest value. Furthermore, the two-sides wet structure shows energy dissipation as a function of time.

As the kinetic energy of the stiffened structure is compared under three different surrounding medias, as shown in Figure 6, the dry structure shows a very significant oscillatory behavior. On the other hand, the oscillation of kinetic energy is suppressed quickly for the wet cases. The kinetic energy of the two-sides wet structure is the lowest. The two-sides wet structure displays the fastest decay rate of the kinetic energy.

The normal and shear strains for this clamped case, for each of the locations of interest (center, side and quarter), are shown in Figure 7, with normalization with respect to dry plate x-axis normal strain. Comparison of the normal strain along the x-axis also indicates reduced strains for wet structures. Wet structures have very high frequency components in the strain response. However, the base frequencies of both-side wet structures are clearly shown lower than those of the dry structure. Average strain values are more or less similar even though the dry structure has greater amplitudes of strain oscillation.

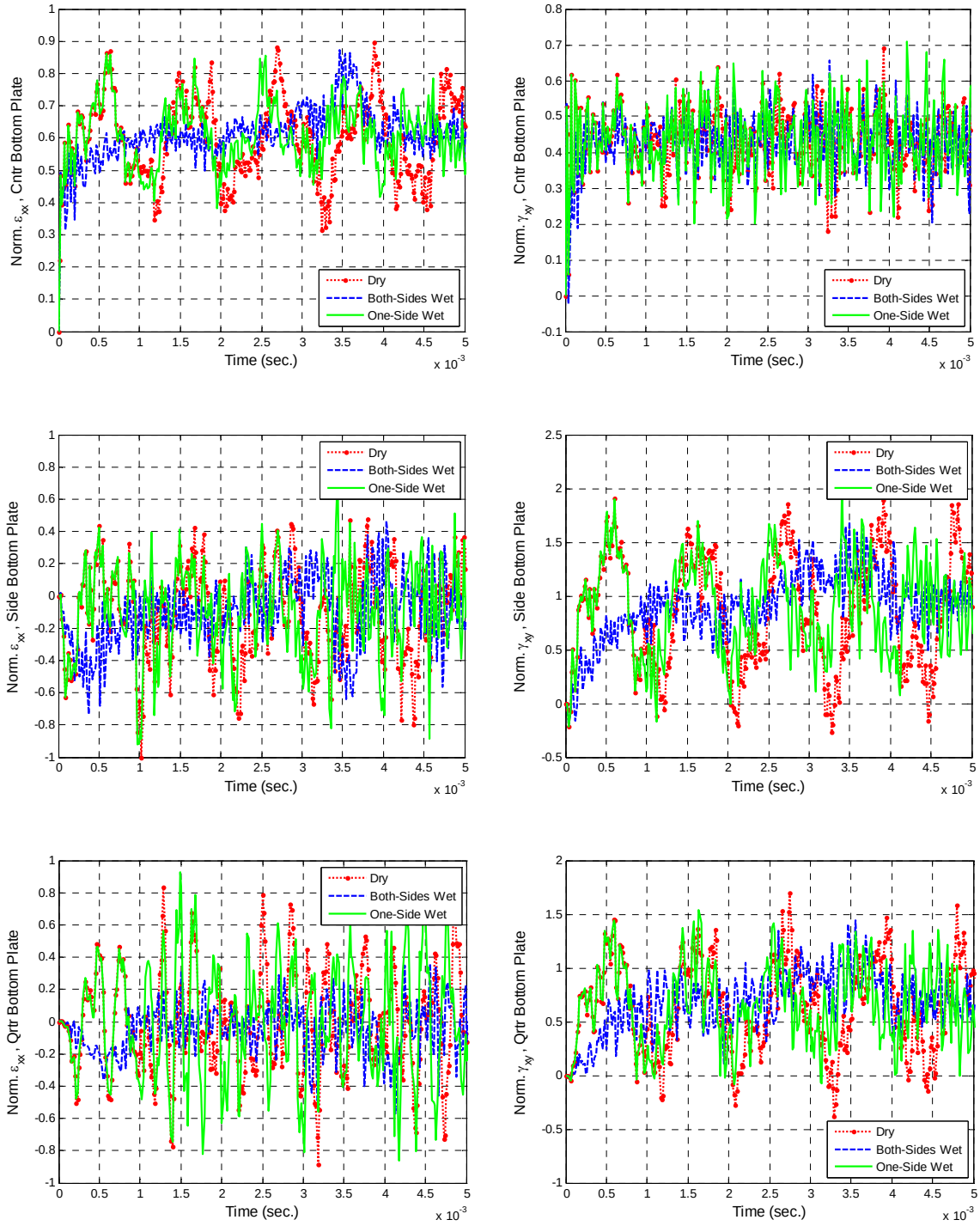

Figure 7. Normal and Shear Strains for Clamped Boundary with Concentrated Force

C. CLAMP VERSUS SIMPLE SUPPORT BOUNDARY CONDITION WITH CONCENTRATED FORCE

Comparison of clamped versus simple boundary shows little difference in dynamic response for concentrated force loading. The displacement and strain energy plots are shown in Appendix A. The kinetic energy responses shown in Figures 8, 9 and 10 shows the comparison for the dry, two-sides wet and one-side wet structures respectively. There is almost no difference for the dry structure; however, the wet structures show slight increase in energy. This is expected due to the increased degree of freedom, although the increased energy is not significant.

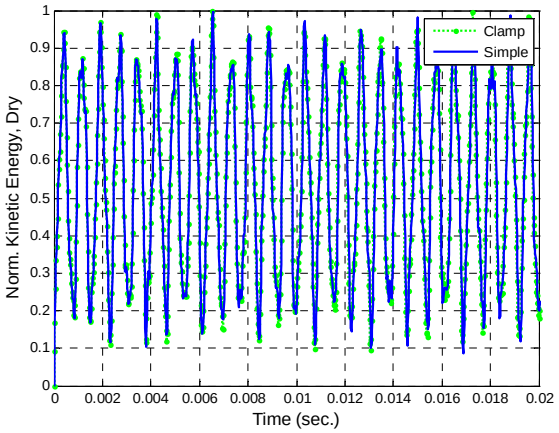

Figure 8. Comparison of Kinetic Energy of Dry Structure between Clamped and Simple Boundary

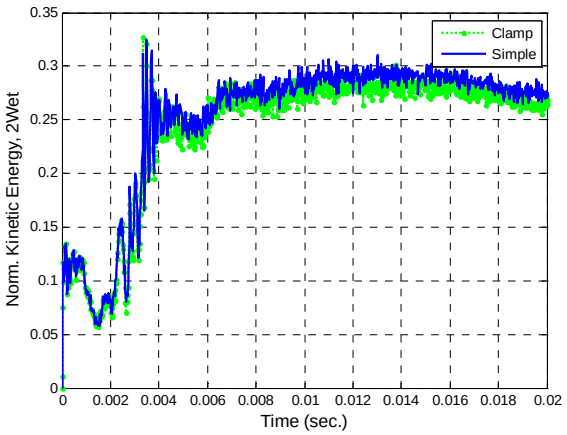

Figure 9. Comparison of Kinetic Energy of Two-sides Wet Structure between Clamped and Simple Boundary

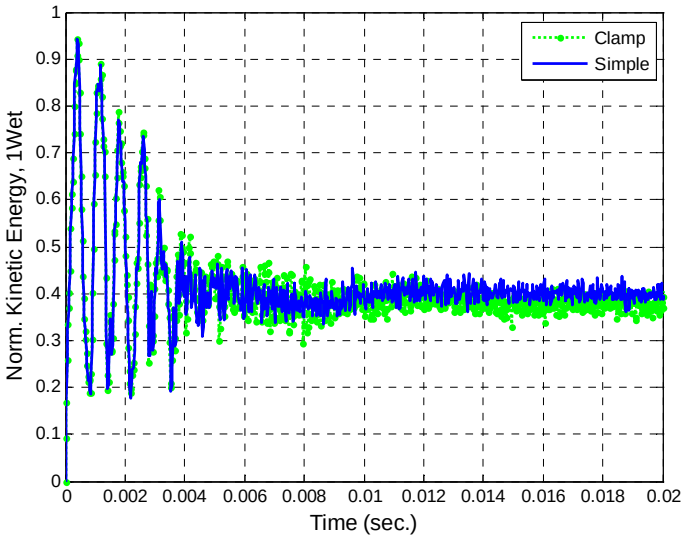

Figure 10. Comparison of Kinetic Energy of One-side Wet Structure between Clamped and Simple Boundary

Similarly, the strains at the center and side locations are nearly identical and are shown in Appendix A. Of interest are the quarter location strains, which show some variance between the boundary condition types, with the clamp condition having slightly higher strains for the dry and wet structures as shown in Figure 11. The increase in strain for the clamped boundary was expected due to restricted degree of freedom; however it is surprising to be evident at only the quarter location.

With an applied concentrated force, there is little difference between the two types of boundary conditions, clamped or simple support. While there is minor increase in kinetic energy of the wet cases for simple support and minor decrease in strain at the quarter location of the composite plate for the simple support, it is not significant. The FSI effects are consistent between the two boundary conditions.

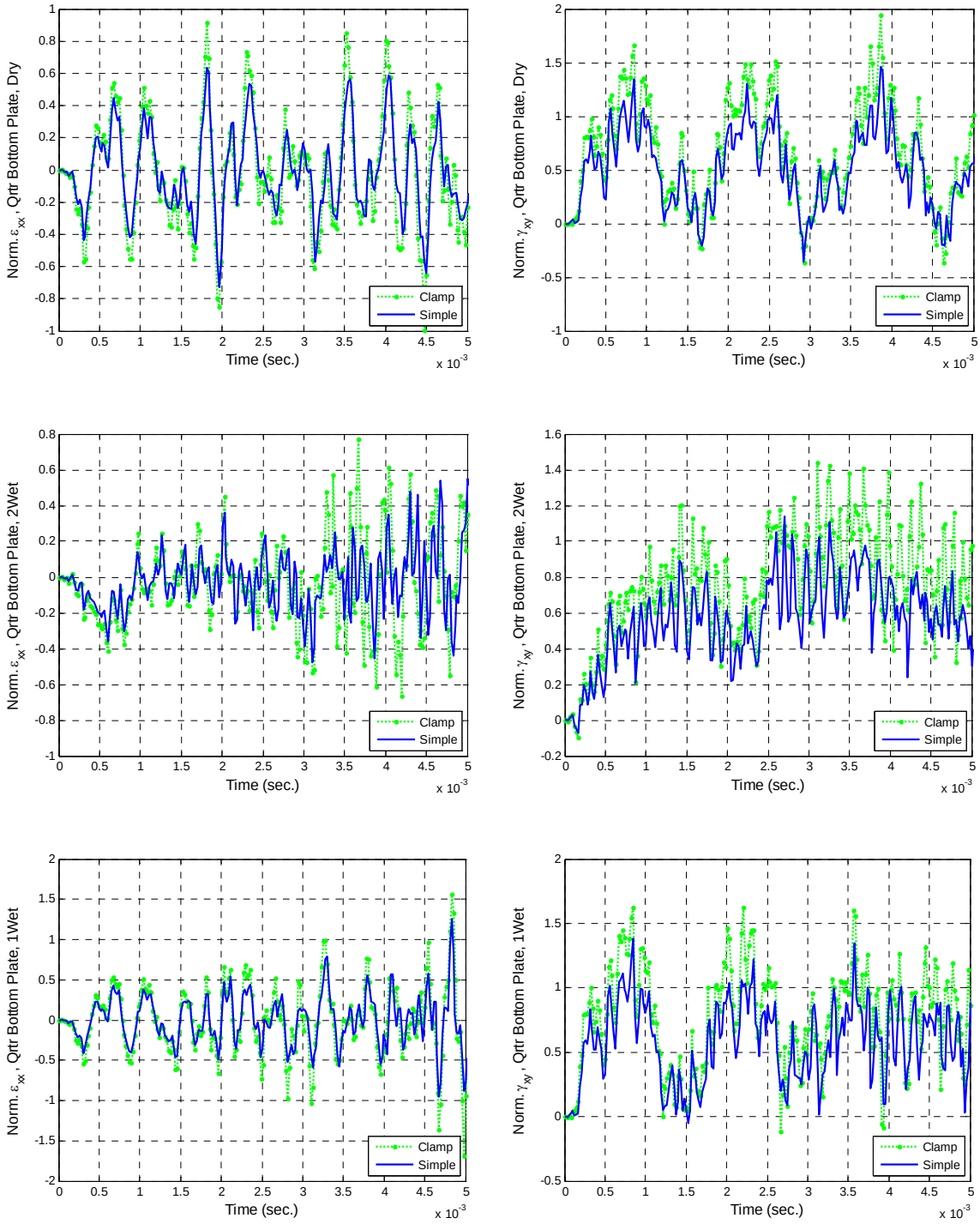

Figure 11. Normal and Shear Strain Comparison at Quarter Position for Clamped versus Simple Boundary with Concentrated Force

D. CONCENTRATED FORCE VERSUS PRESSURE LOADING WITH CLAMPED BOUNDARY

Next, the dynamic response of thin composite plate was compared under different loading conditions: constant concentrated force and equivalent uniform pressure, each with clamped boundary. The basis for comparison is clamped boundary with constant concentrated force of 1000 N applied at center of plate. The equivalent uniform pressure loading is determined from the concentrated force being uniformly applied over the surface of the 0.3m by 0.3m plate, giving a uniform pressure load of 11,111 Pa.

The comparison for the dry structure under the two loading conditions is shown in Appendix B. Under dry conditions, the pressure loading versus concentrated force increases the amplitude of oscillation for displacement, strain energy, and kinetic energy with no shift in frequency. The strain at the center location has increased amplitude but lower average strain. The normal average strain at the side location is increased, while the shear strain is comparable between the two loading conditions. The quarter location exhibits similar strain behavior for applied force and pressure loading.

The dry structure is used to normalize the wet structure responses and the displacement response showing the FSI effects are shown in Figure 12. The wet structure comparison of strain and kinetic energy for force versus pressure load is shown in Figures 13 and 14, respectively.

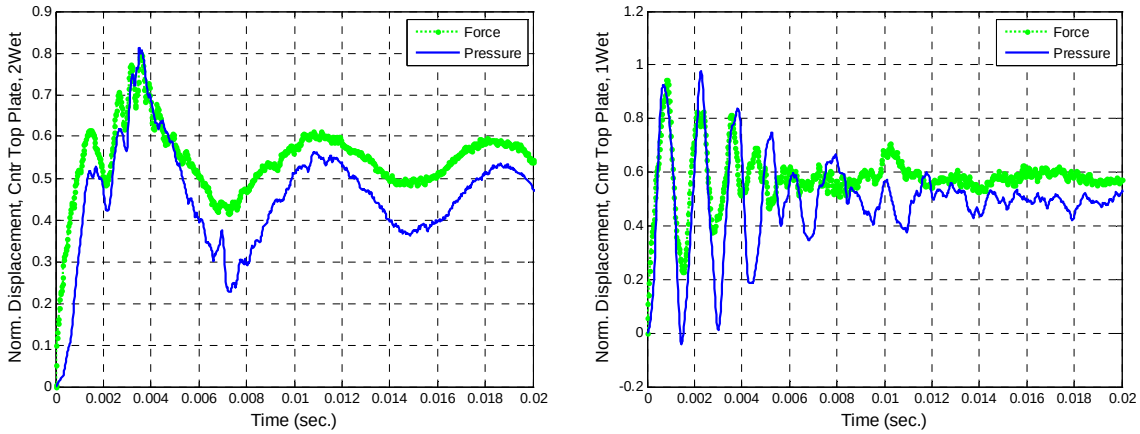

Figure 12. Wet Structure Displacement Comparison between Force and Pressure Loading with Clamped Boundary

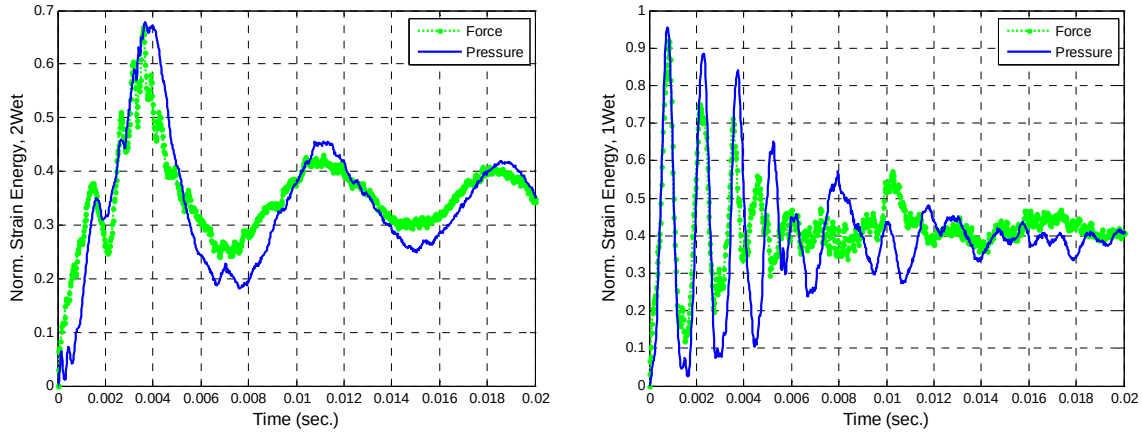

Figure 13. Wet Structure Strain Energy Comparison between Force and Pressure Loading with Clamped Boundary

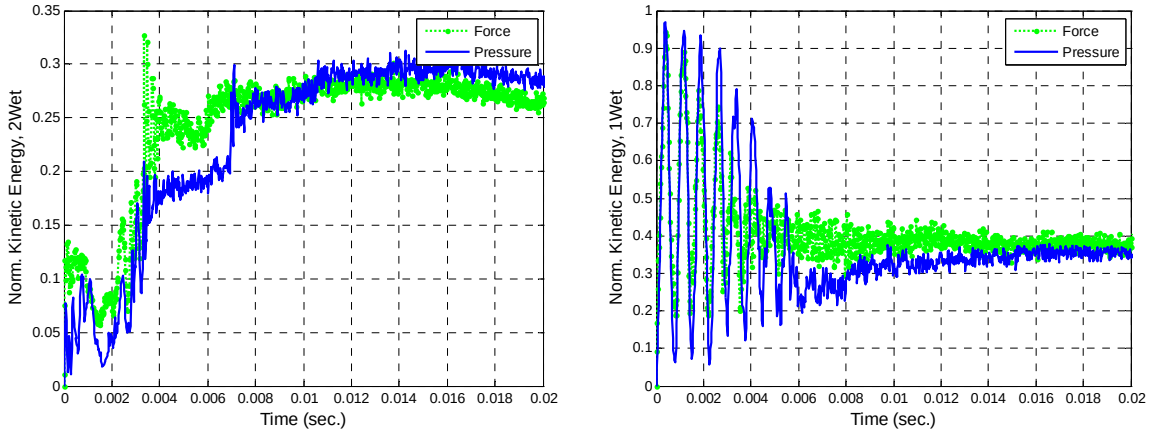

Figure 14. Wet Structure Kinetic Energy Comparison between Force and Pressure Loading with Clamped Boundary

Figures 12 to 14 show t he com parison between one-side wet and two-sides wet structural responses. The FSI with both one-side and two-sides wet reduces the oscillating m agnitude and frequency of the response over dry structure. The pressure load tends to produce larger am plitude of os cillation than concentrated force, but th e average energy is similar, while the mean displacement under pressure load is less. Two-sides wet FSI results in the lowest peak en ergy, peak displacement, and frequency among the three cases. However, the m agnitude of oscillatory behavior is the lea st for the two-sides wet s tructure. The figures sho w the effects of FSI, wi th average displacement and

energy being reduced through the fluid interaction. Additionally, FSI causes a decrease in frequency and magnitude of structural responses with significantly more rapid damping effects than the dry case. Of note in Figure 14 is the slower initial response of kinetic energy under pressure load.

The strain behavior for the dry structure is shown in Appendix B. The pressure load vice concentrated force comparison show increased amplitude of strain oscillation at center location and reduced average strain as well. The strain response at the side and quarter locations was similar for both normal and shear strains, with exception of normal strain at the side location having a slightly higher magnitude under applied pressure than applied force. The strain behavior for wet structures, also shown in Appendix B, was similar to that of dry, with an increased amplitude oscillation at center location, but with reduced average strain. The side and quarter location strain response of wet structures also followed that of dry, with same differences of the normal side location strain exhibiting higher magnitude under pressure loading. This means the concentrated force has a greater FSI effect than the pressure at the side and quarter locations.

E. CONCENTRATED FORCE VERSUS PRESSURE LOADING WITH SIMPLE SUPPORT BOUNDARY

Next the dynamic response of a thin composite plate was compared under different loading conditions, constant concentrated force and equivalent uniform pressure, with a simple support boundary. The basis for comparison is simple support boundary with constant concentrated force.

The comparison for the dry structure under the two loading conditions with simple support is shown in Appendix C. Under dry conditions the pressure and concentrated force loading have nearly identical responses with no discernable change in amplitude or frequency for displacement, strain energy and kinetic energy. The strains at the center locations have nearly identical response for applied force and pressure loading. The normal average strains at the side and quarter location is increased for pressure loading, while the shear strain shows higher amplitude of oscillation for the pressure loading condition.

The wet structure response com parison with simple boundary for force versus pressure load is shown in Figures 15, 16 and 17 for displacem ent, strain energy and kinetic energy respectively.

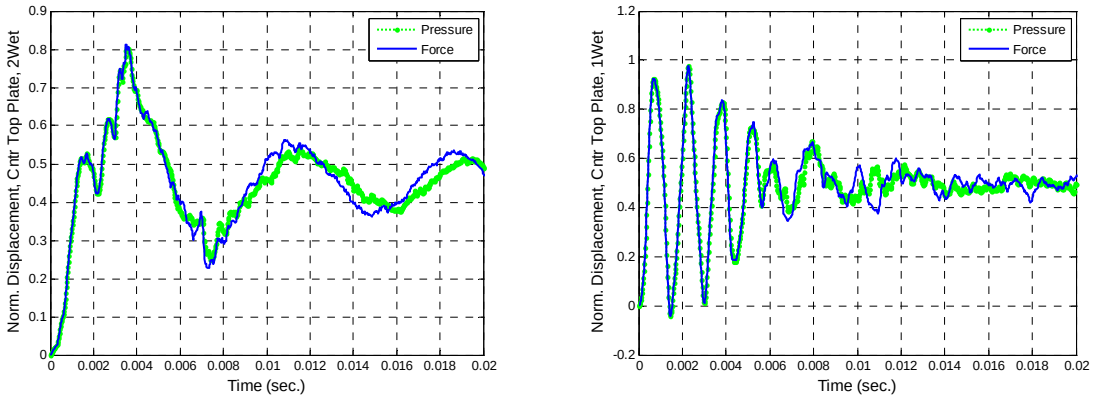

Figure 15. Wet Structure Displacement Comparison of Force and Pressure Loading with Simple Support Boundary

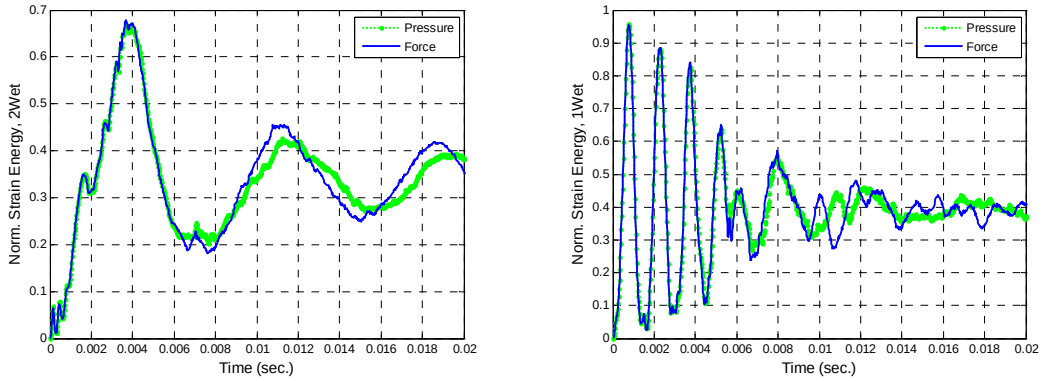

Figure 16. Wet Structure Strain Energy Comparison of Force and Pressure Loading with Simple Support Boundary

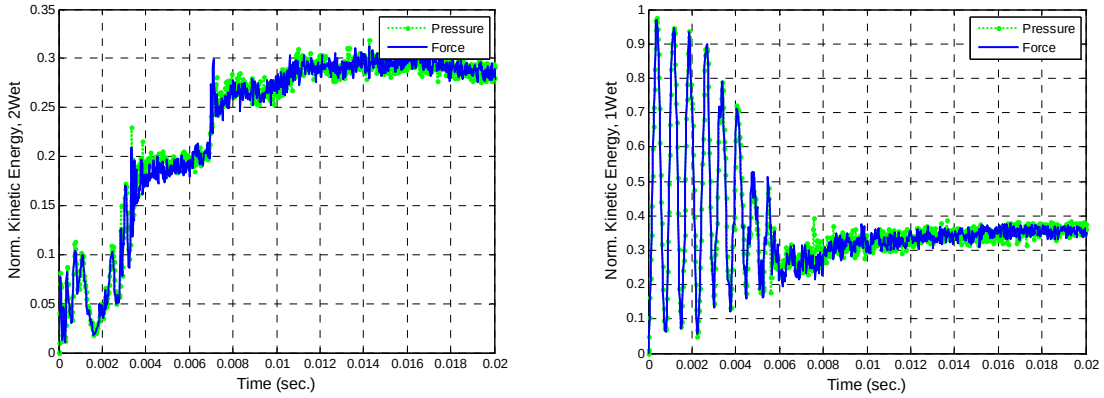

Figure 17. Wet Structure Kinetic Energy Comparison of Force and Pressure Loading with Simple Support Boundary

The FSI with both one-side and two-sides wet structures reduce the oscillating magnitude and frequency of the response over the dry structure. With a simple boundary, the pressure and force load track very well with one another, with only minor difference in frequency evident in the two-sides wet structure displacement and strain energy. Unlike the clamped boundary, there is no delay in response of kinetic energy with a simple boundary for the force and pressure load. Again, the two-sides wet FSI results in the lowest peak energy, peak displacement and frequency among the three cases. The figures show the effects of FSI, with average displacement and energy being reduced through the fluid interaction.

The strain behaviors for the three structures are shown in Appendix C. The pressure and force load strains track each other using a simple support boundary at the center location. The strain response at the side location has similar amplitude of oscillation, with the normal strains slightly higher under pressure load. The strain behavior at the quarter location is similar for wet structures, although the two-sides wet structure has less amplitude, the wet structures overall have approximately equal average strain.

F. SIZE OF COMPOSITE PLATE

Next the influence of composite plate size on FSI is examined by increasing the size of the square plate from 0.3m to 0.5m on a side. The comparison is made using

clamped boundary condition with applied concentrated force. The displacement response for the three structures is shown in Appendix D, and indicates that increases in plate size yield a decrease in frequency, with the two-sides wet structure having a substantial decrease in frequency. Also, FSI damping is slower as the plate size increases. Similar results are visible in strain and kinetic energy response between the two sizes of plates shown in Figures 18, 19 and 20, for the dry, two-sides wet and one-side wet structures respectively.

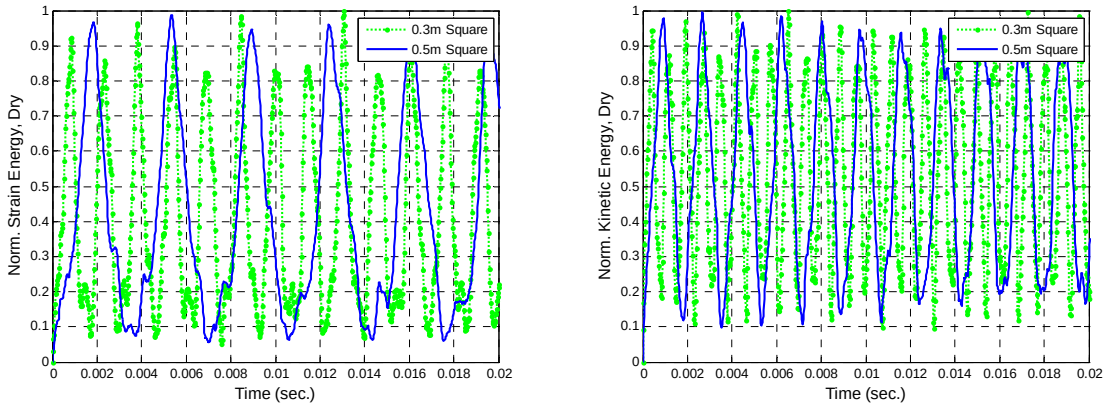

Figure 18. Dry Structure Strain and Kinetic Energy Comparison for Plate Size Variations with Concentrated Force and Clamped Boundary

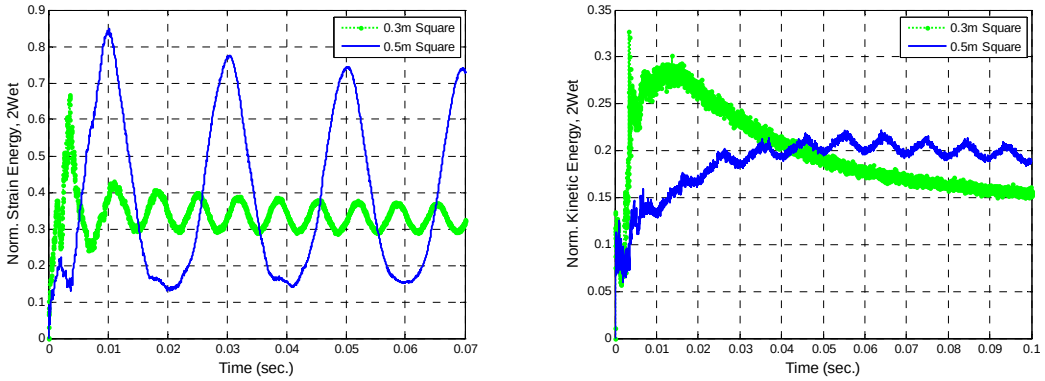

Figure 19. Two-sides Wet Structure Strain and Kinetic Energy Comparison for Plate Size Variations with Concentrated Force and Clamped Boundary

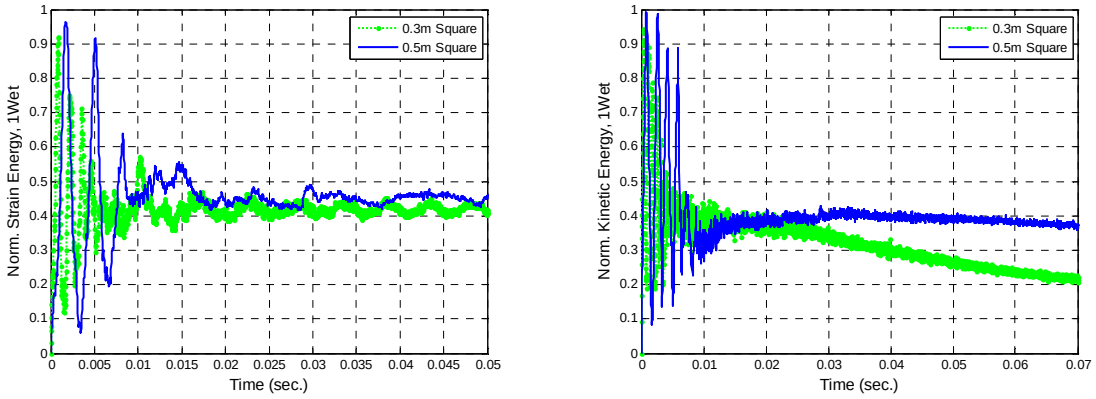

Figure 20. One-side Wet Structure Strain and Kinetic Energy Comparison for Plate Size Variations with Concentrated Force and Clamped Boundary

The larger size plate has lower frequency, slower initial response, and slower long-term damping. The FSI of the larger plate is less and thus has higher amplitude oscillations. The dry structure has similar average energies between the two plate sizes, while the steady state energy of the larger plate is marginally greater for the one-side wet structure. The difference in energy between the two plate sizes is more pronounced in the two-sides wet structure, where the kinetic energy clearly shows the significant delay in response due to the damping effect of fluid.

The comparison of strain between the two sized plates is shown in Appendix D. However, there is no clearly identifiable characteristic between the strains with exception of some decreased frequency and comparable average normal and shear strains.

G. SHAPE OF COMPOSITE PLATE

The influence of composite plate shape on FSI is examined next by changing the shape of the plate from square to rectangular while maintaining equivalent area, thus the rectangular plate is 0.2 m by 0.45m. As with comparison of plate size, the shape comparison is made using clamped boundary conditions with applied concentrated force. The displacement response for the three structures is shown in Appendix E, and indicates the rectangular shape has increase in frequency and decrease in amplitude of oscillation over the square plate of equivalent area, with the average displacement of the three structures (dry, two-sides wet, one-side wet) slightly greater for the rectangular shape.

The strain and kine tic energy response between the two shap es of plates are shown in Figures 21, 22 and 23, for the dry, two-sides wet and one-s ide wet structures respectively. The rectan gular plate has a hi gher frequency and faster dam ping rate. T he rectangular plate has lo wer a mplitude of oscillations. The average energies of the rectangular plate are higher th an those of the square plat e. The difference in energy between the two plate shapes is m ore pronounc ed in the two-sides wet structure, w hich clearly sho ws the FSI effect is greates t fo r tw o-sides wet structur e and the overall FSI effect is less for the rectangular vice square plate since the peak energy is greater.

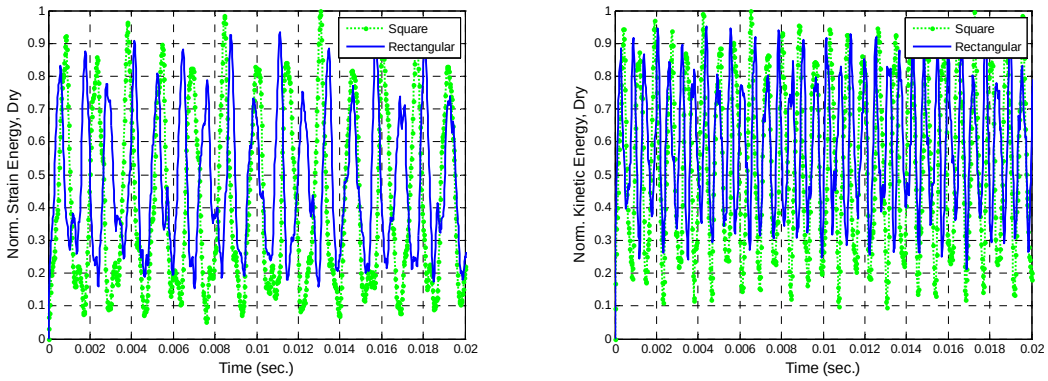

Figure 21. Dry Structure Strain and Kinetic Energy Comparison for Plate Shape Variations with Concentrated Force and Clamped Boundary

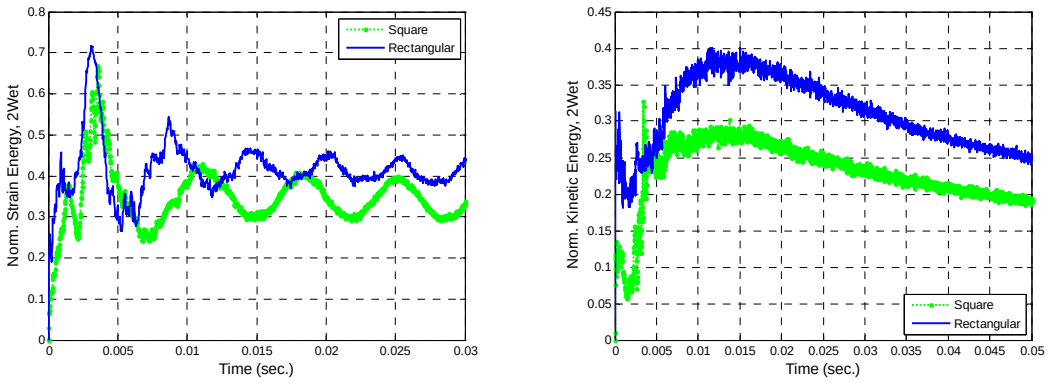

Figure 22. Two-sides Wet Structure Strain and Kinetic Energy Comparison for Plate Shape Variations with Concentrated Force and Clamped Boundary

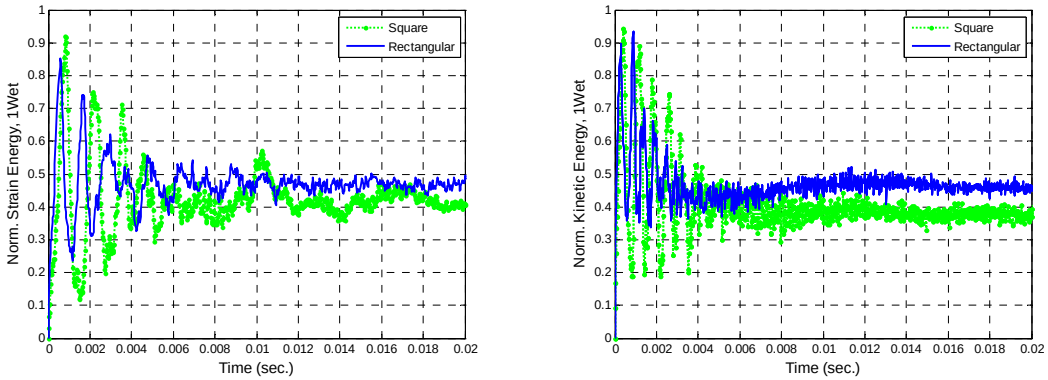

Figure 23. One-side Wet Structure Strain and Kinetic Energy Comparison for Plate Shape Variations with Concentrated Force and Clamped Boundary

The comparison of strain between the two shaped plates is shown in Appendix E. The shear strains for the rectangular plate are all less than for the equivalent area square plate. The average normal strain at center location of all three structures is a little more for the rectangular vice the square plate, while the normal strains at the side and quarter locations are very similar. Overall, the reduction in energy due to FSI effects of the rectangular plate shape is less than the square plate.

H. COMPOSITE DENSITY

Next the influence of composite material density on dynamic response is examined. Since the response of displacement is similar to strain energy, only the strain energy will be used here and displacement plots are in Appendix F. Figures 24, 25 and 26 show the strain and kinetic energy for the dry, two-sides wet and one-side wet structures respectively, with each using a composite plate of density 2020 kg/m ^{3} and elastic modulus of 1.7e ^{10} Pa, with concentrated force and clamped boundary for normalization. For the dry structure it is clearly visible that increasing density causes a decrease in frequency, however, due to FSI this feature is not as pronounced in the wet structures. The wet structures show only slight difference in frequency and the peak strain energy occurs in lowest density with only minimal decrease in peak energy as density increases. The kinetic energy shows a faster rate of damping with increasing density for the wet structures.

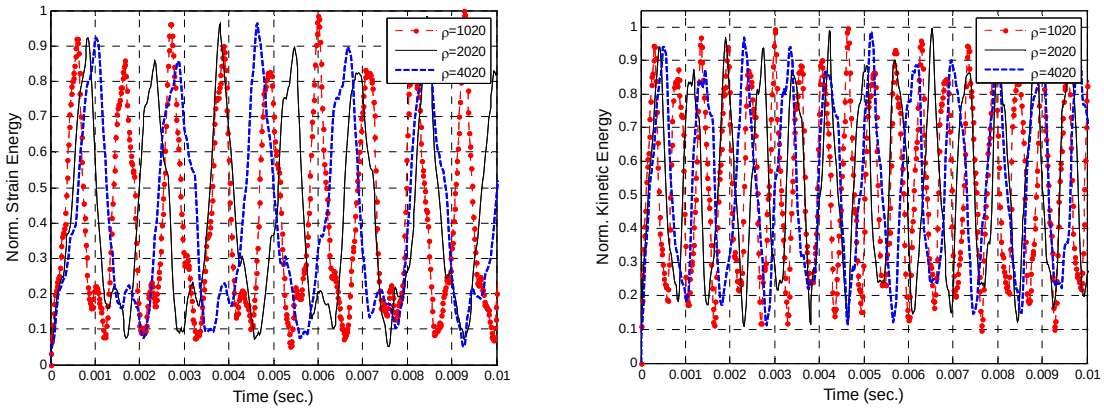

Figure 24. Dry Structure Strain and Kinetic Energy Comparison for Density Variations with Concentrated Force and Clamped Boundary

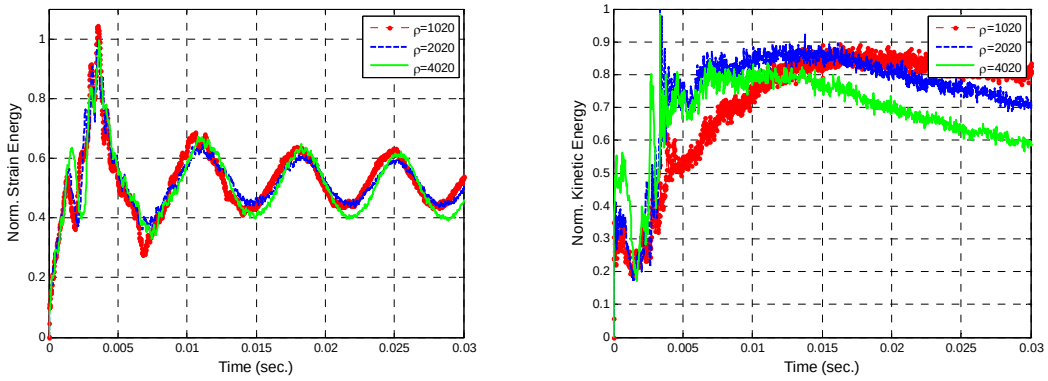

Figure 25. Two-sides Wet Structure Strain and Kinetic Energy Comparison for Density Variations with Concentrated Force and Clamped Boundary

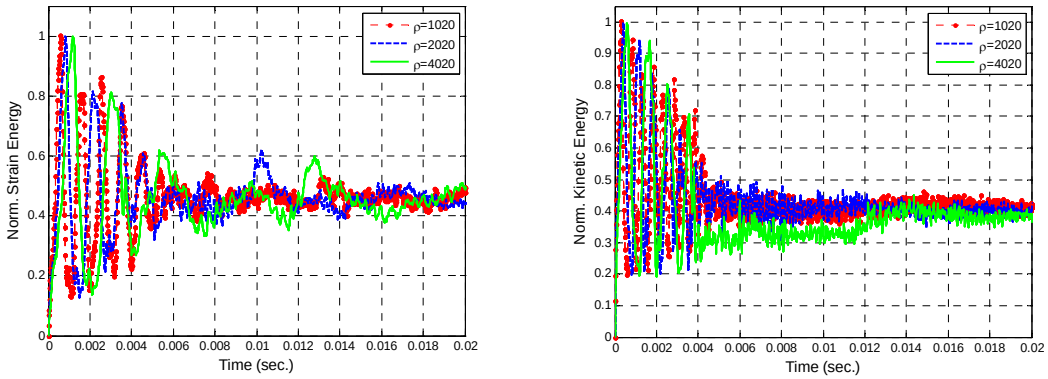

Figure 26. One-side Wet Structure Strain and Kinetic Energy Comparison for Density Variations with Concentrated Force and Clamped Boundary

To highlight the specific FSI effects, the method of normalization was altered such that each wet structure is normalized to its respective dry structure and the three different densities are plotted together to show its effect on response. With this alternate normalization, the strain and kinetic energy is shown in Figures 27 and 28 for the two-sides wet and one-side wet structures, respectively. In this representation, it is clear FSI gives a reduction in peak energy, is more significant in two-sides wet structure and drastically reduces the high frequency oscillation from the dry structure. Also, the two-sides wet structure kinetic energy shows faster response, as density increases, from initial load application to peak energy value and subsequent decay toward steady state value.

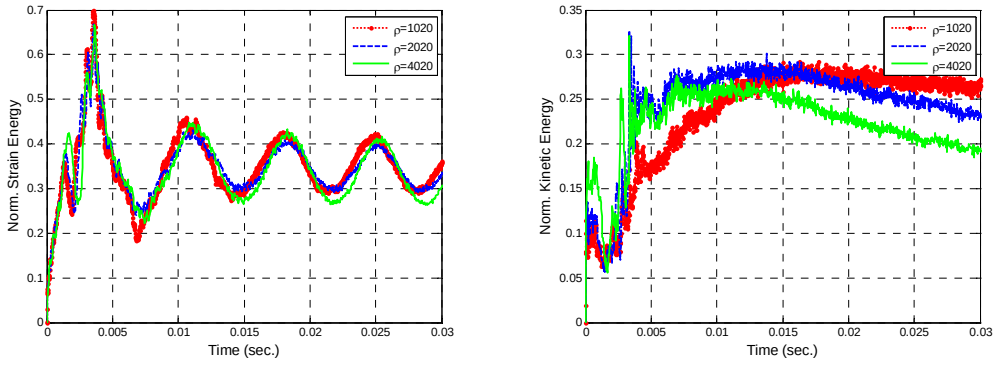

Figure 27. Two-sides Wet Structure Strain and Kinetic Energy Comparison for Density Variations with Concentrated Force and Clamped Boundary (Alternate Normalization)

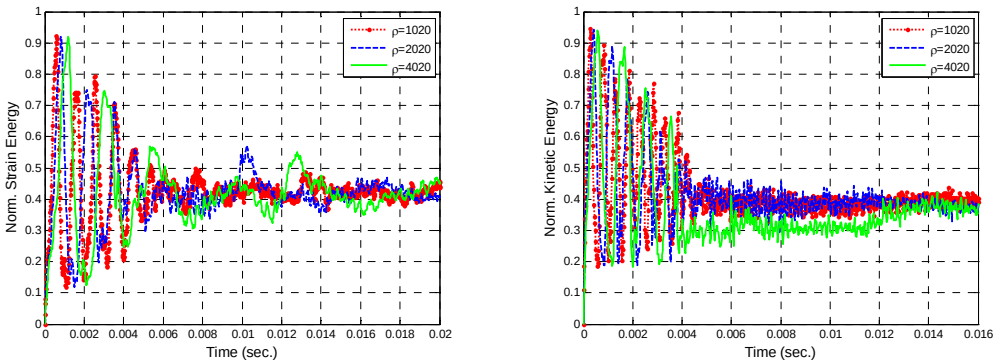

Figure 28. One-side Wet Structure Strain and Kinetic Energy Comparison for Density Variations with Concentrated Force and Clamped Boundary (Alternate Normalization)

The variations in strain of the three structures are shown in Appendix F. For the dry and one-side wet structure, a decrease in frequency as density increases is evident, but is not identifiable for the two-sides wet structure. None of the structures exhibit significant variation in magnitude of strain for the different density values. As shown in Figure 29, using the previously discussed alternate normalization, the strains for the two-sides wet structure have similar relative magnitude, for the three locations (center, side, quarter), with no discernable shift in frequency due to density variations, while Figure 30 shows the one-side wet structure having a decrease in frequency from density increases with similar relative strain magnitude.

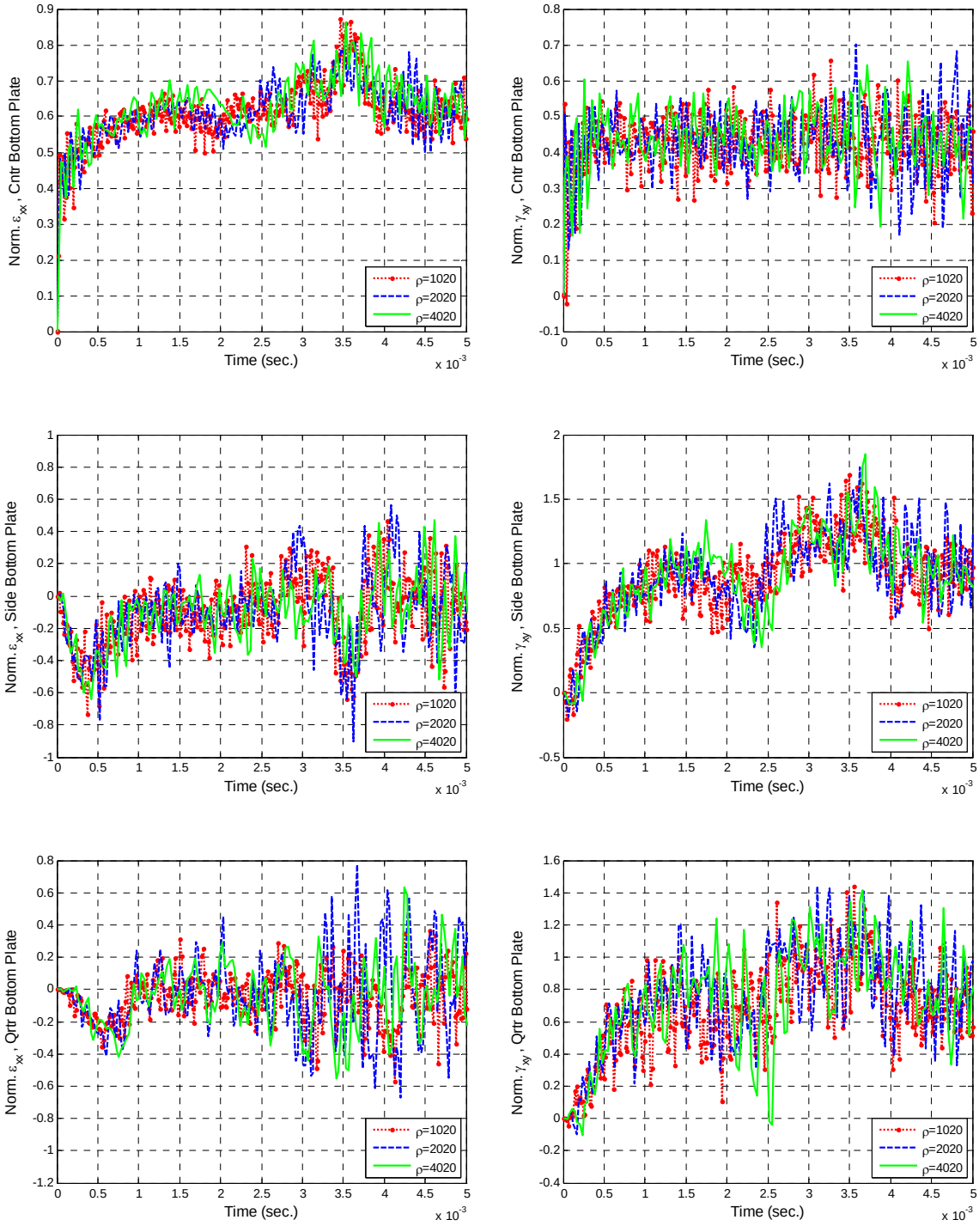

Figure 29. Normal and Shear Strains for Comparison of Differ Density for Two-sides Wet Structure with Concentrated Force and Clamped Boundary (Alternate Normalization)

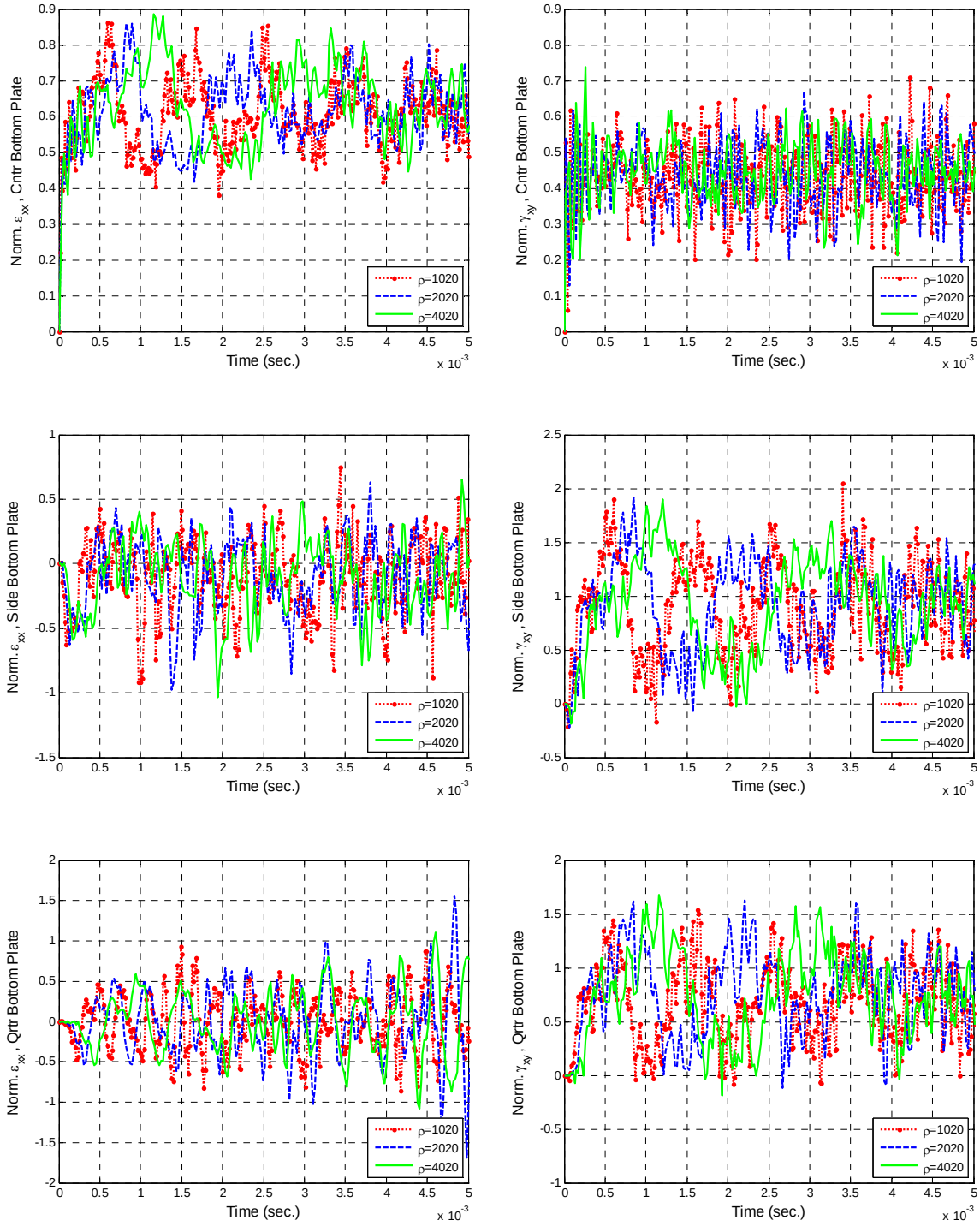

Figure 30. Normal and Shear Strains for Comparison of Differ Density for One-side Wet Structure with Concentrated Force and Clamped Boundary (Alternate Normalization)

I. COMPOSITE MODULUS

The influence of composite material elastic modulus on dynamic response is examined next. The displacement response for different elastic modulus is shown in Appendix G. Figures 31, 32 and 33 show the strain and kinetic energy for the dry, two-sides wet and one-side wet structures respectively, with each using a composite plate of density 2020 kg/m ^{3} and elastic modulus of 1.7e ^{10} Pa, with concentrated force and clamped boundary for normalization. For the three structures, an increase in frequency and decrease in amplitude is clearly visible for increasing elastic modulus. As the composite elastic modulus increases, the structure becomes stiffer and as the strain and kinetic energy plots show, the average energy decreases with increasing modulus. Also, the amplitude of oscillation decreases with increasing modulus. The wet structures show a similar rate of damping with increasing modulus.

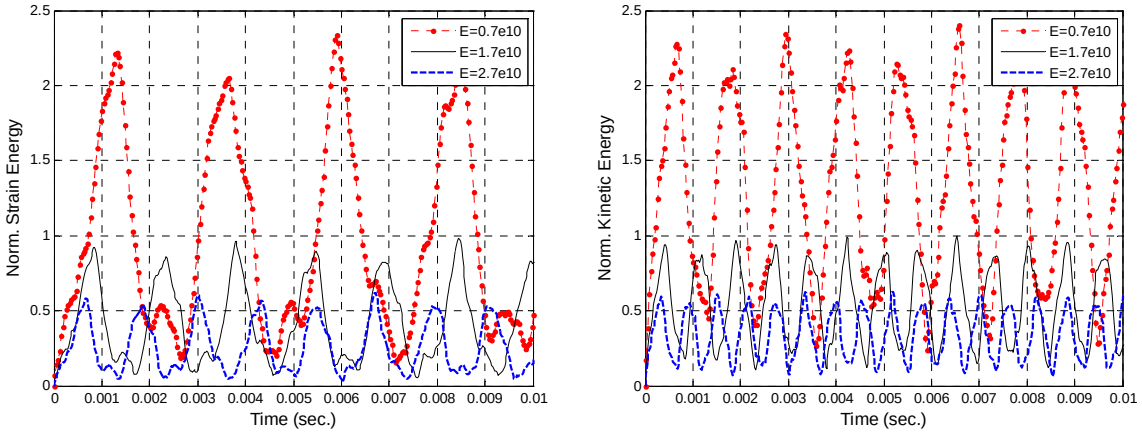

Figure 31. Dry Structure Strain and Kinetic Energy Comparison for Elastic Modulus Variations with Concentrated Force and Clamped Boundary

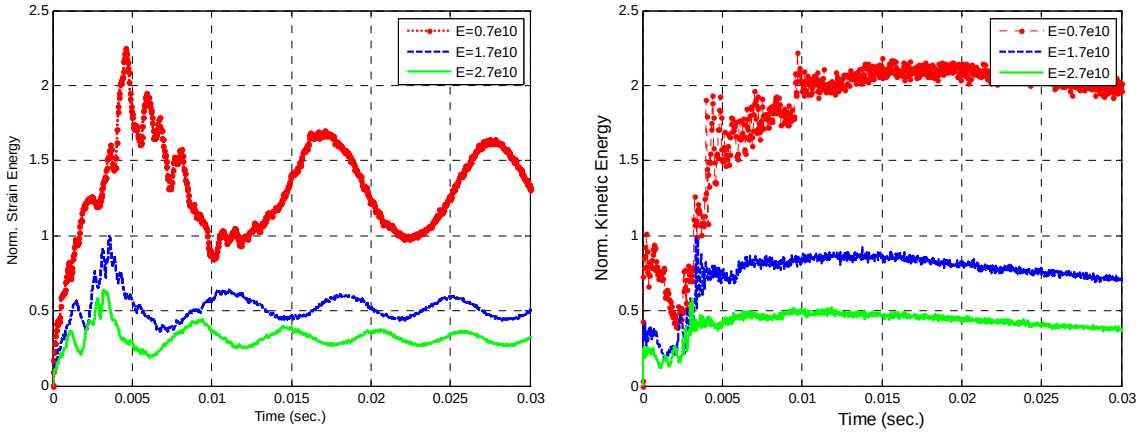

Figure 32. Two-sides Wet Structure Strain and Kinetic Energy Comparison for Elastic Modulus Variations with Concentrated Force and Clamped Boundary

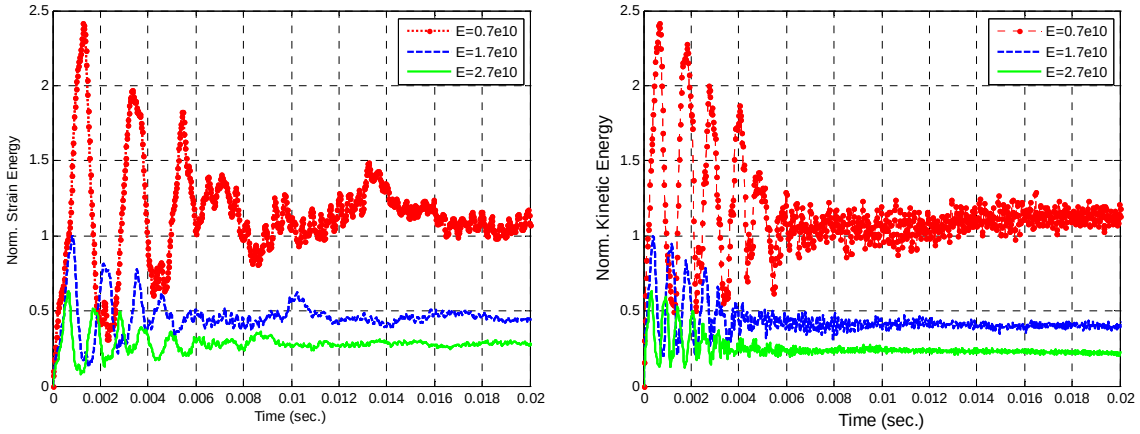

Figure 33. One-side Wet Structure Strain and Kinetic Energy Comparison for Elastic Modulus Variations with Concentrated Force and Clamped Boundary

To highlight the specific FSI effects, the method of normalization was altered as discussed in the previous section. With this alternate normalization, the strain and kinetic energy is shown in Figures 34 and 35 for the two-sides wet and one-side wet structures, respectively. In this representation, it is clear FSI gives a reduction in peak energy, is more significant in two-sides wet structure and drastically reduces the high frequency oscillation. The average strain energy is comparable at each of the different elastic modulus values, with only the frequency and amplitude varying, while the kinetic energy tends to decrease with increasing modulus.

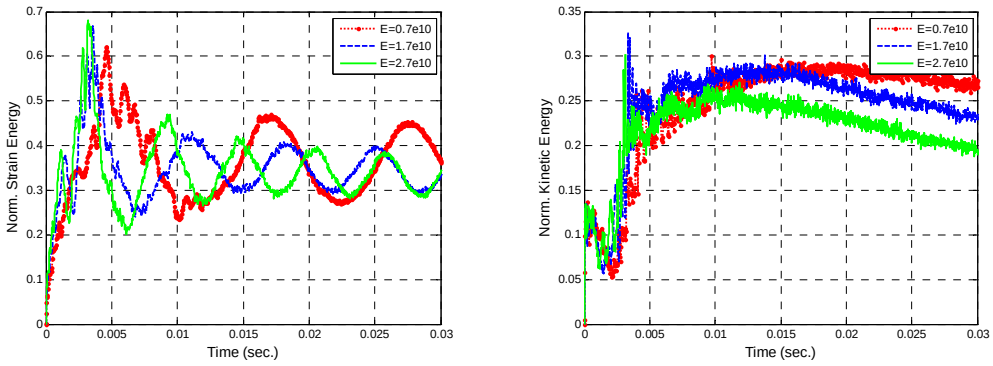

Figure 34. Two-sides Wet Structure Strain and Kinetic Energy Comparison for Elastic Modulus Variations with Concentrated Force and Clamped Boundary (Alternate Normalization)

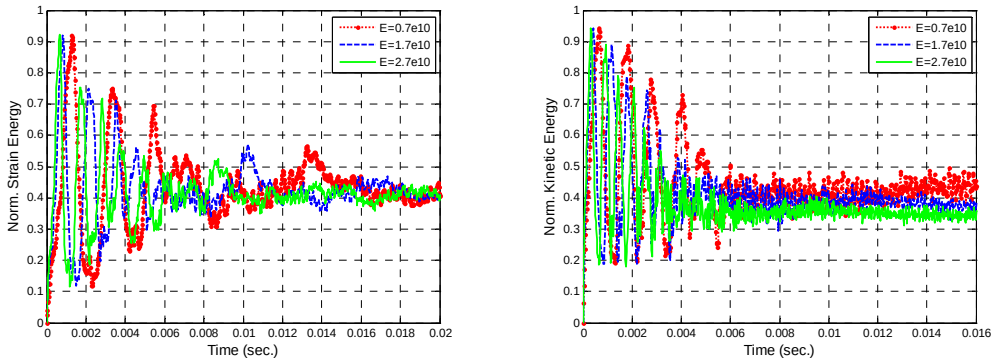

Figure 35. One-side Wet Structure Strain and Kinetic Energy Comparison for Elastic Modulus Variations with Concentrated Force and Clamped Boundary (Alternate Normalization)

The strain variations of the three structures are shown in Appendix G. For these structures, the decrease in amplitude of oscillation as elastic modulus increases is evident while the increase in frequency less noticeable in the strain plots. The most notable feature is the large reduction in strain as the modulus increases; this is due to the increased stiffness. Using the alternate normalization, so that specific influences of elastic modulus and FSI can be highlighted for strain, the strain responses of the two-sides wet and one-side wet structures are shown in Figures 36 and 37, respectively. For the two-sides wet structure, the relative magnitude of strain is consistent for each of the three moduli across the three different locations on the plate, with minor indication of the

increase in frequency with increasing m odulus. The frequency shift is m uch more evident in the one -side wet s tructure, whil e again the rela tive stra in m agnitude is consistent for the various modulus values.

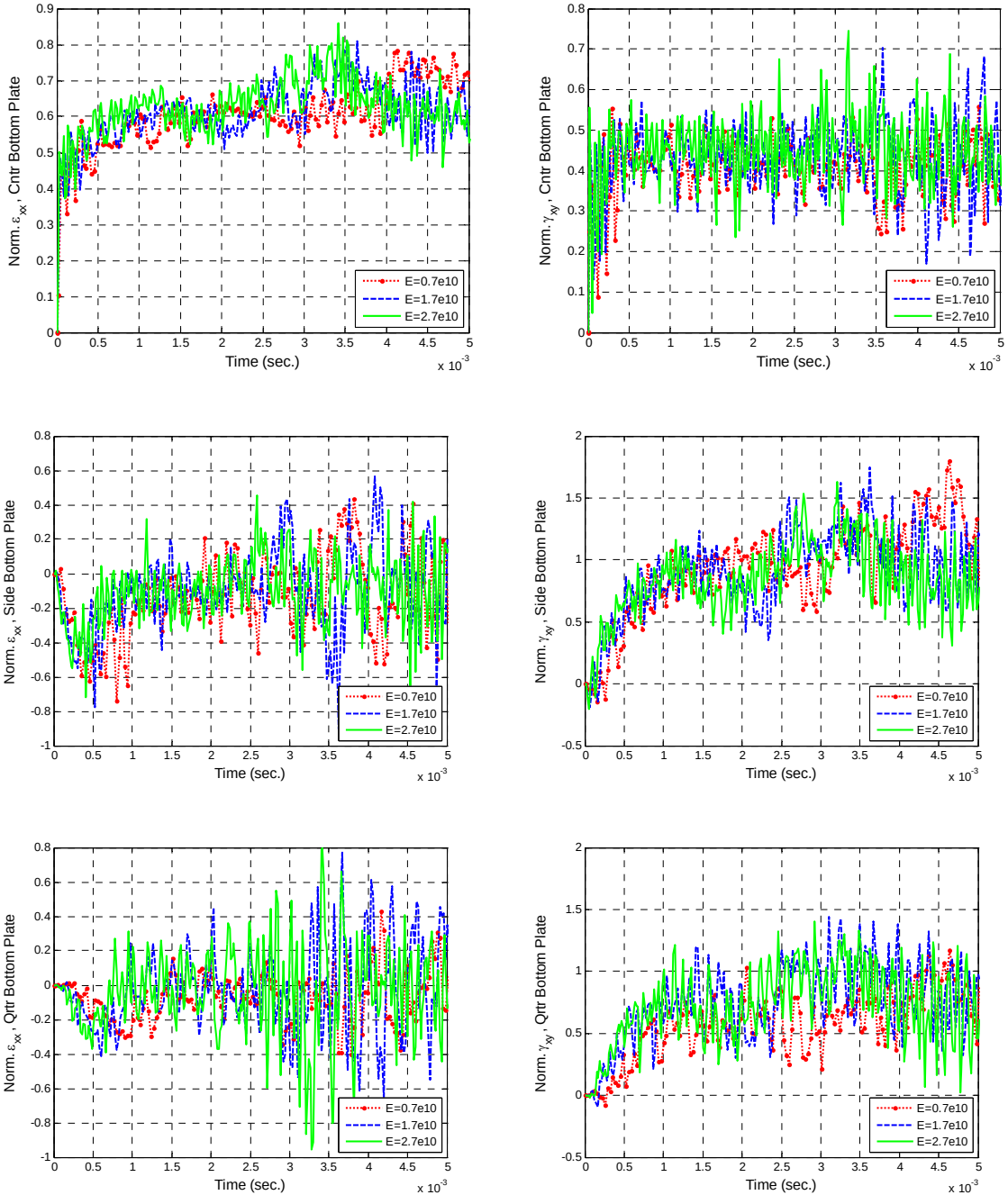

Figure 36. Normal and Shear Strains for Comparison of Differ Elastic Modulus for Two-sides Wet Structure with Concentrated Force and Clamped Boundary (Alternate Normalization)

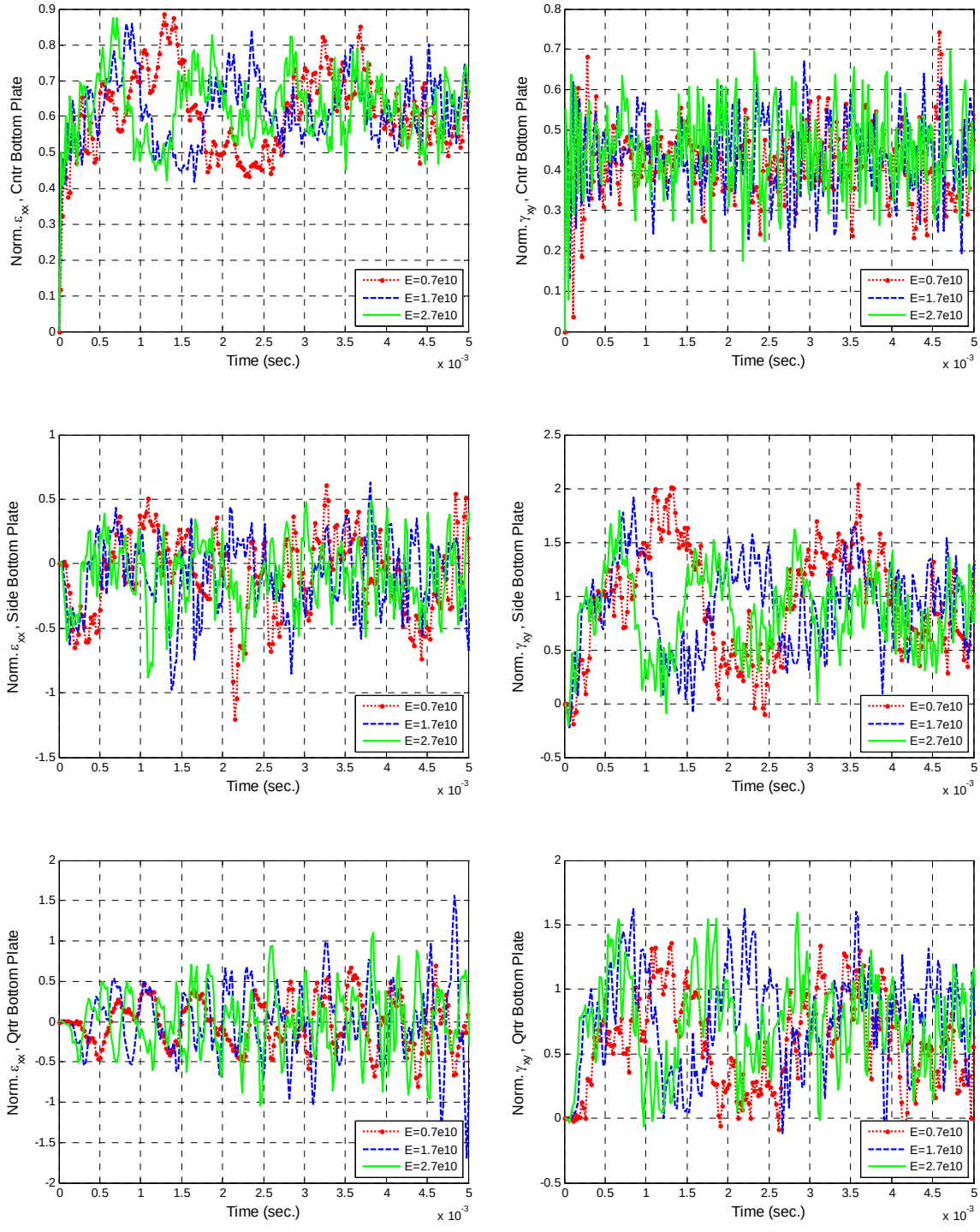

Figure 37. Normal and Shear Strains for Comparison of Differ Elastic Modulus for One-side Wet Structure with Concentrated Force and Clamped Boundary (Alternate Normalization)

J. IMPACT LOADING

The final dynamic behavior examined is the impact response of composite plate from a steel projectile. Three velocities are examined for the projectiles: 1 m/s, 5 m/s and 10 m/s. In addition, the response due to two impact face shapes are compared, each having the same surface area for impact and equal mass. A cylindrical shaped impactor has a circular shape area of impact and a rectangular shaped impactor has a square shape area of impact. Each projectile contacts the composite plate at the center.

1. Shape of Impactor

To investigate any dependence on shape of the impact object, a fixed velocity of 10 m/s is used to compare the difference in response between the two shapes of impact projectiles. Figures 38, 39 and 40 compare the displacement, strain energy and kinetic energy response of the three structures to the circular and square shape impactor. The figures show FSI gives a significant reduction in amplitude and frequency and the square impact face has less amplitude for dry and one-side wet structure than the circular face impactor. The two-sides wet structure shows similar initial response between the two shapes of impact and then the square face impactor response steadies out with higher amplitude of oscillation. The average displacement is comparable between the two impact shapes, while the average energy is less for the square face impact for each of the three structures.

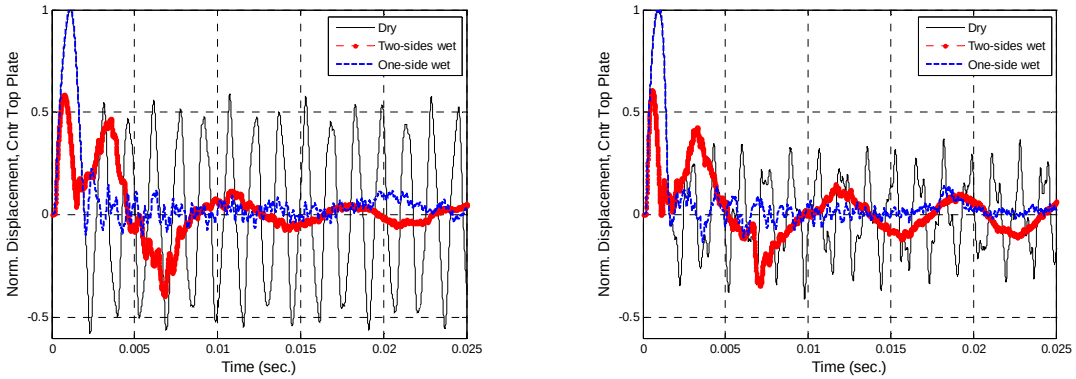

Circular Impact Area Square Impact Area

Figure 38. Displacement Comparison of Three Structures Due to Different Impactor Shapes at 10 m/s

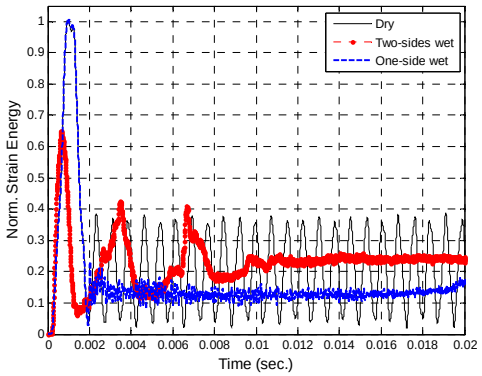

Circular Impact Area

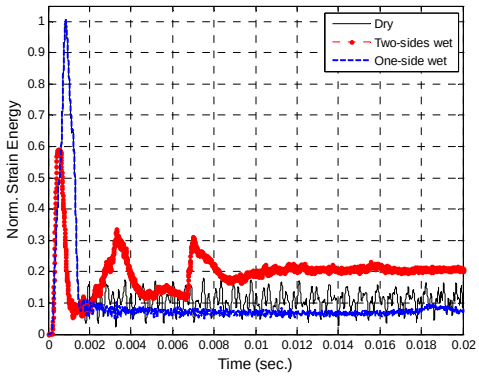

Square Impact Area

Figure 39. Strain Energy Comparison of Three Structures Due to Different Impactor Shapes at 10 m/s

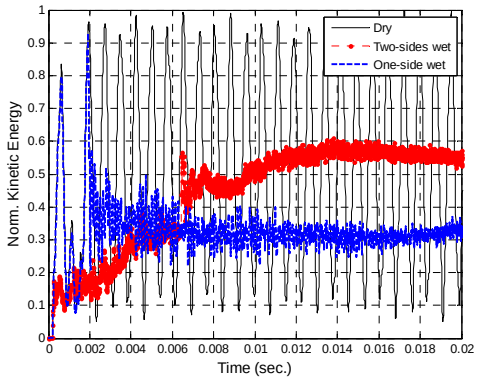

Circular Impact Area

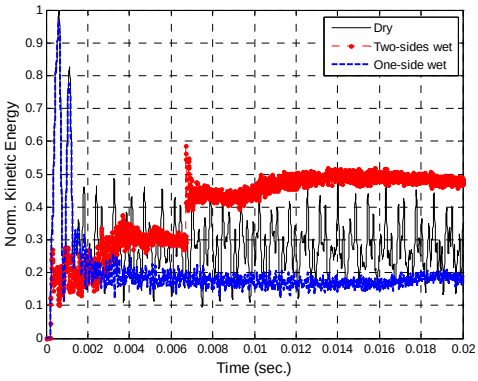

Square Impact Area

Figure 40. Kinetic Energy Comparison of Three Structures Due to Different Impactor Shapes at 10 m/s

The normal strain at each location is compared in Figure 41 for the two shapes of impactor. The FSI decreases slightly the strain amplitude with minor decrease in frequency. The two-sides wet structure has a larger peak strain for the center and side locations for the square faced impactor over the circular faced impactor, while the cylindrical impactor has peak strain in dry and one-side wet structure. The shear strain is slightly higher for square face impactor at center location, while the shear strains are comparable between impactor at the side and

quarter locations. The FSI is more pronounced for the square impactor one-side wet, and more for the cylindrical impactor two-sides wet case.

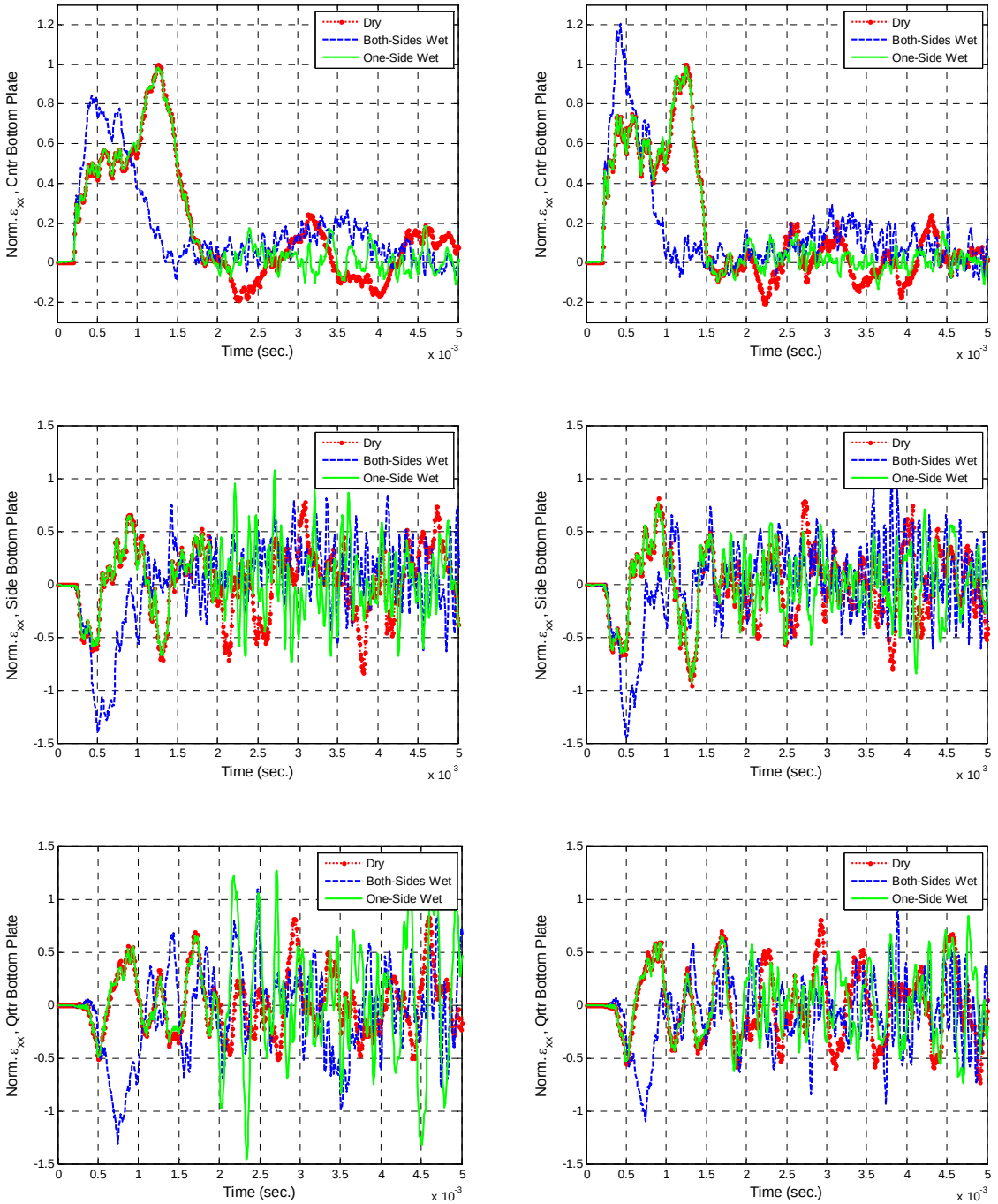

Figure 41. Normal Strain Comparison of Three Structures Due to Different Impactor Shapes at 10 m/s

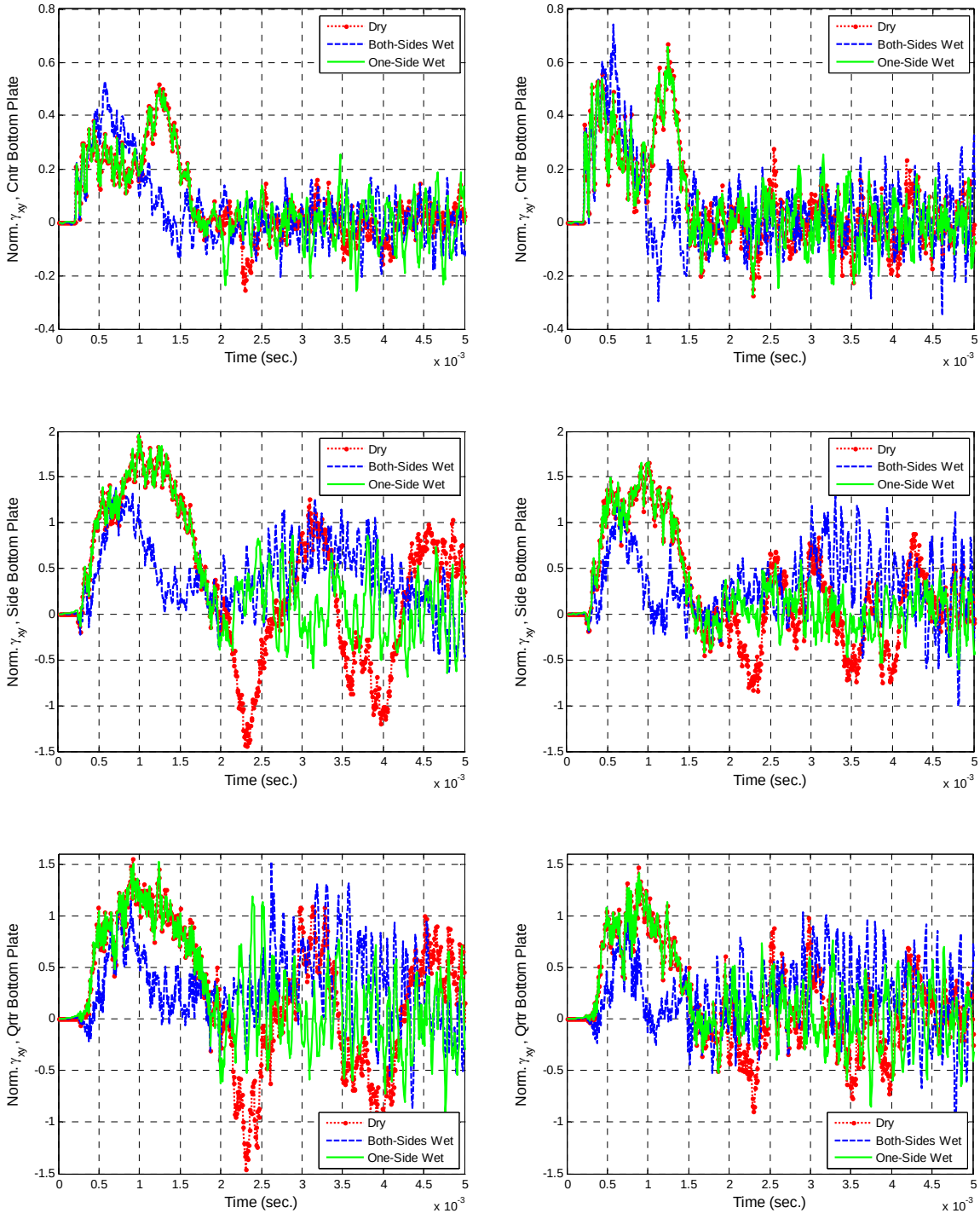

Circular Impact Area Square Impact Area

Figure 42. Shear Strain Comparison of Three Structures Due to Different Impactor Shapes at 10 m/s

Additional figures comparing the response between the square and circular faced impactor are contained in Appendix H. These additional figures highlight the FSI differences for the two different shapes of impactor for the two-sides wet and one-side wet structures by normalizing each to their respective dry structure response. To summarize, FSI slightly decreases the strain amplitude and frequency of oscillation with the square impactor having a slight increase in frequency and amplitude of oscillation over the circular impactor for both two-sides and one-side wet. The square impactor also has slightly less average energy (strain and kinetic). The strains are nearly the same between the cylinder and square impactor with the square having higher peak strain at center position and comparable for the side and quarter positions. The average strains are roughly the same except for the center position which is higher due to higher peak strain initially.

2. Velocity of Impact

The effect of impact velocity is straight forward; increasing impact velocity gives increased magnitude of plate displacement, strain and kinetic energies. When combining the varying impact velocities with different shaped impactors, there are some slight differences in response. The shift in initial response when comparing the three velocities is due to the time difference required for the impactor to traverse the distance to the composite plate and should not be misinterpreted as a frequency shift.

The response of each of three structures to different initial impact velocities is shown in Appendix I for both circular and square faced impactors. Increasing impact velocity simply increases the response. Generally, the square faced impactor has less amplitude of oscillation and average values for the dry and one-side wet structure and the two-sides wet structure amplitude of oscillation and average value is similar for the two different impactors. The normal strains are comparable with only very slight decrease in amplitude of oscillation for the square impactor for each of the three structures. The shear strain is also similar among the three structures and two impactors for the three impact velocities.

To focus on the FSI effects, each of the impact velocities for the two-sides and one-side wet structures are normalized to a respective dry structure. These normalized responses are shown in Figures 43, 44 and 45 for displacement, strain energy and kinetic energy respectively. Using this normalization, it is clear FSI causes significant decreases in frequency and amplitude range of response. The two-sides wet structure shows decreased peak values while the one-side wet has slightly increased peak values over the strictly dry structure due to effects of the water layer on one side of plate. The square faced impactor has higher relative amplitude of oscillation for displacement, but slightly lower energies than those of circular faced impactor.

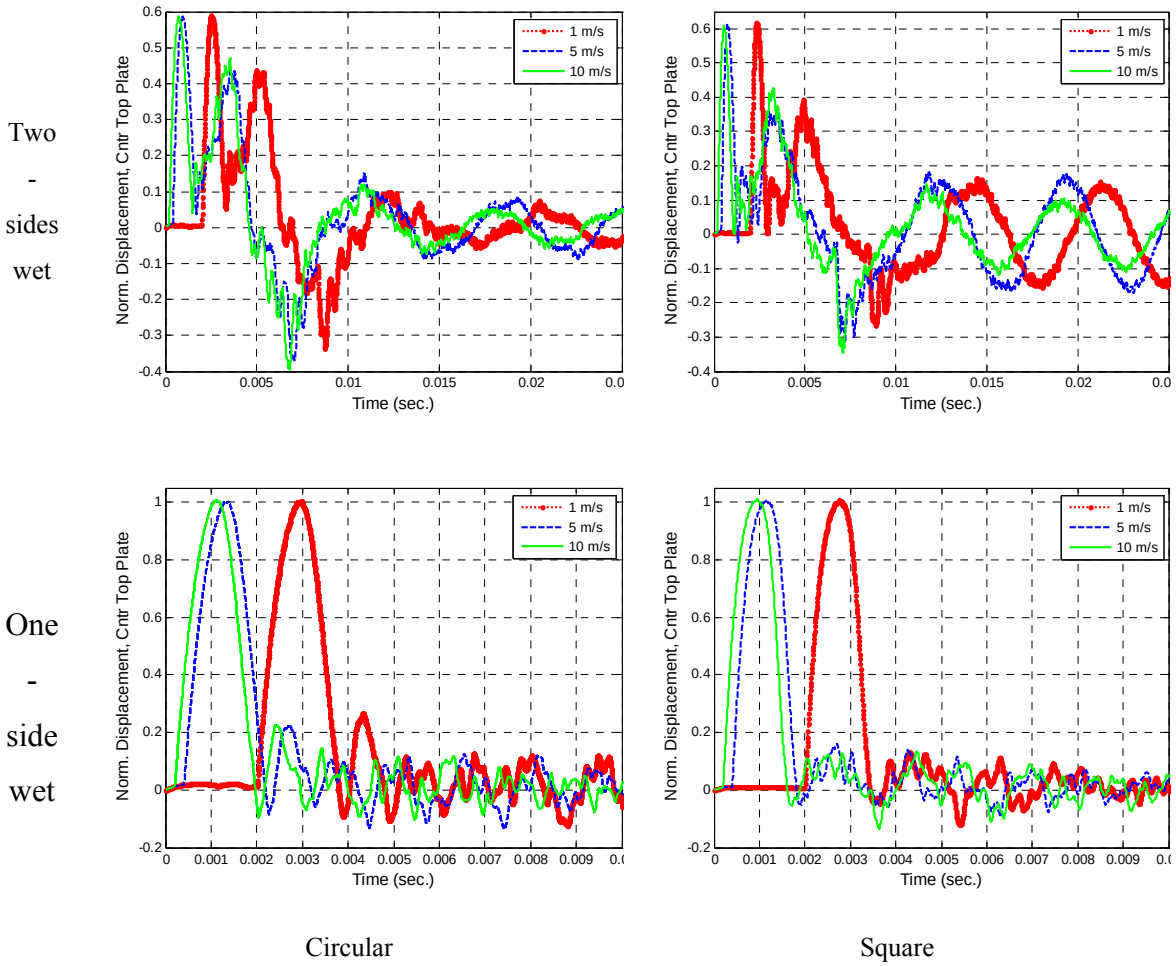

Figure 43. Comparison of Displacement Response Due to Impact Velocity Effects for Circular and Square Faced Impactor

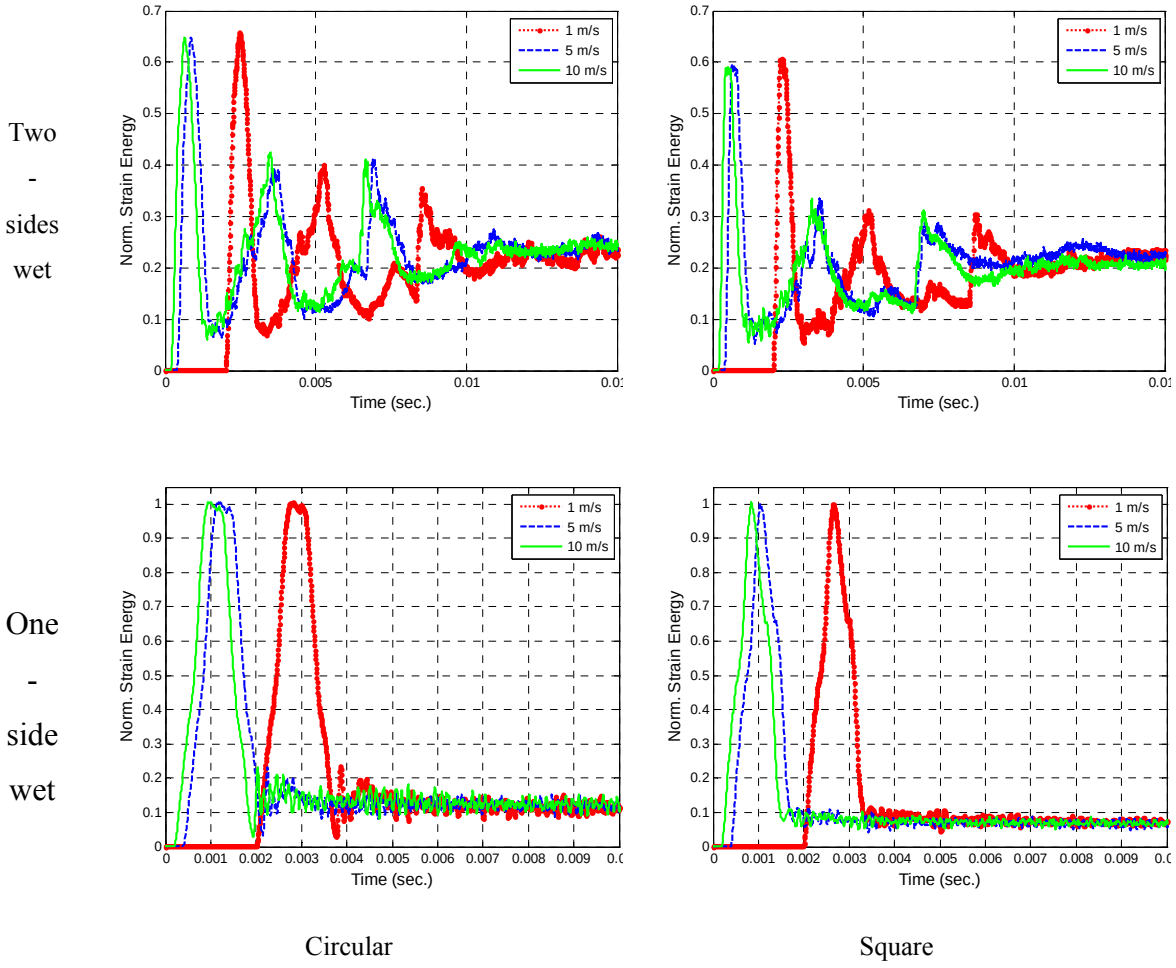

Figure 44. Comparison of Strain Energy Response Due to Impact Velocity Effects for Circular and Square Faced Impactor

The normal and shear strains using the normalization to highlight the FSI effects are shown in Figures 46 and 47, respectively. These figures show the relative magnitudes of strain for all three velocities are similar with the exception of the two-sides wet structure with square face impactor has slightly increased peak strain.

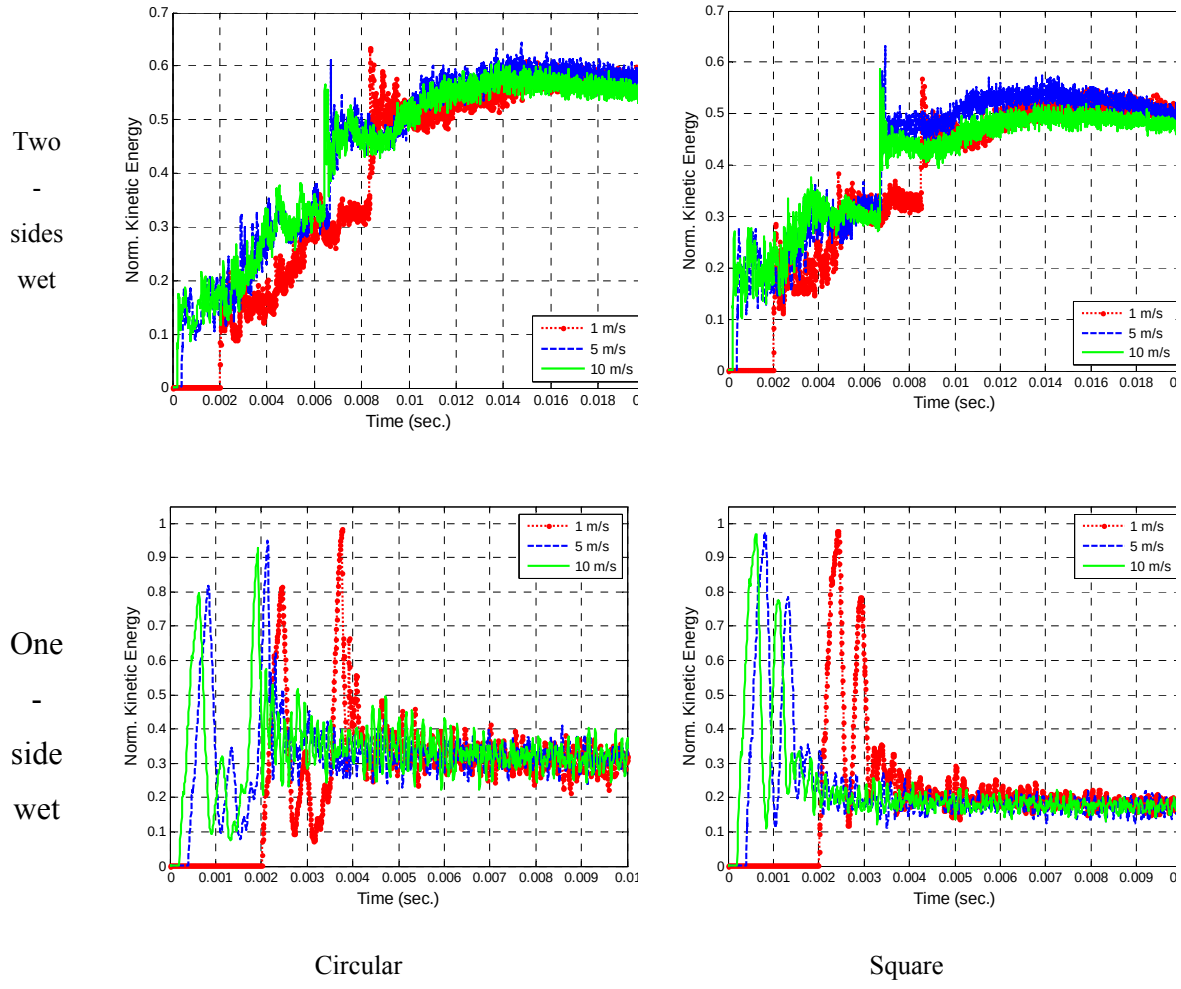

Figure 45. Comparison of Kinetic Energy Response Due to Impact Velocity Effects for Circular and Square Faced Impactor

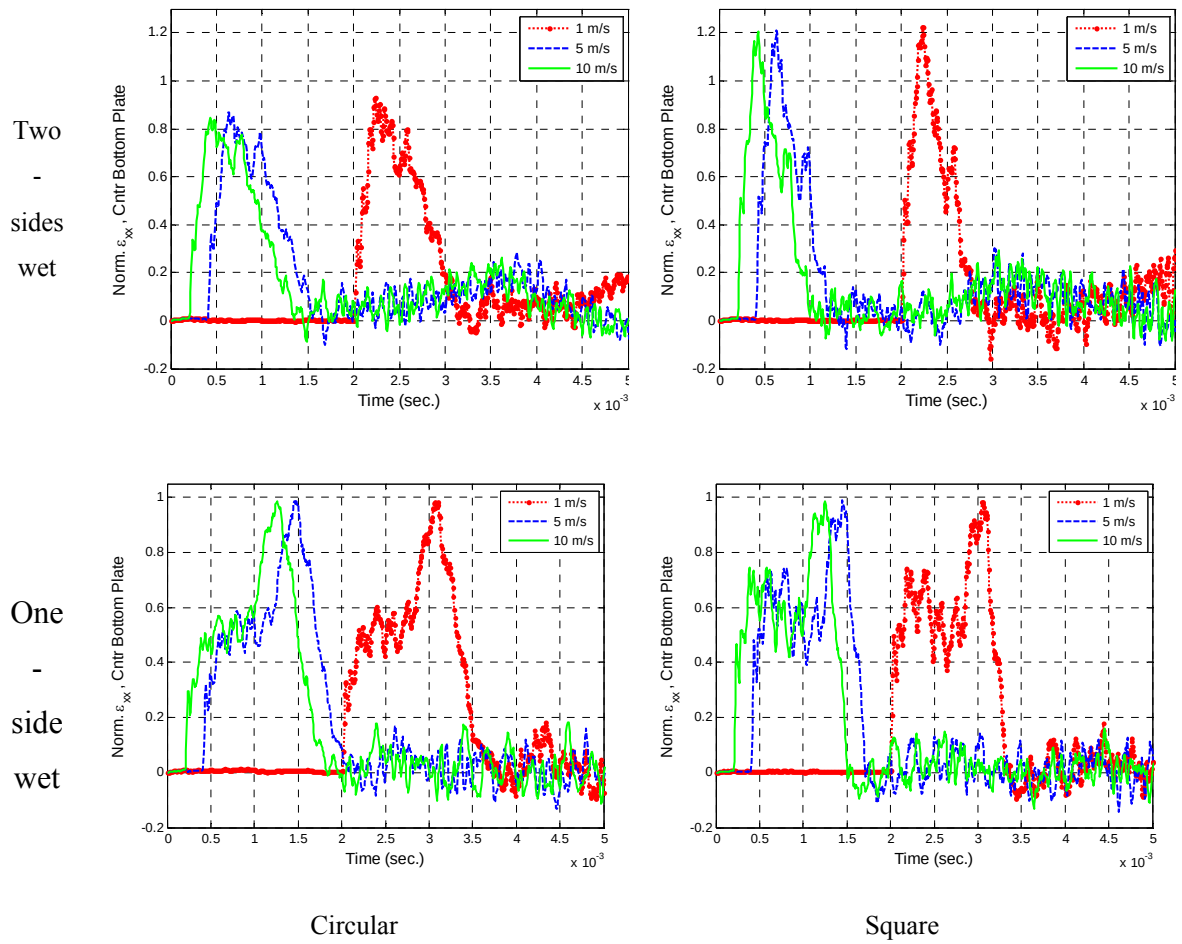

Figure 46. Comparison of Normal Strain Due to Impact Velocity Effects for Circular and Square Faced Impactor

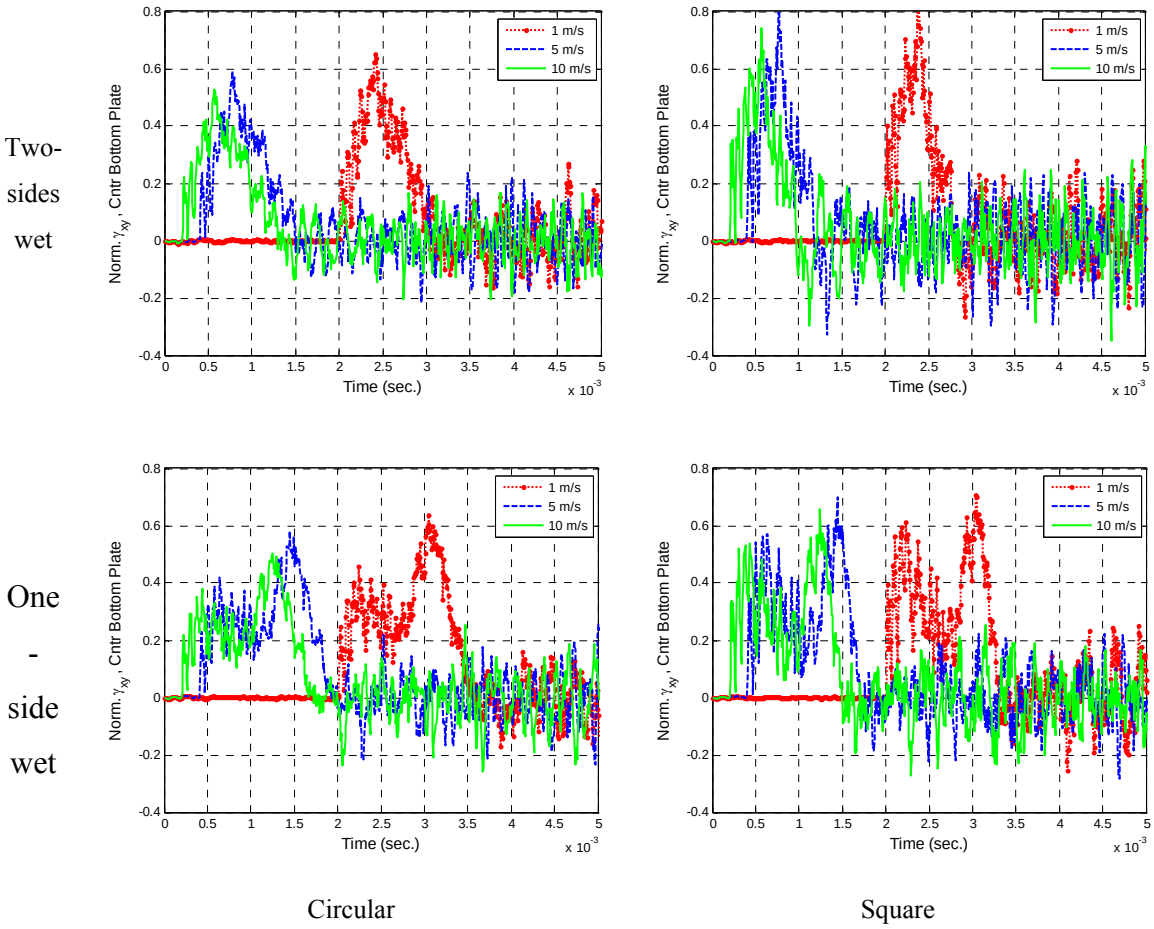

Figure 47. Comparison of Shear Strain Due to Impact Velocity Effects for Circular and Square Faced Impactor

THIS PAGE INTENTIONALLY LEFT BLANK

V. NUMERICAL MODEL COMPARISON TO EXPERIMENT

The principal focus of this work is numerical study of various parameters which affect the dynamic behavior of composite plates. A separate study conducted experimentally examines the behavior of dry and wet plates subjected to impact. Numerical and experimental studies each have their respective advantages and disadvantages and are used to complement each other. In particular, the various parametric studies conducted in this work were only possible utilizing numerical modeling. Experimental testing is limited to measuring forces and strains through gages. Preliminary comparison of experimental and numerical work is noted here to determine methods for improvement to follow on research.

A. EXPERIMENTAL SETUP FOR IMPACT LOADING

Preliminary experimental behavior study of thin composite plates is conducted on 12 inch square and 1/16 inch thick plate clamped in the frame of an impact testing device. The device uses a weighted sled system to strike a cylindrical impactor. Multiple impacts are prevented using a large spring opposing the cylindrical impactor such that only one impact event takes place. There is a force measuring gage mounted on the end of the cylindrical impactor to measure the force during contact with the composite plate. The schematic of the experimental device setup is shown in Figure 48. The underside of the composite plate is instrumented with strain gages, bonded to the plate with epoxy, in the layout shown in Figure 49. The strain gages measure approximately 1 cm square. Gage 2 is in the center location for comparison to the numerical model and is directly below impact site. Gages 1 and 4 are representative of a side location similar to the numerical model and gages 3 and 5 are similar to the quarter location. The data acquisition software measures the transient force and strain data at 1000 Hz sampling rate.

B. NUMERICAL MODEL

The $1/16^{th}$ inch thick, 12 inch by 12 inch composite plate is modeled using shell elements with a mesh seed of 60 nodes per side. The mesh size is chosen to adequately approximate the impact force gage area and strain gage size reasonably. The impact

force measured experimentally is converted to equivalent pressure and applied to elements approximating a cylindrical impactor striking the plate. In the numerical model, stress is computed and strains are calculated using standard stress-strain transformation equations. The strain over the area of the numbered experimental strain gages is calculated by averaging the elements which approximate the size of the strain gage to compare with the experimentally measured strains.

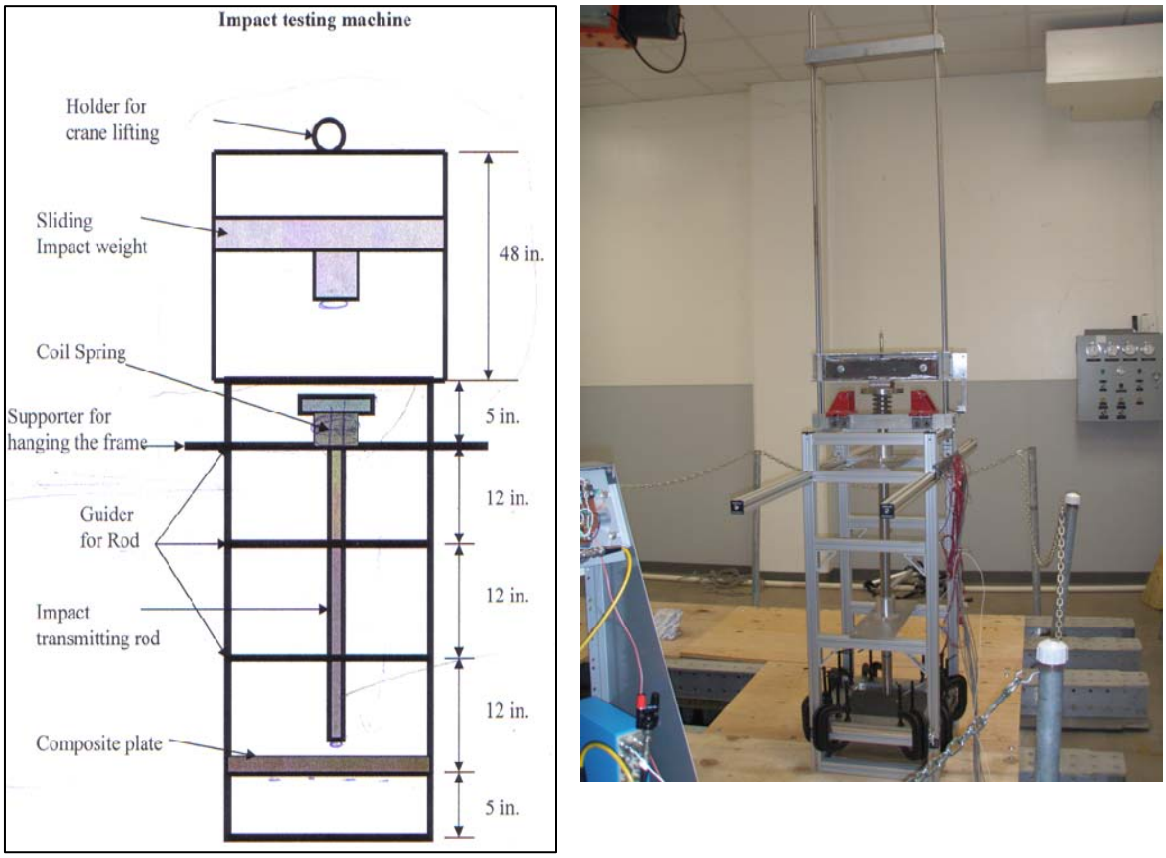

(a) Schematic (b) As-built

Figure 48. Impact Device Experimental Setup

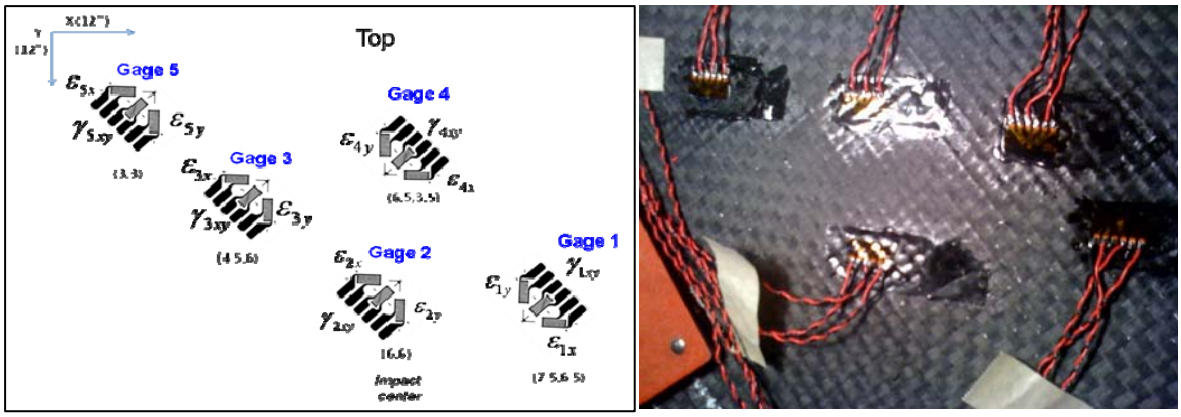

(a) Strain Gage Layout (b) Actual Composite Plate

Figure 49. Experiment Strain Gage Layout on Underside of Composite Plate (Dimensions in parenthesis are given in inches)

C. COMPARISON OF EXPERIMENTAL AND NUMERICAL RESULTS

One of the challenges experimental work presents when measuring strains is getting a good bond between the strain gages and the composite plate. Another is having the strain gages aligned perfectly with the direction of fibers in the composite and minimizing the area of the gage covering the matrix which forms the composite. The experiment is conducted in a one-side wet scenario using an anechoic tank to minimize water disturbance effects, with the side opposite of impact on the composite plate kept dry through a plexi-glass box bound to the underside of the composite plate. The experiment is also run in a completely dry condition. Both dry and wet cases use the same impact force by dropping the weighted sled from full height, giving the steel impact rod roughly a 5 m/s initial velocity. The experiments were first conducted in the wet condition and then dry. Following the wet experiments it was identified that the strain gage labeled Gage 1 had broken free from the composite plate and hence was not available for the dry experiment.

The comparison of normal strain for gage 1 location, between the experiment and simplified Finite Element model is shown in Figure 50. As shown, there is not a good comparison between the experiment and model results for the one-side wet condition (note that the strain gage fell off prior to dry experiment and there is no experimental data

to compare). Because the strain gage fell off after the wet experiment, the data shown is possibly erroneous due to the strain gage disbonding and any comparison at the gage 1 location is suspect.

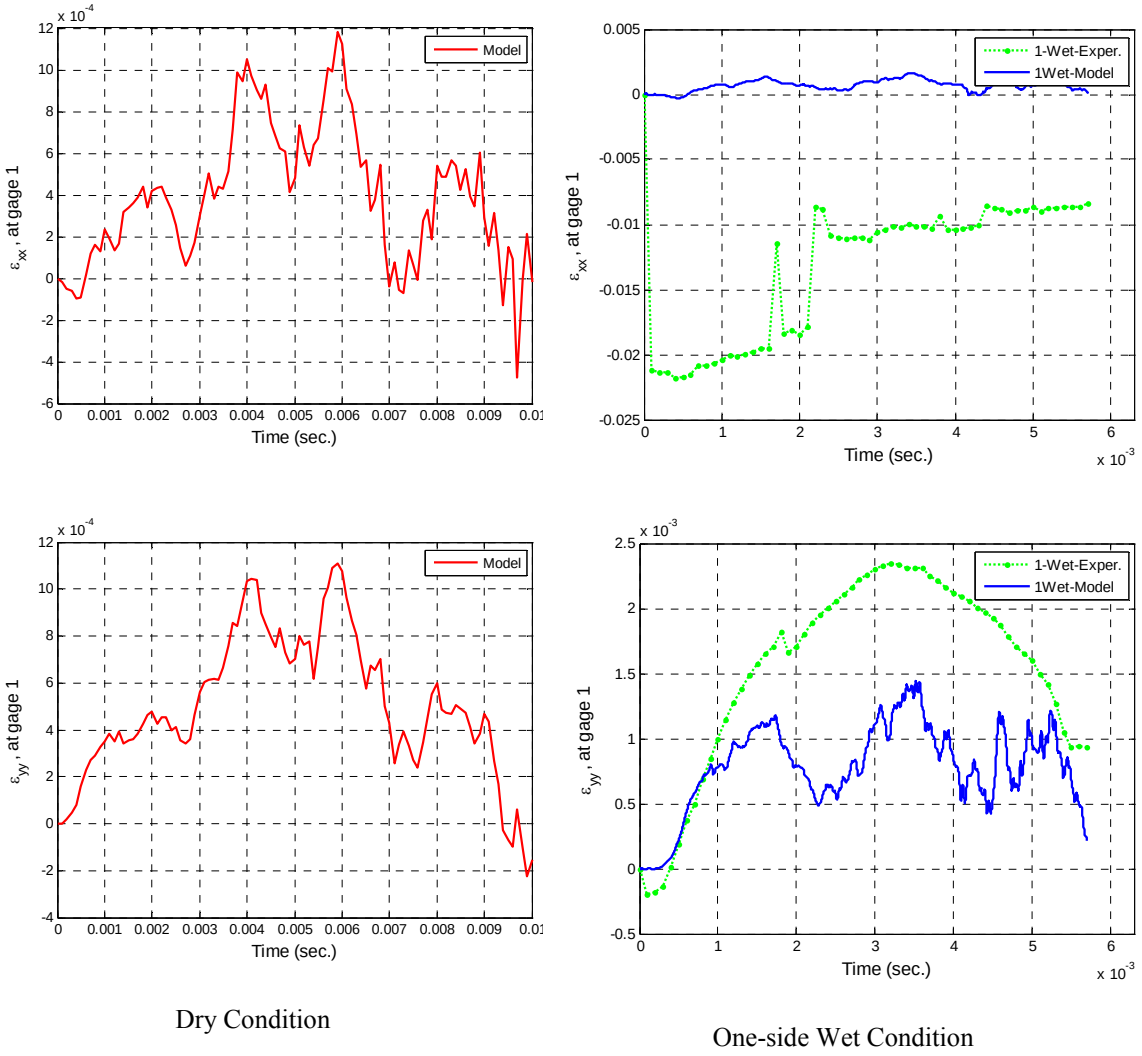

Figure 50. Comparison of Normal Strain at Gage 1 Location Between Experiment and FEM in Dry and One-side Wet Condition

The comparison of normal strain for gage 2 location, between the experiment and simplified FEM model is shown in Figure 51. As shown, the comparisons between the experiment and model results are quite good for both the one-side wet and dry condition. This good agreement between the experiment and numerical model is evidence of the feasibility to accurately predict composite plate response using finite element models.

This gives more flexibility for researchers as many more parameters can be varied with a numerical model. The fact that the x-axis model strain is higher than the experiment and the y-axis is lower is an indication there may be some misalignment of the strain gage with the fiber direction. If this is the case, some improvement can be obtained through use of a Mohr Circle transformation.

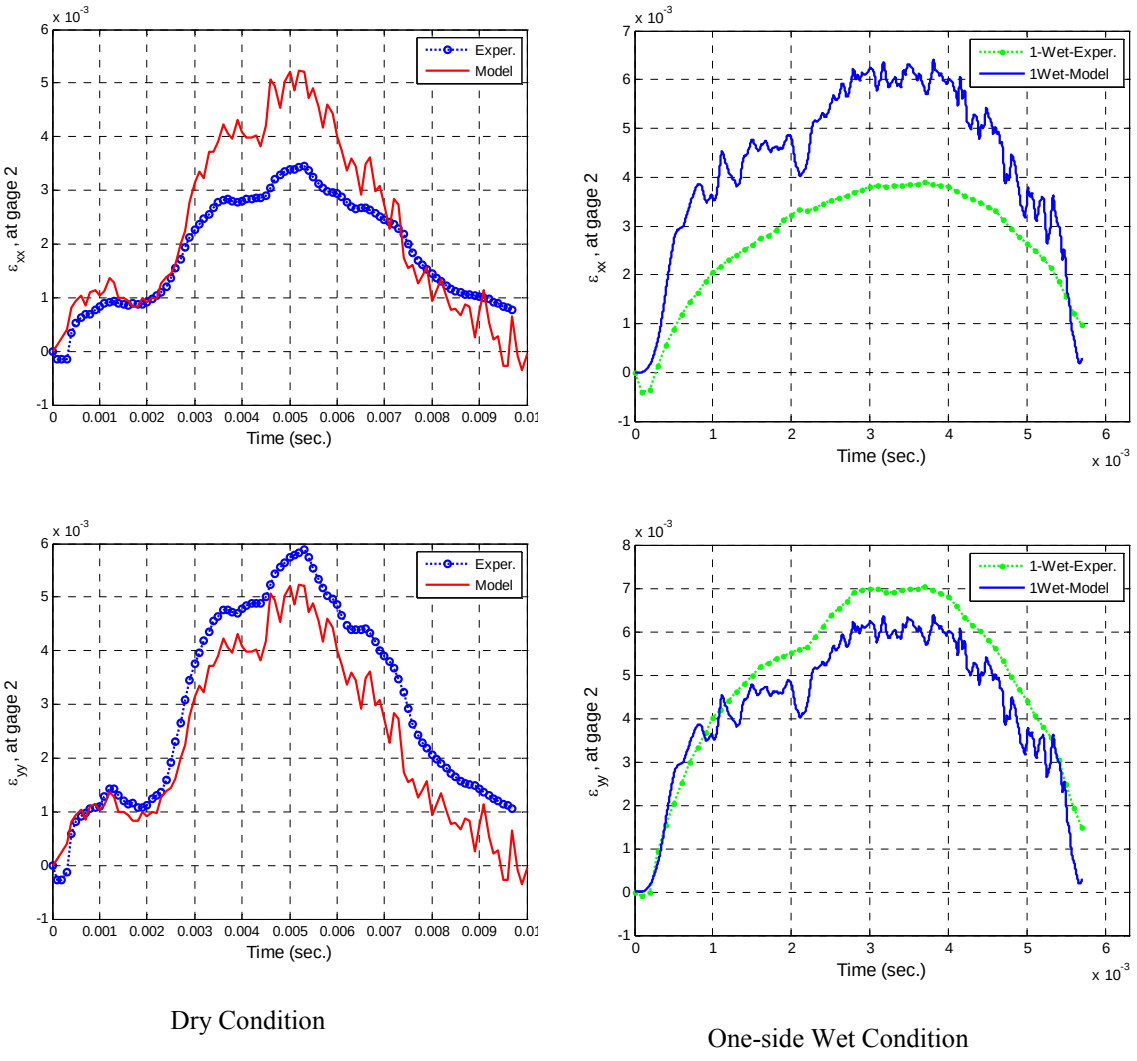

Dry Condition

One-side Wet Condition

Figure 51. Comparison of Normal Strain at Gage 2 Location Between Experiment and FEM in Dry and One-side Wet Condition

The comparison of normal strain for the gage 3 location, between the experiment and simplified FEM model is shown in Figure 52. As shown, the comparisons between the experiment and model results are quite good for the dry condition but not the one-side

wet condition. Use of Mohr Circle transf ormation m ay i mprove the dry com parison. What is encouraging is the trend between e xperiment and model tr acks. Unfortunately, there is not a good explanation of why the dr y condition is in such good agreem ent but the one-side wet condition is not.

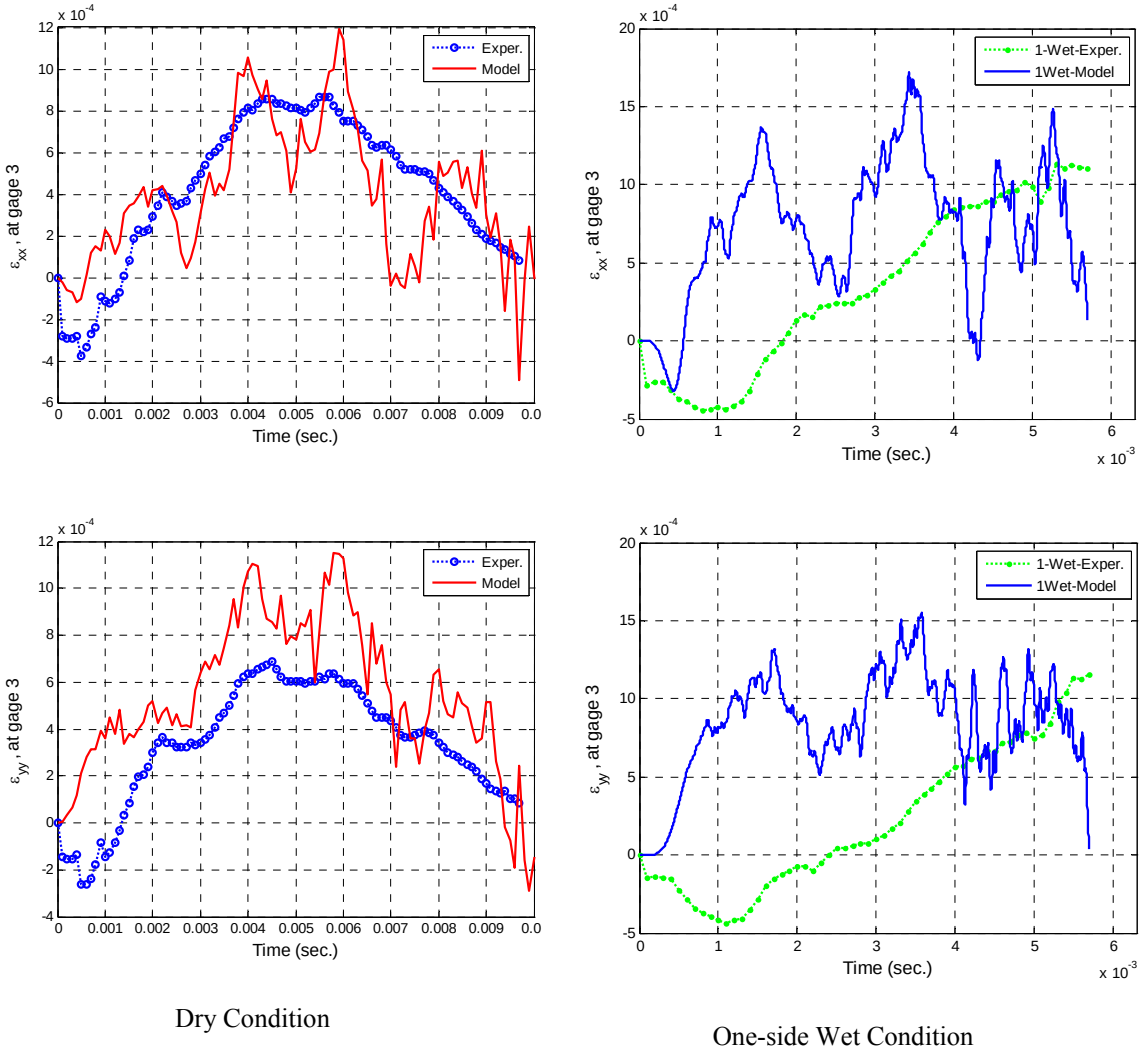

Dry Condition

One-side Wet Condition

Figure 52. Comparison of Normal Strain at Gage 3 Location Between Experiment and FEM in Dry and One-side Wet Condition

The comparison of normal strain for gage 4 location, between the experim ent and simplified FEM m odel is shown in Figure 53. As shown, there is good agreem ent between the experiment and m odel results f or the dry cond ition and th e trends agree for

the one-side wet condition, although the m agnitudes are off. Again a Mohr Circle transformation could improve the dry and wet comparison.

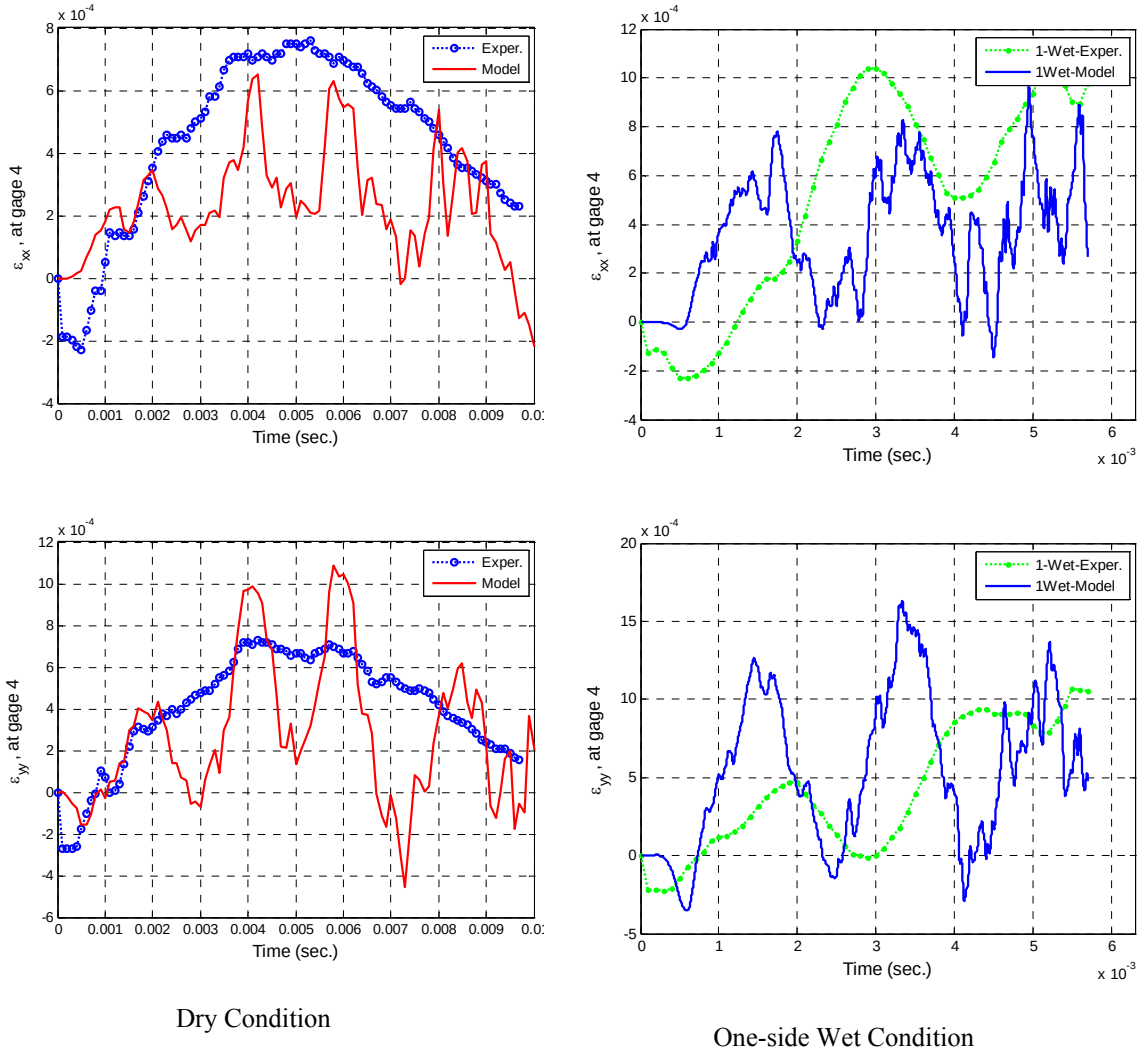

Dry Condition

One-side Wet Condition

Figure 53. Comparison of Normal Strain at Gage 4 Location Between Experiment and FEM in Dry and One-side Wet Condition

The comparison of normal strain for gage 5 location, between the experim ent and simplified FEM m odel is shown in Figure 54. As shown, the trends between the experiment and m odel are sim ilar, but the magnitudes are not, and application of Mohr Circle will not im prove the va lues as both the x-axis and y- axis normal strains are over predicted in the numerical model.

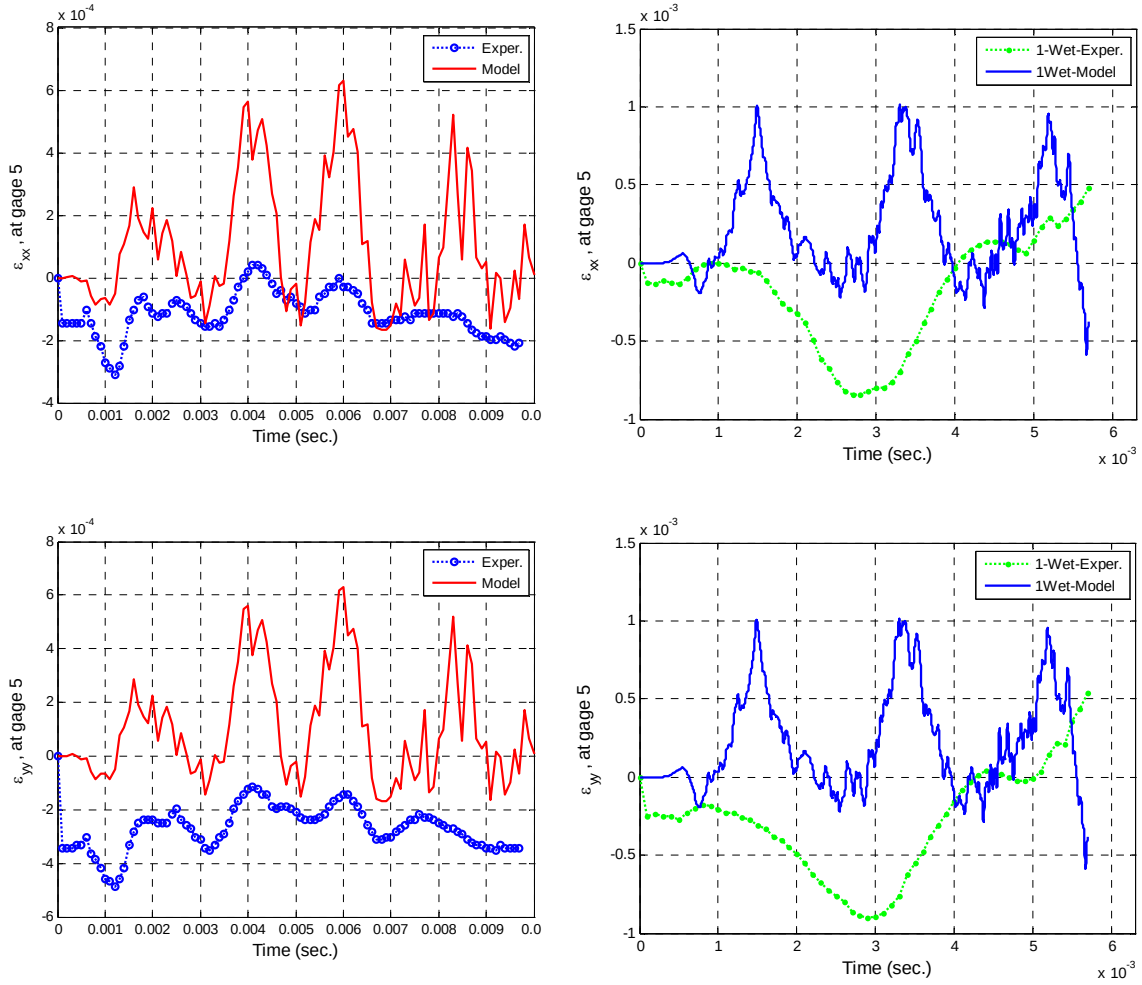

Figure 54. Comparison of Normal Strain at Gage 5 Location Between Experiment and FEM in Dry and One-side Wet Condition

In summary, the strain in the vicinity of impact, at gage 2 location, compares very well between model and experiment. Moving away from impact location either to side or quarter location results in less agreement between the experiment and model. This indicates that proper strain gage alignment with fiber direction and good bonding over fiber vice matrix is important. Other things to consider in future work are altering the element size in the model and adjusting the quantity of elements used in averaging to determine the strain at a gage location for comparison to the experimental data.

VI. CONCLUDING REMARKS AND RECOMMENDATIONS

Thin composite plate structures were examined under various conditions to investigate the effect of FSI on dynamic behaviors. Overall, water influenced significantly both kinetic and strain energies of the composite structures by greatly reducing their magnitudes and frequencies. The FSI greatly suppressed the oscillatory nature of dynamic responses of the structures. Whether a structure is wet on one-side or two-sides, the FSI effect was very clear even though the two-sides wet structures showed a greater FSI effect.

The boundary condition, either clamped or simple, has similar behaviors and is thereby not a significant contributor for FSI. The size and shape of the composite plates was shown to have minor differences in FSI. The method of loading the plate, either concentrated force, uniform pressure or impact, showed some difference on the degree of FSI. Interestingly, the shape of the impacting object (contact shape) gave different degrees of FSI for equivalent impact velocities. The largest variation of FSI was due to differences in material properties such as density and elastic modulus. As a result, it is critical to understand and incorporate the FSI effects when designing reliable composite structures employed in an underwater environment.

Future work should examine the dynamic behavior of composites which include moisture absorption effects. Additionally, various types of composites should be compared for determination of the best response behavior properties and minimal moisture absorption. Finally, both numerical and experimental work should be conducted to monitor composite behavior in failure. The failure modes should be investigated as to whether they are matrix or fiber failure, delamination or a mixture of failure modes.

THIS PAGE INTENTIONALLY LEFT BLANK

APPENDIX A: ADDITIONAL FIGURES FOR CLAMPED AND SIMPLE BOUNDARY WITH CONCENTRATED FORCE LOAD

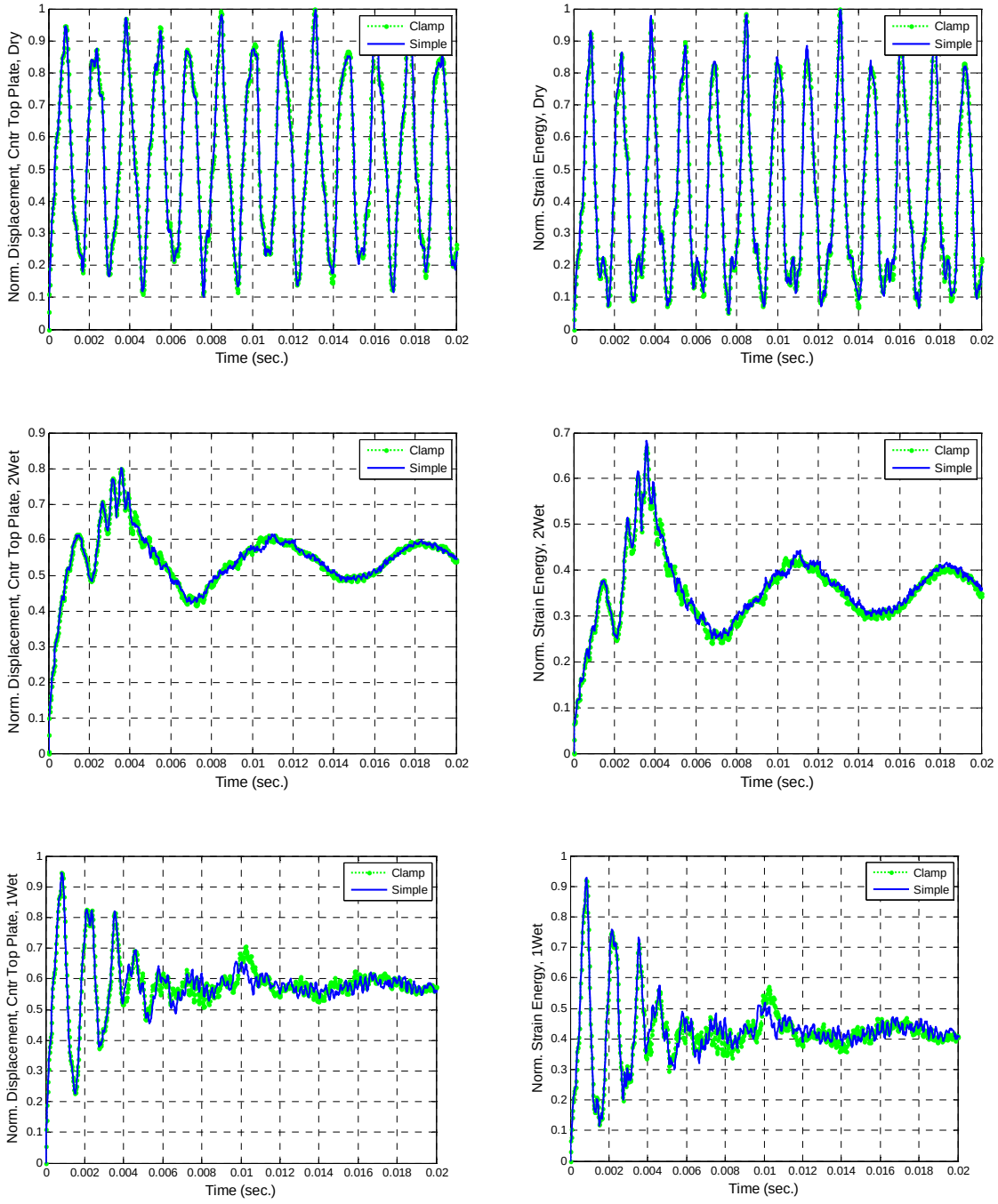

Figure 55. Displacement and Strain Energy Comparison of Clamped and Simple Boundary with Concentrated Force Load

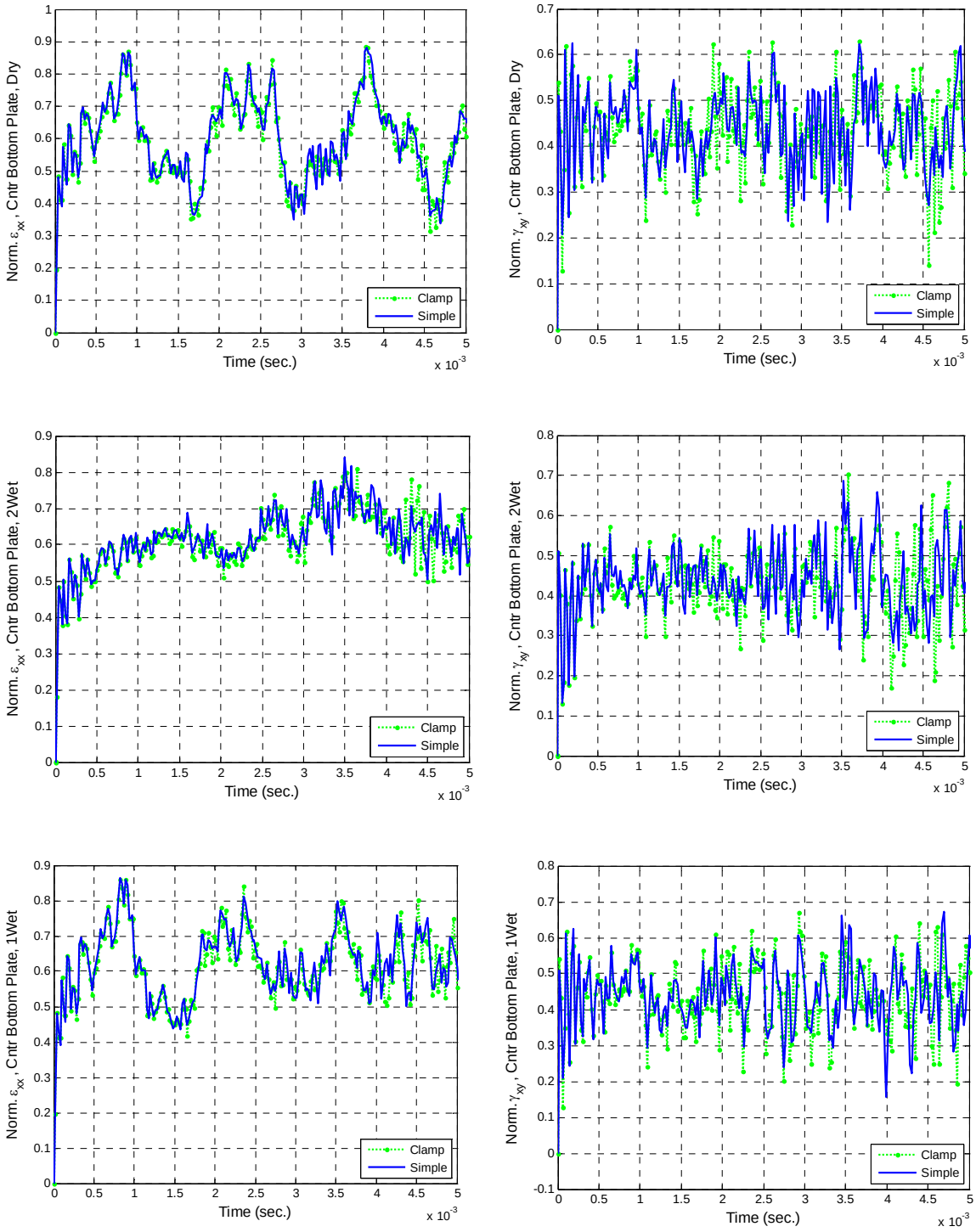

Figure 56. Normal and Shear Strain Comparison at Center Position for Clamped versus Simple Boundary with Concentrated Force Load

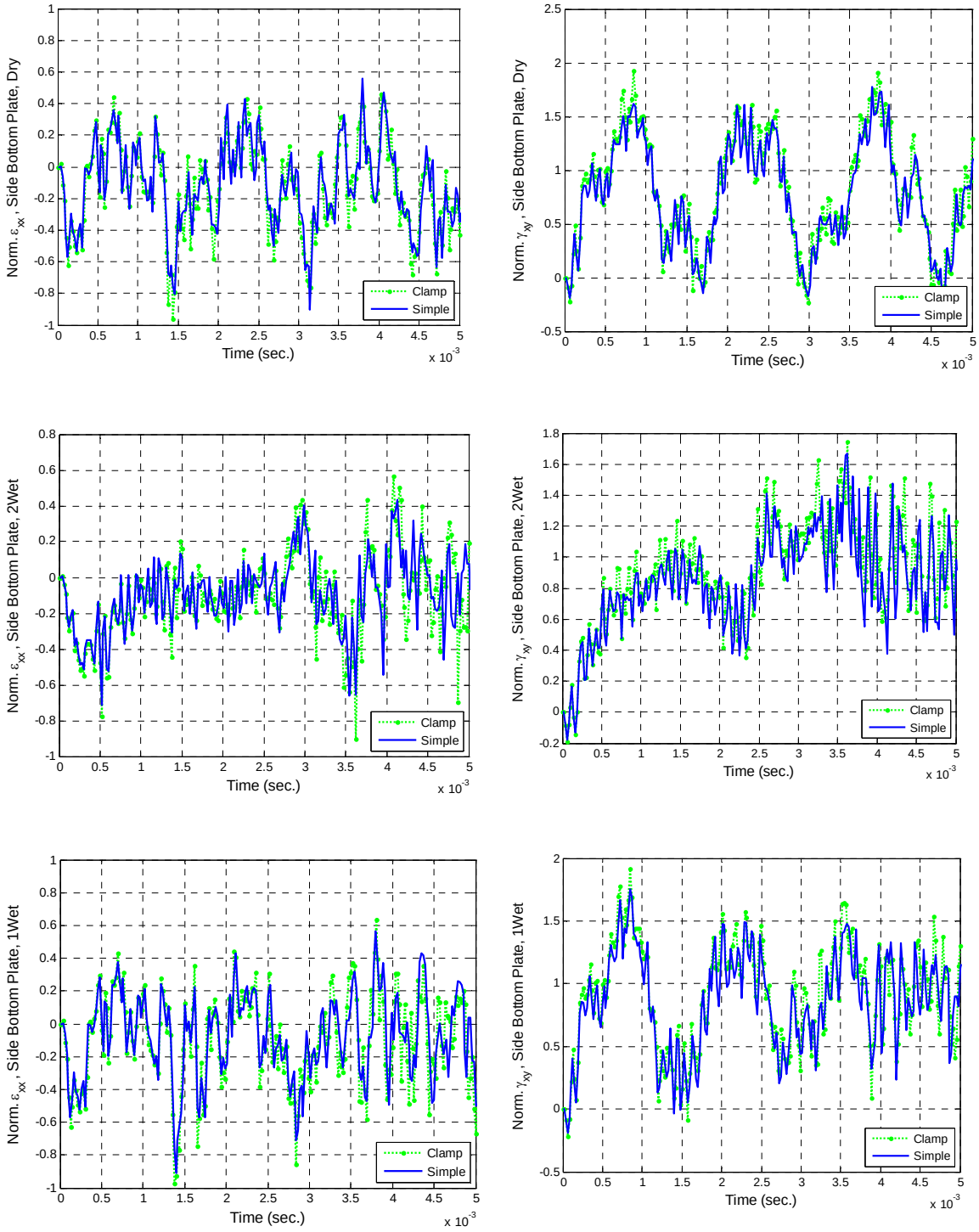

Figure 57. Normal and Shear Strain Comparison at Side Position for Clamped versus Simple Boundary with Concentrated Force Load

THIS PAGE INTENTIONALLY LEFT BLANK

APPENDIX B: ADDITIONAL FIGURES FOR FORCE AND PRESSURE LOAD COMPARISON WITH CLAMPED BOUNDARY

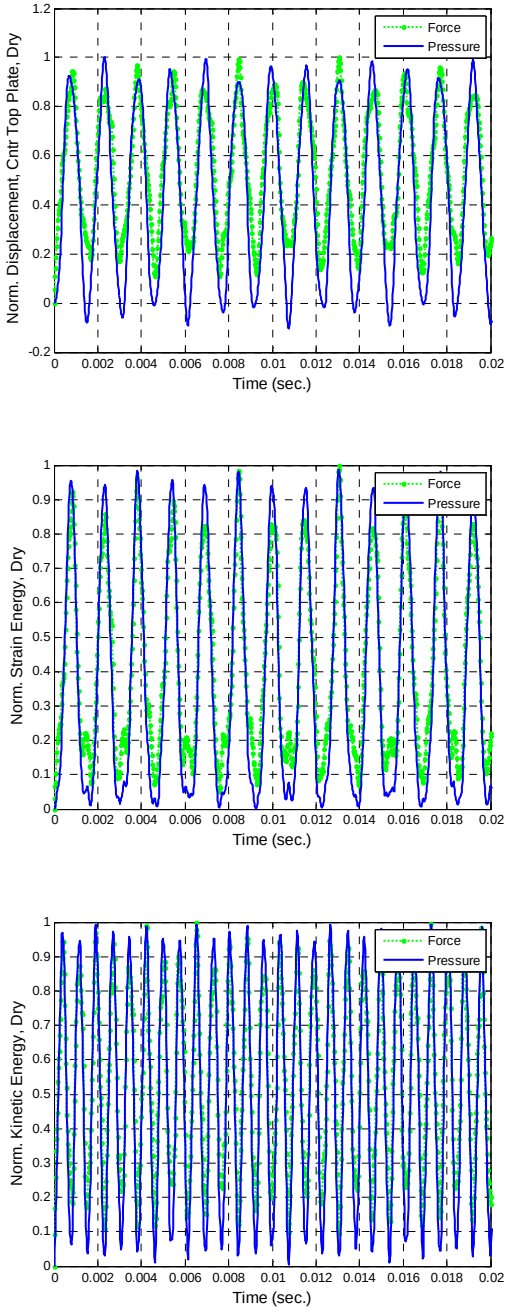

Figure 58. Comparison of Dry Structure Response for Displacement, Strain and Kinetic Energies Between Force and Pressure Loading with Clamped Boundary

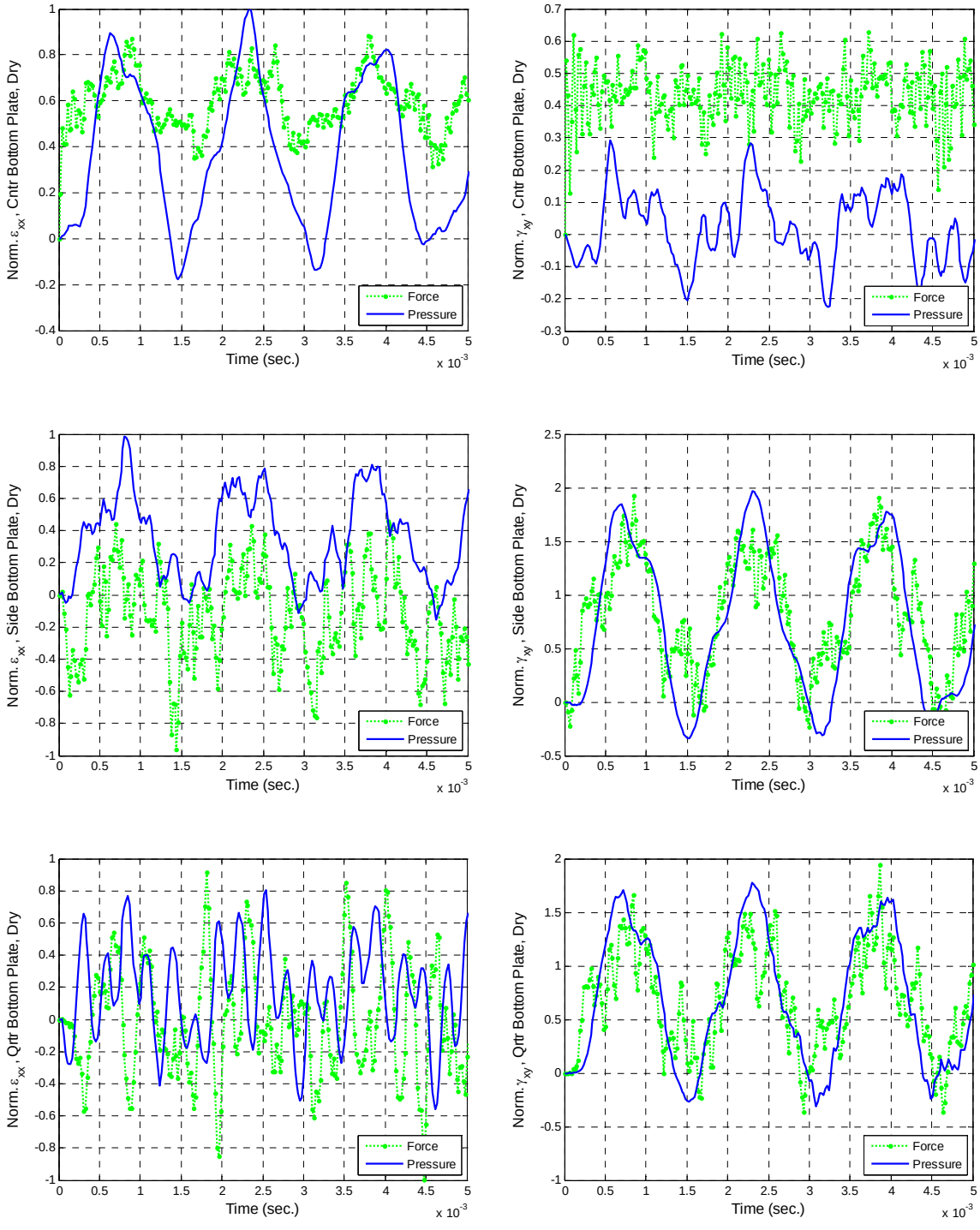

Figure 59. Normal and Shear Strains for Comparison of Dry Structure with Clamped Boundary between Force and Pressure Loading

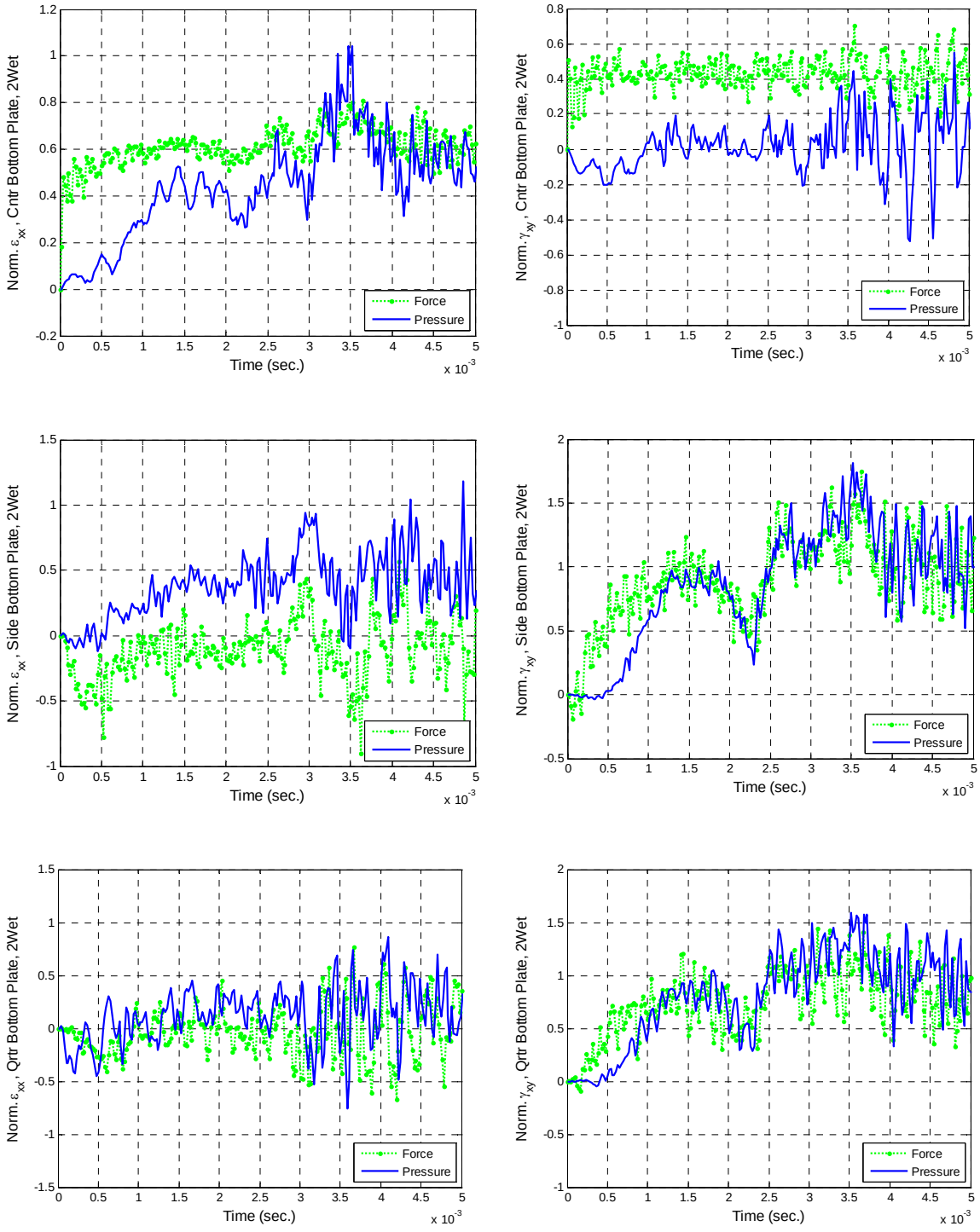

Figure 60. Normal and Shear Strains for Comparison of Two-sides Wet Structure with Clamped Boundary between Force and Pressure Loading

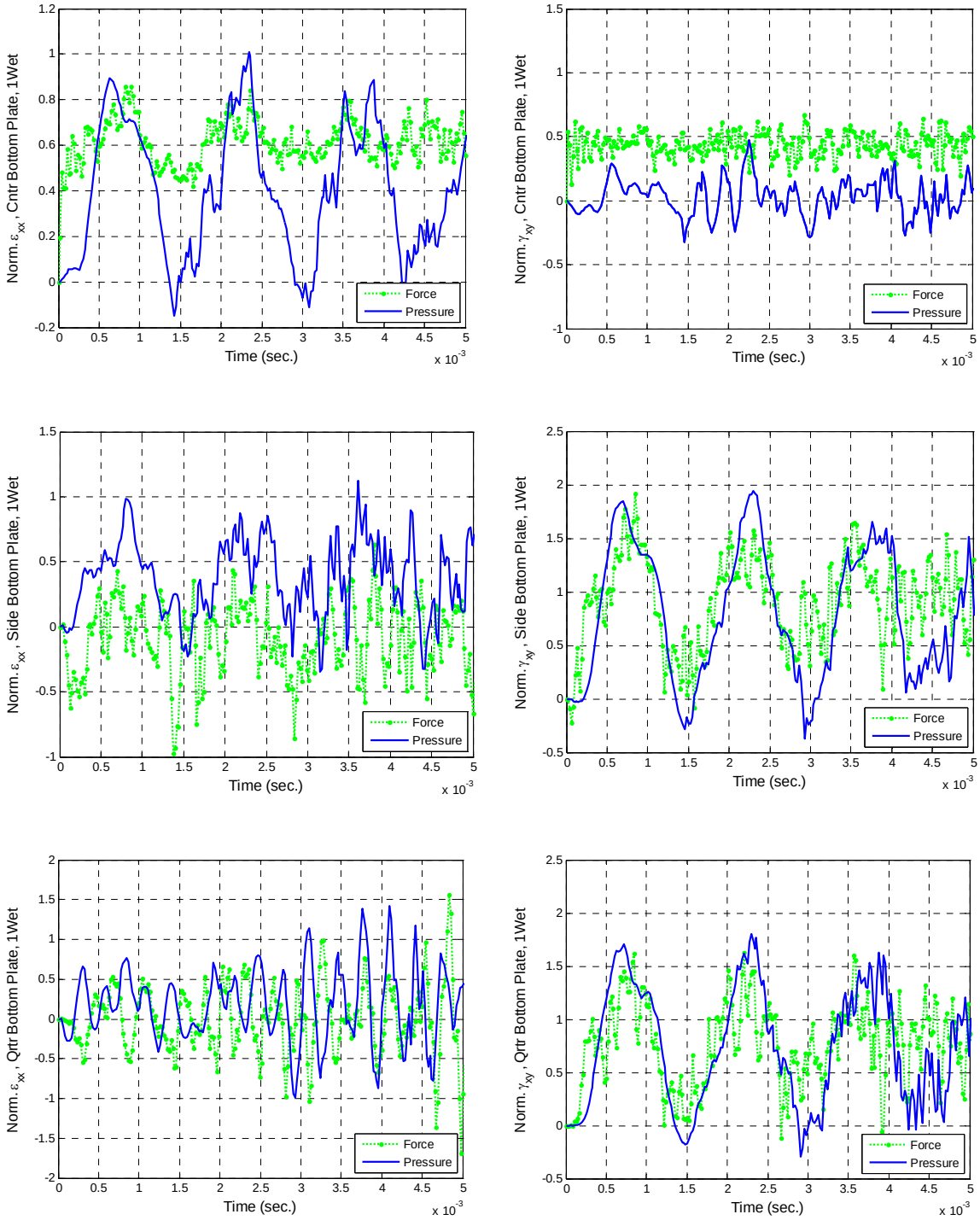

Figure 61. Normal and Shear Strains for Comparison of One-side Wet Structure with Clamped Boundary between Force and Pressure Loading

APPENDIX C: ADDITIONAL FIGURES FOR FORCE AND PRESSURE LOAD COMPARISON WITH SIMPLE BOUNDARY

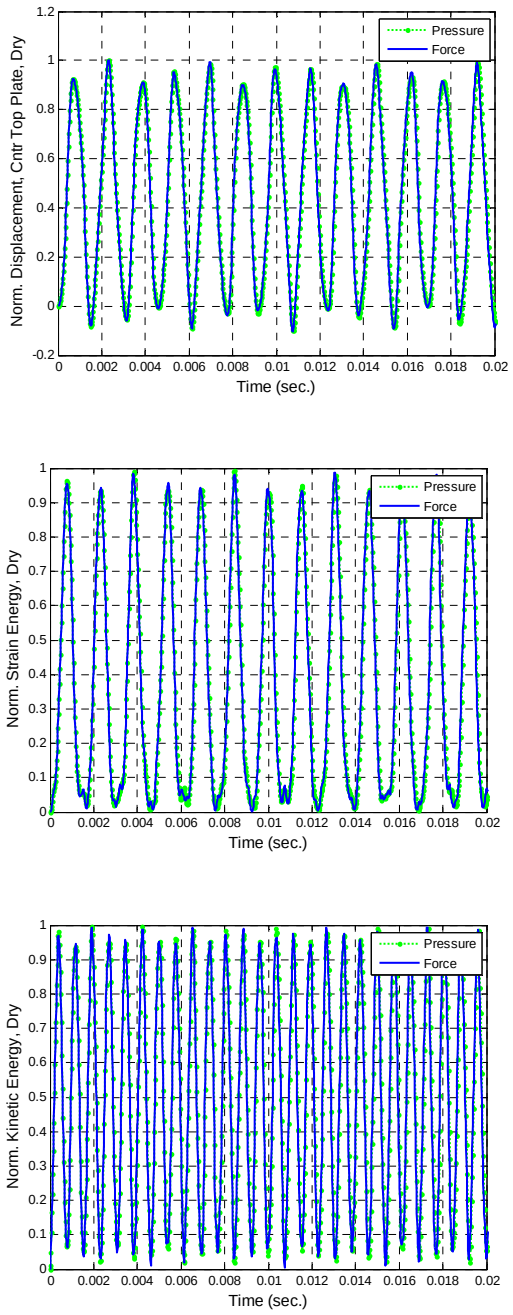

Figure 62. Comparison of Dry Structure Response for Displacement, Strain and Kinetic Energies between Force and Pressure Loading with Simple Boundary

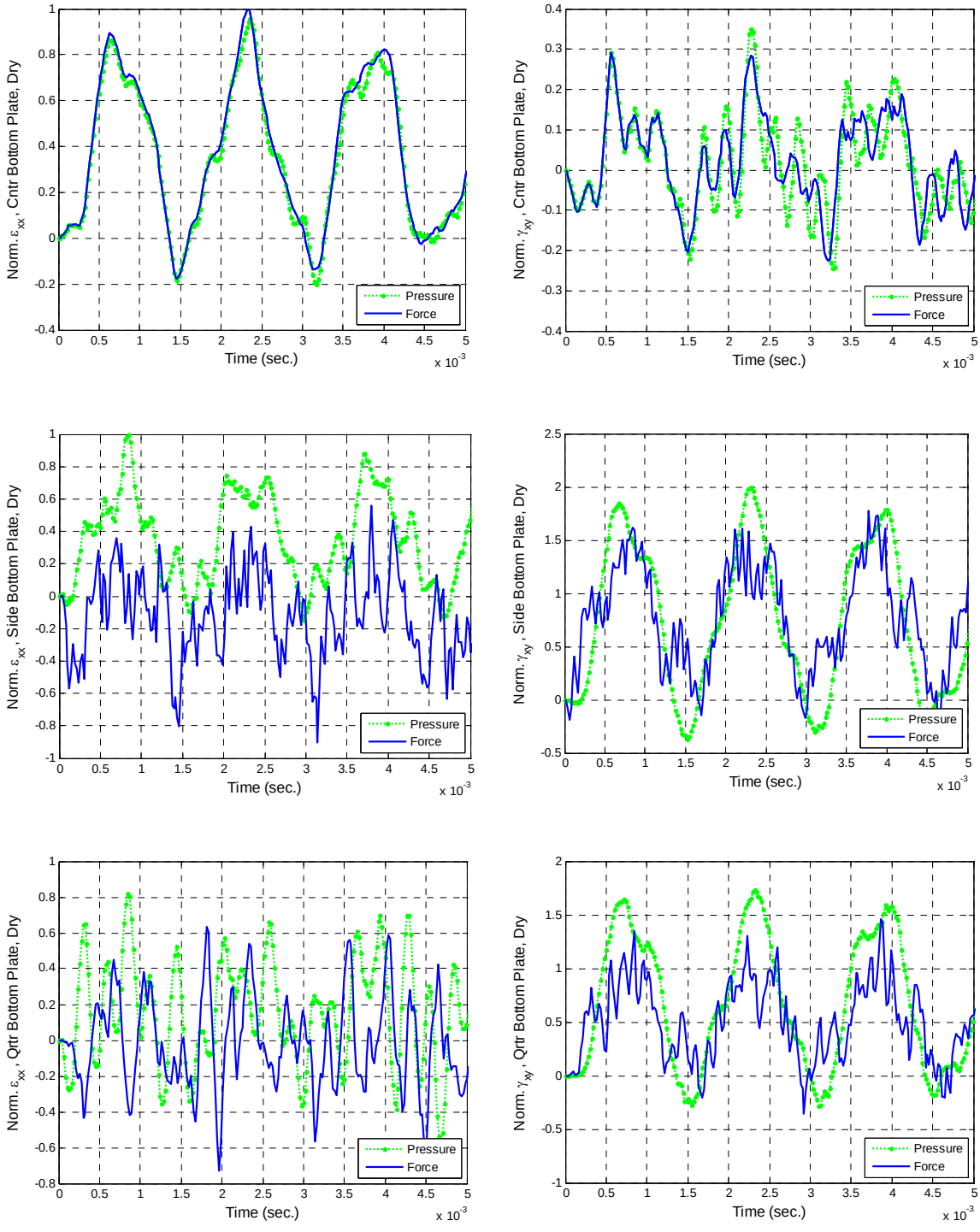

Figure 63. Normal and Shear Strains for Comparison of Dry Structure with Simple Boundary between Force and Pressure Loading

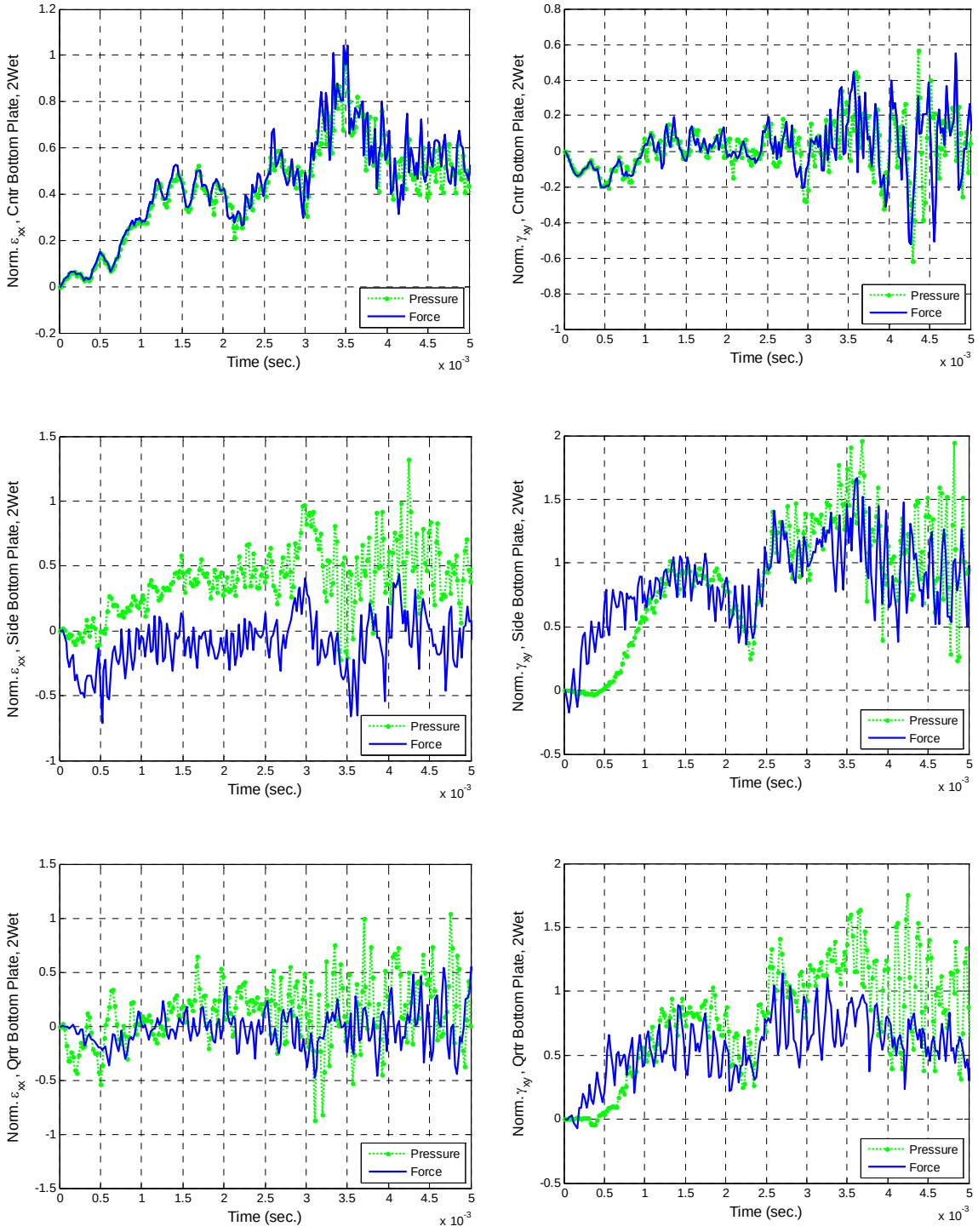

Figure 64. Normal and Shear Strains for Comparison of Two-sides Wet Structure with Simple Boundary between Force and Pressure Loading

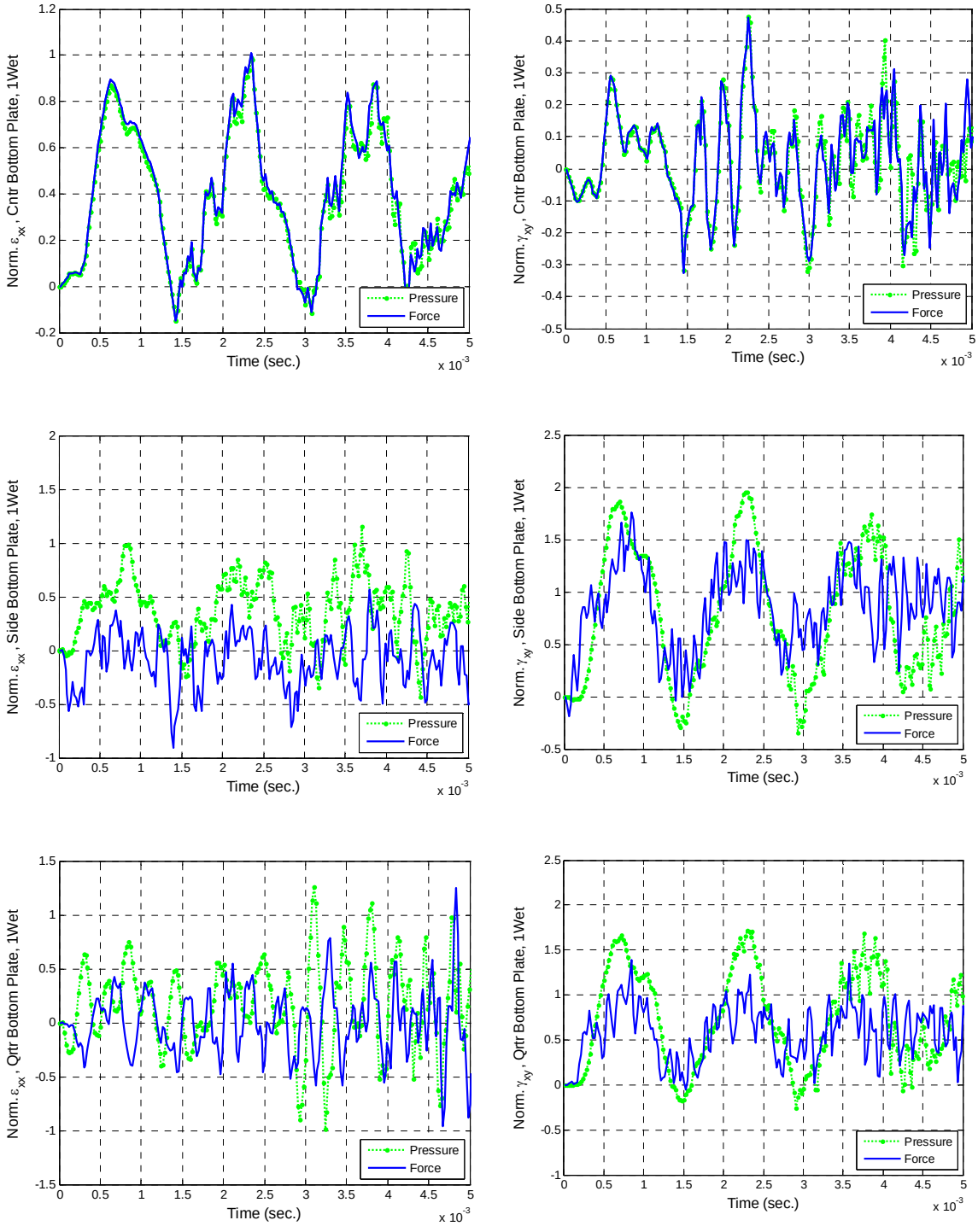

Figure 65. Normal and Shear Strains for Comparison of One-side Wet Structure with Simple Boundary between Force and Pressure Loading

APPENDIX D: ADDITIONAL FIGURES FOR PLATE SIZE EFFECTS WITH CONCENTRATED FORCE LOAD AND CLAMPED BOUNDARY

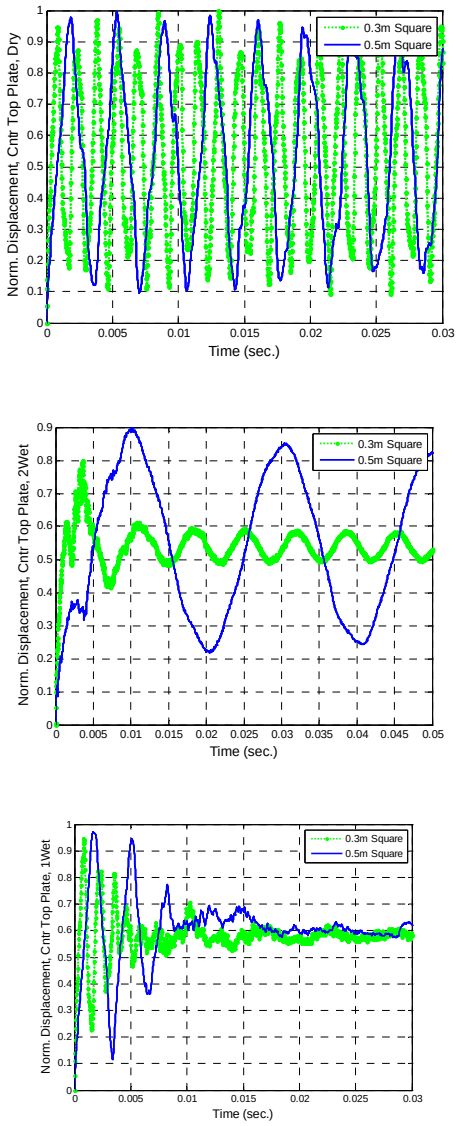

Figure 66. Comparison of Displacement Response for Three Structures Due to Size Variation Effects with Concentrated Force and Clamped Boundary

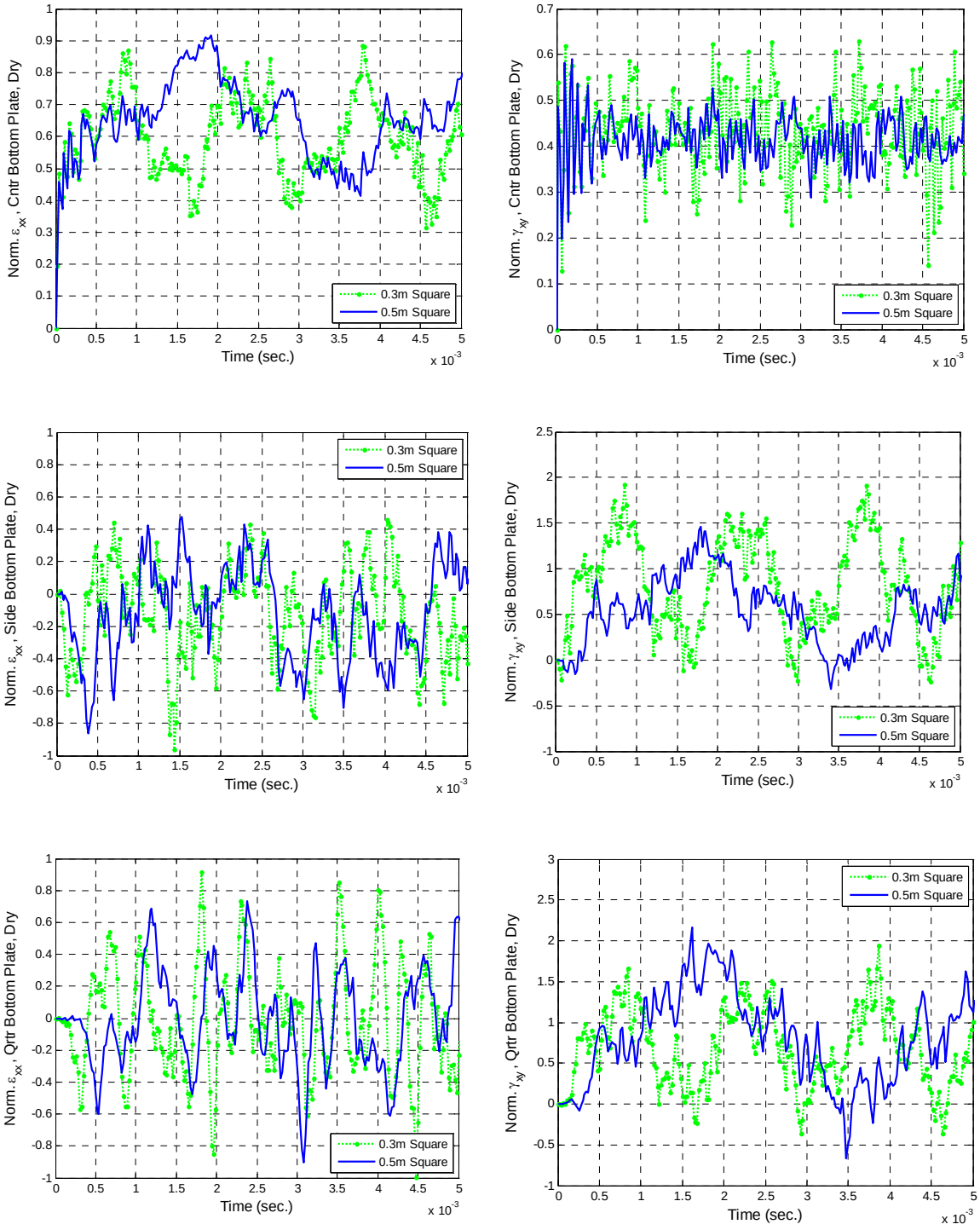

Figure 67. Normal and Shear Strains for Comparison of Differ Plate Sizes for Dry Structure with Concentrated Force and Clamped Boundary

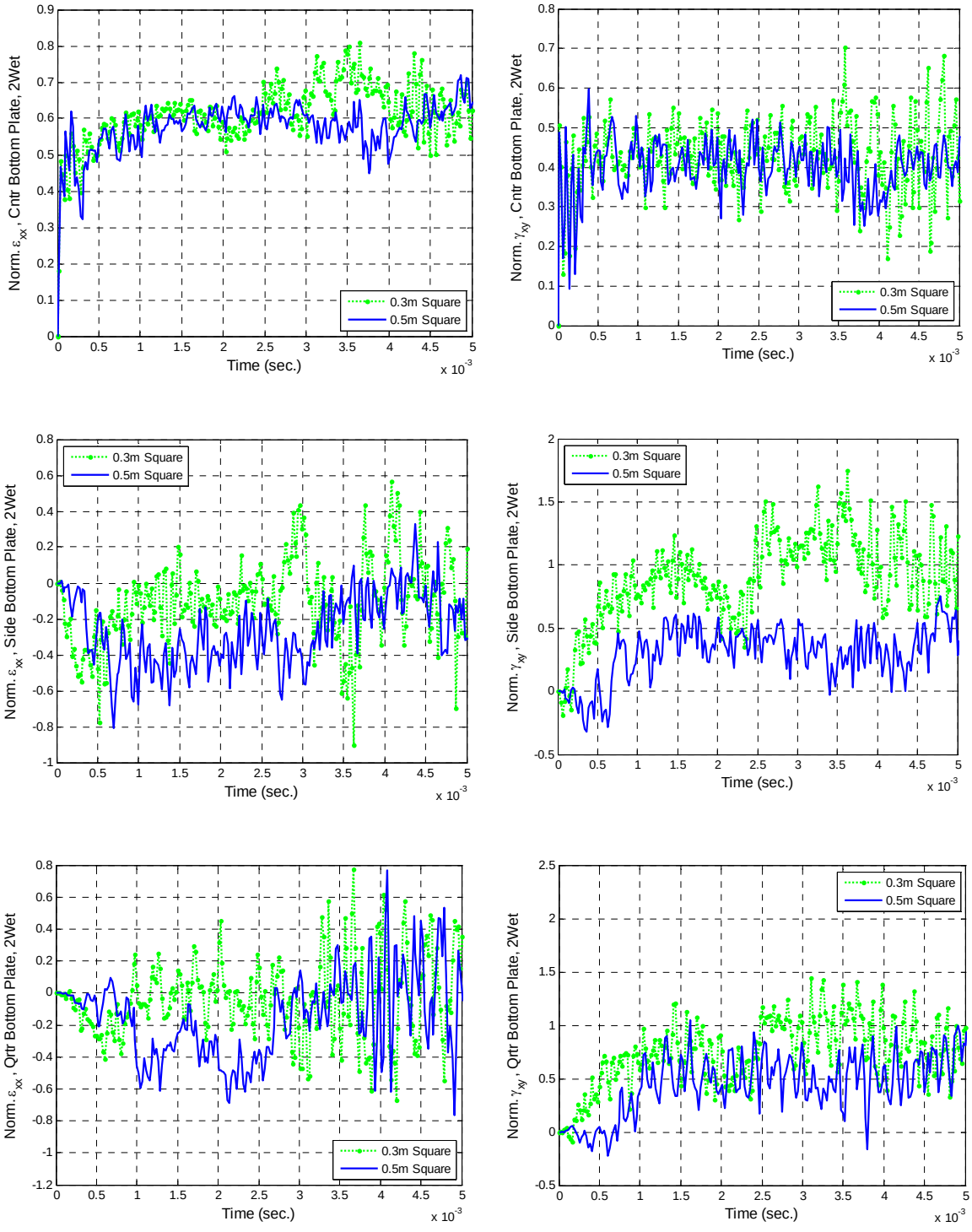

Figure 68. Normal and Shear Strains for Comparison of Differ Plate Sizes for Two-sides Wet Structure with Concentrated Force and Clamped Boundary

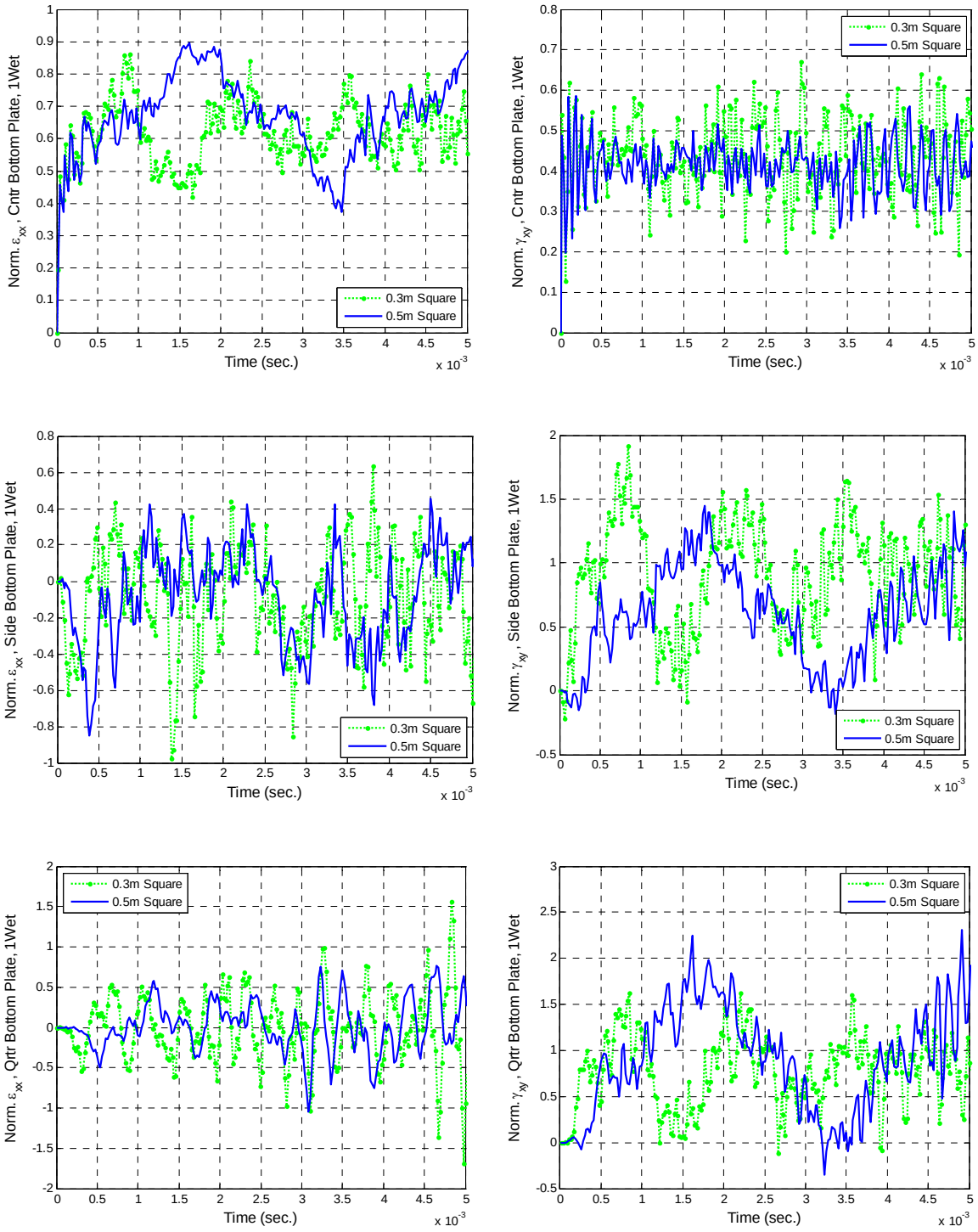

Figure 69. Normal and Shear Strains for Comparison of Differ Plate Sizes for One-side Wet Structure with Concentrated Force and Clamped Boundary

APPENDIX E: ADDITIONAL FIGURES FOR PLATE SHAPE EFFECTS WITH CONCENTRATED FORCE LOAD AND CLAMPED BOUNDARY

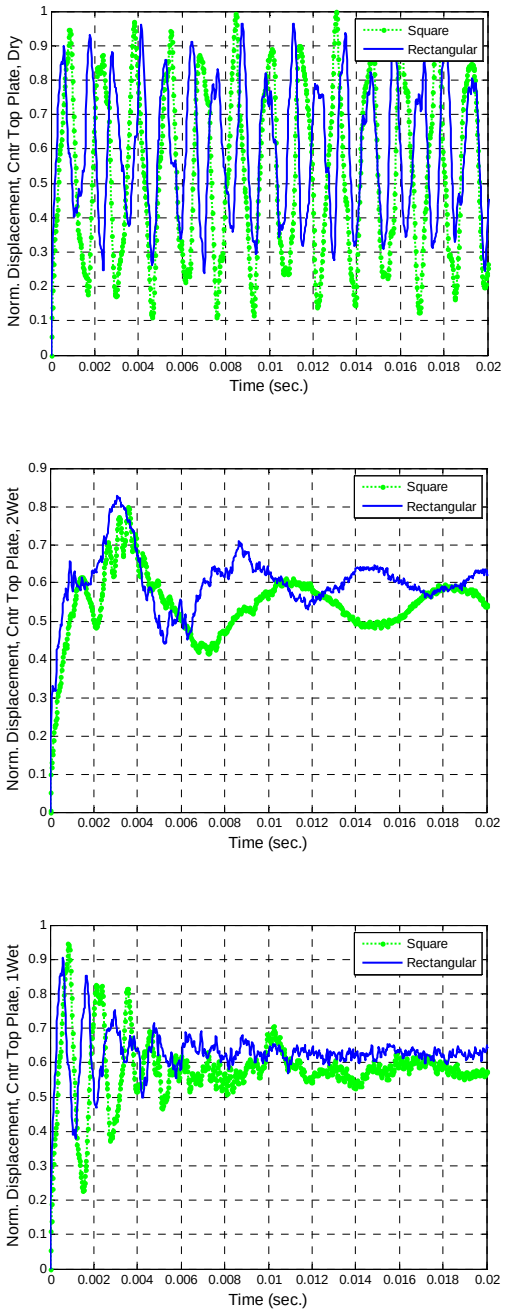

Figure 70. Comparison of Displacement Response for Three Structures Due to Shape Effects with Concentrated Force and Clamped Boundary

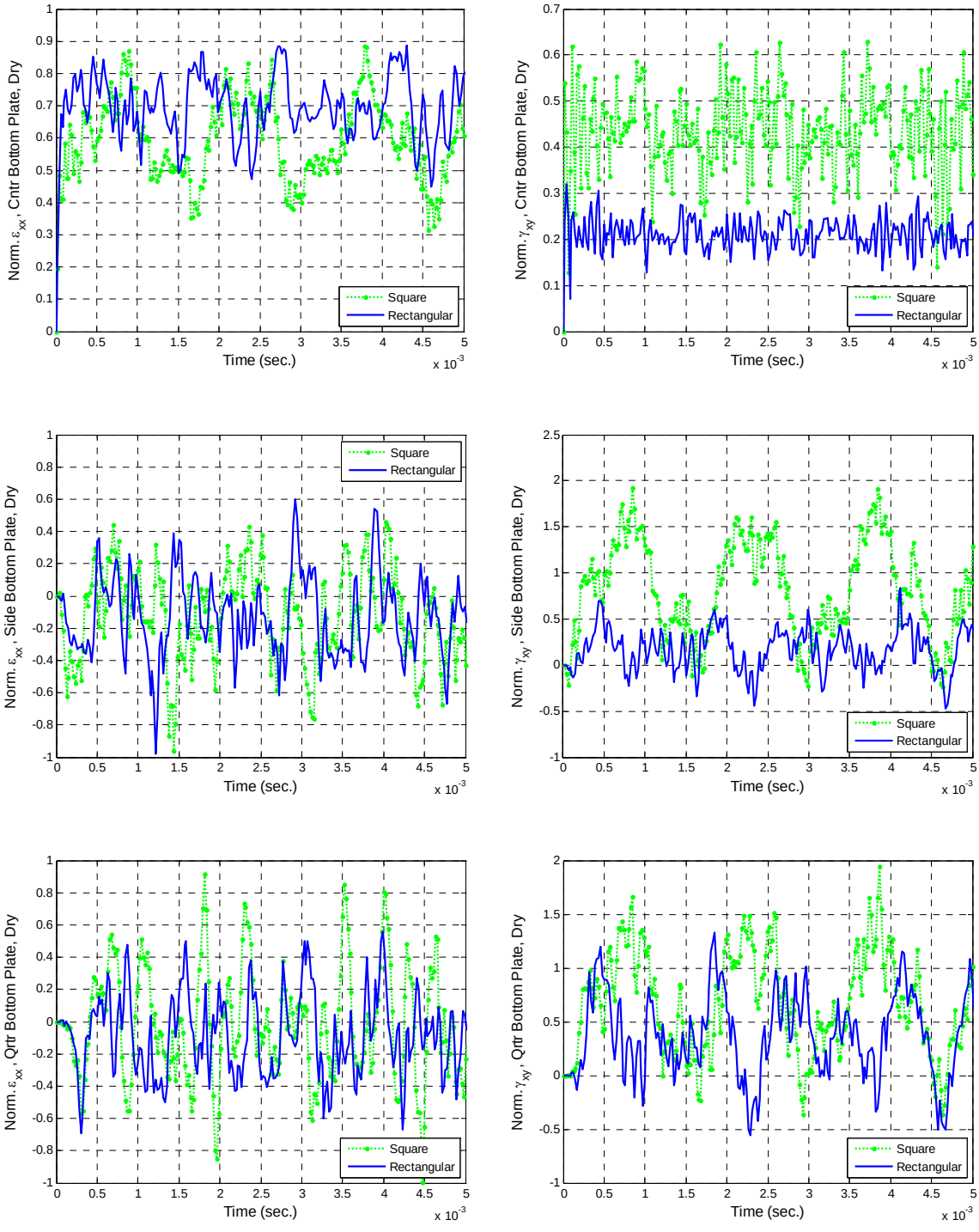

Figure 71. Normal and Shear Strains for Comparison of Differ Plate Shapes for Dry Structure with Concentrated Force and Clamped Boundary

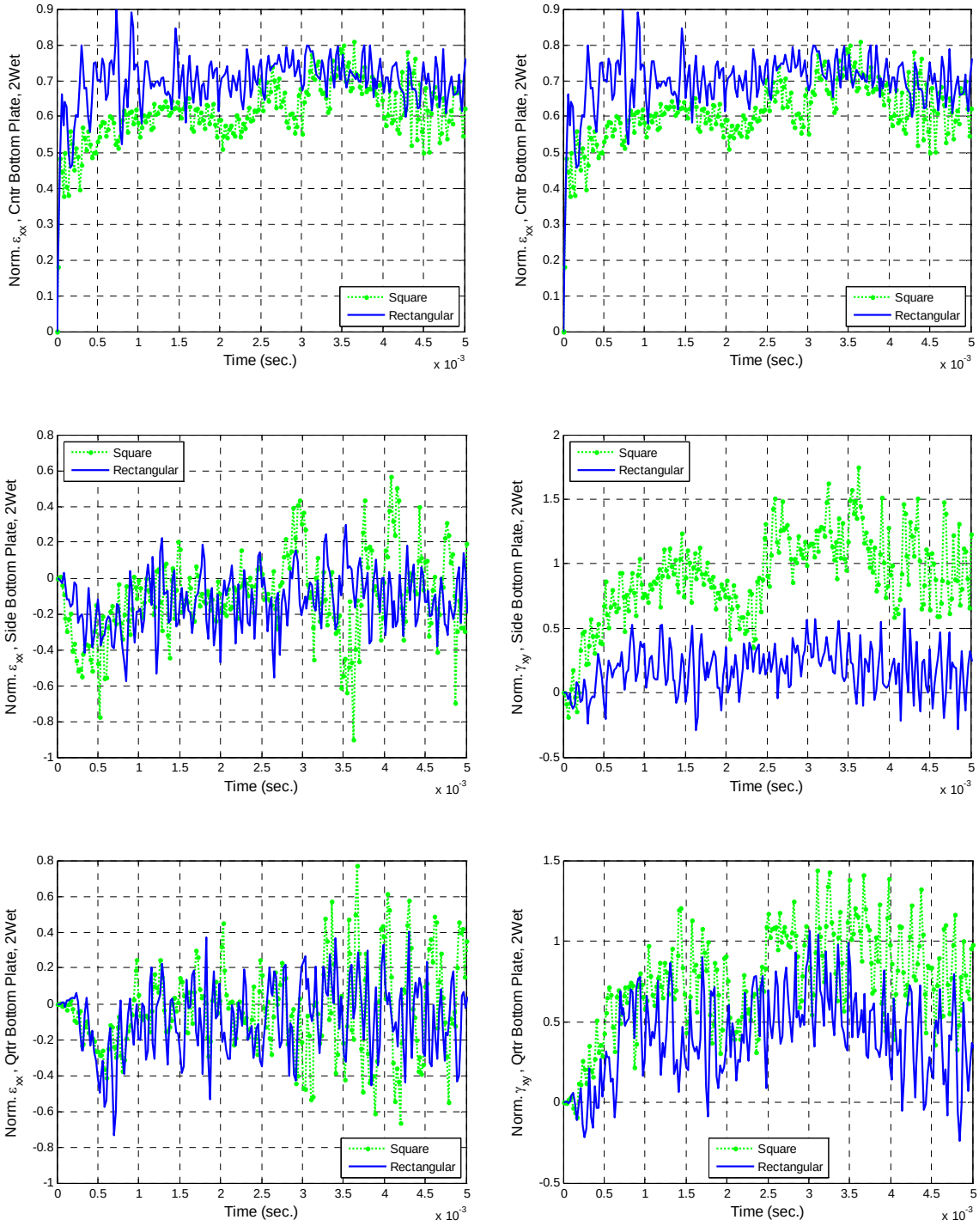

Figure 72. Normal and Shear Strains for Comparison of Differ Plate Shapes for Two-sides Wet Structure with Concentrated Force and Clamped Boundary

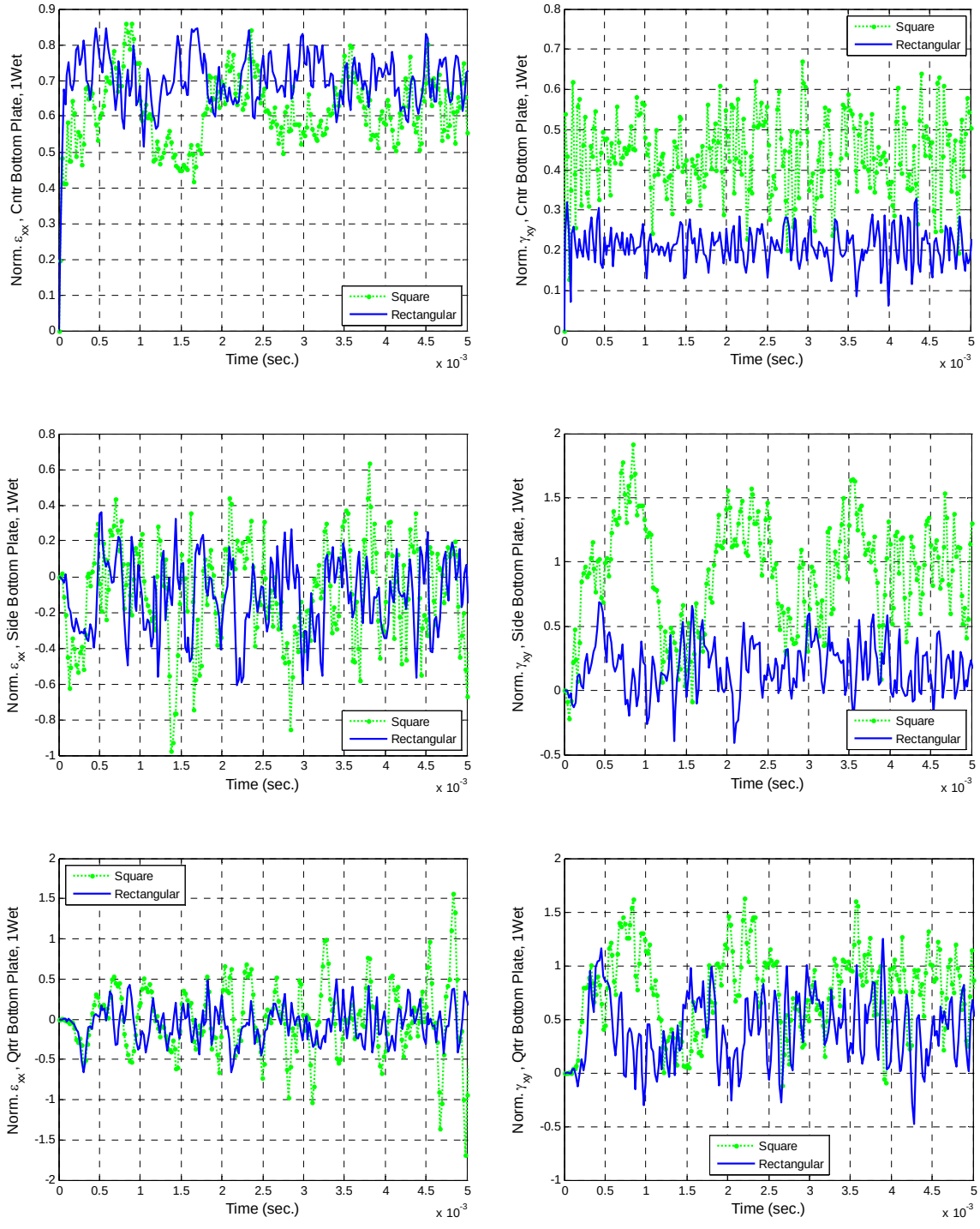

Figure 73. Normal and Shear Strains for Comparison of Differ Plate Shapes for One-side Wet Structure with Concentrated Force and Clamped Boundary

APPENDIX F: ADDITIONAL FIGURES FOR COMPOSITE DENSITY EFFECTS WITH CONCENTRATED FORCE LOAD AND CLAMPED BOUNDARY

The following use composite density of 2020 kg/m ^{3} and modulus 1.7e ^{10} GPa for normalization in each of the three structures.

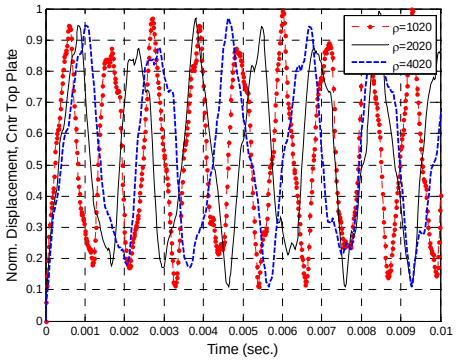

a) Dry Structure

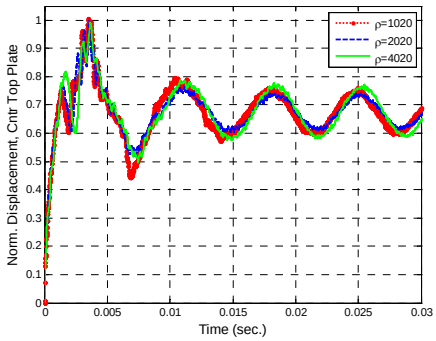

b) Two-sides wet Structure

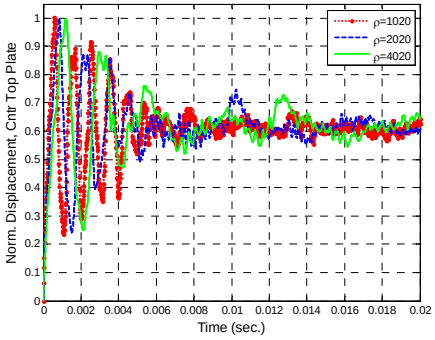

c) One-side Wet Structure

Figure 74. Comparison of Displacement Response for Three Structures Due to Density Effects with Concentrated Force and Clamped Boundary

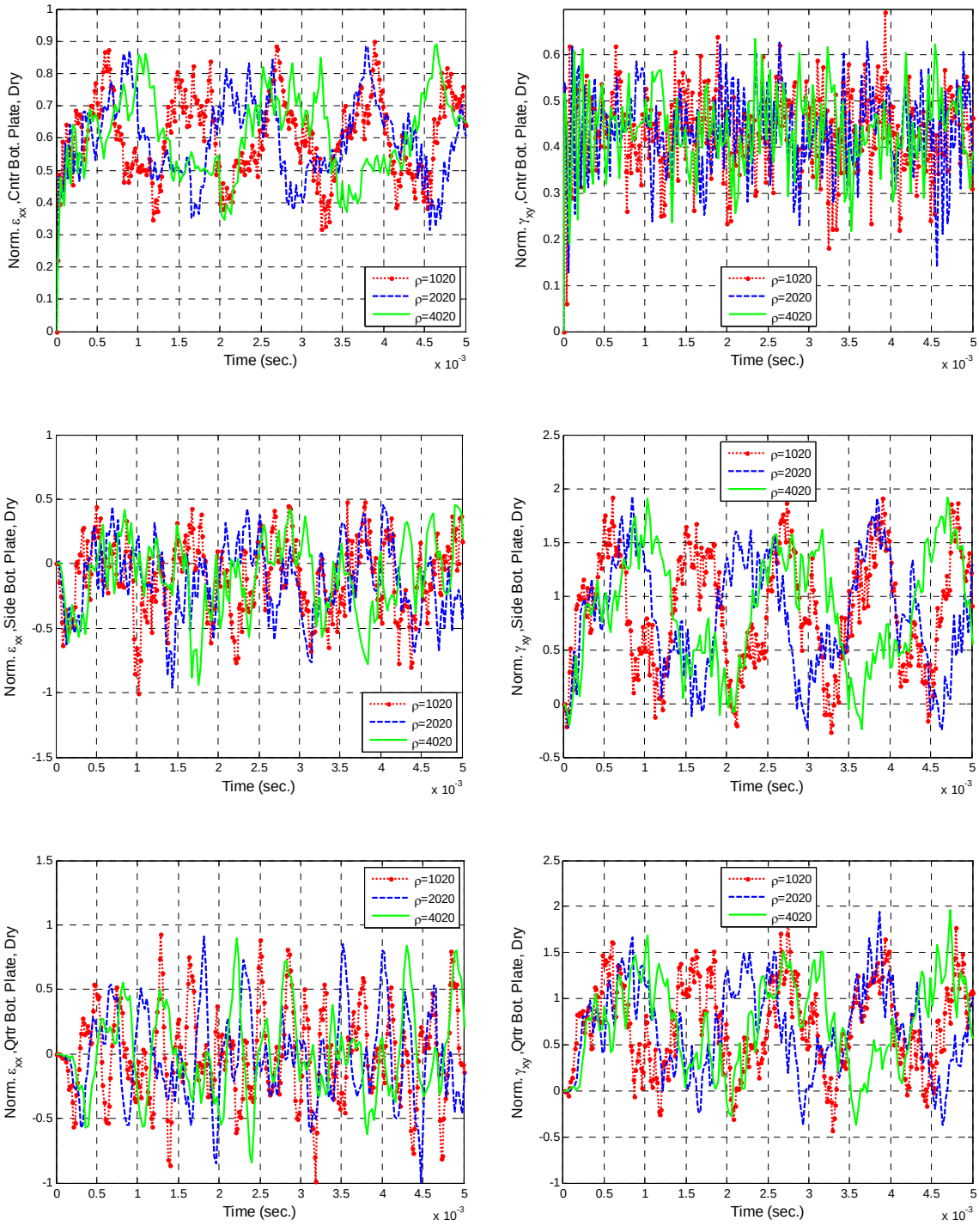

Figure 75. Normal and Shear Strains for Comparison of Differ Density for Dry Structure with Concentrated Force and Clamped Boundary

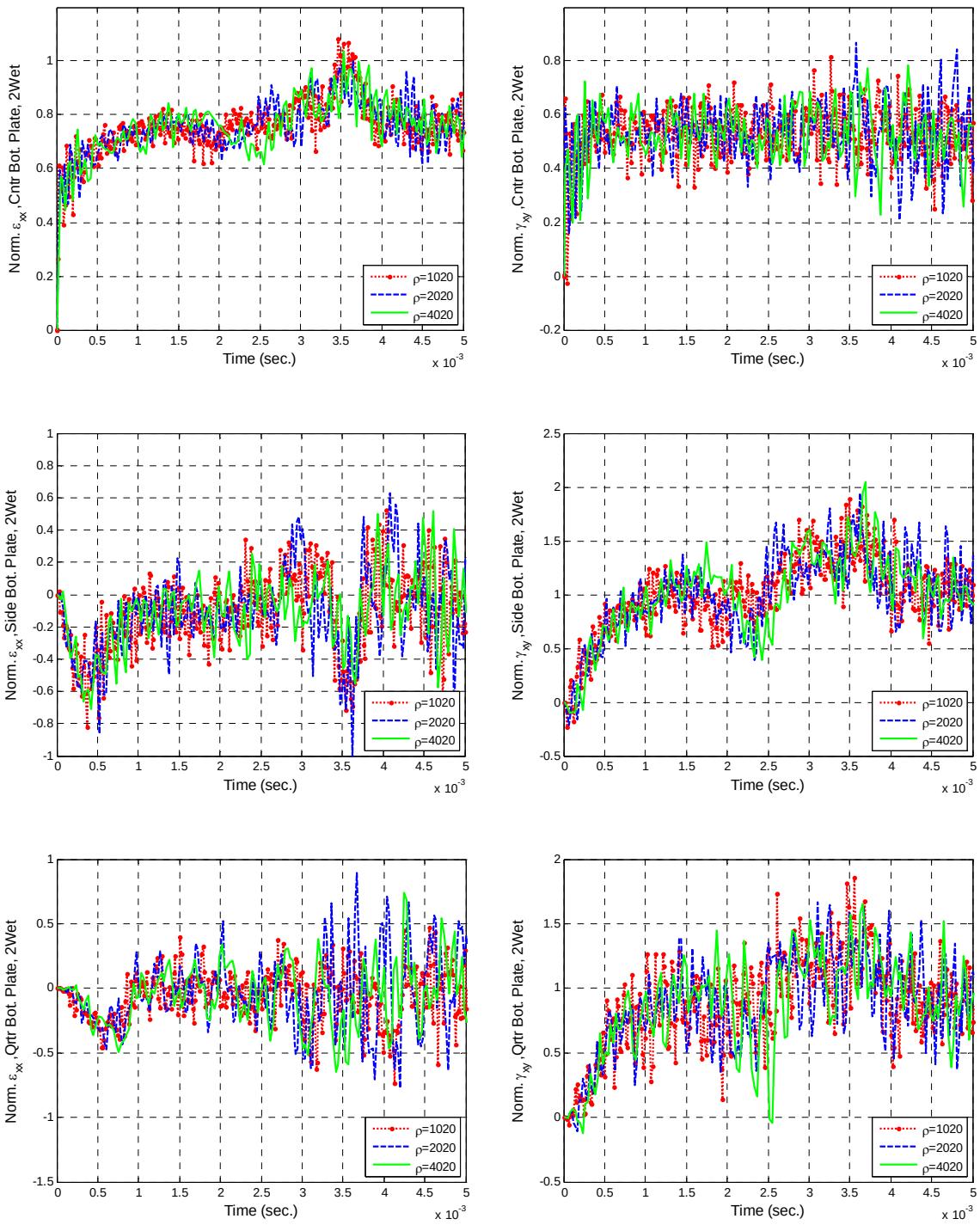

Figure 76. Normal and Shear Strains for Comparison of Differ Density for Two-sides Wet Structure with Concentrated Force and Clamped Boundary

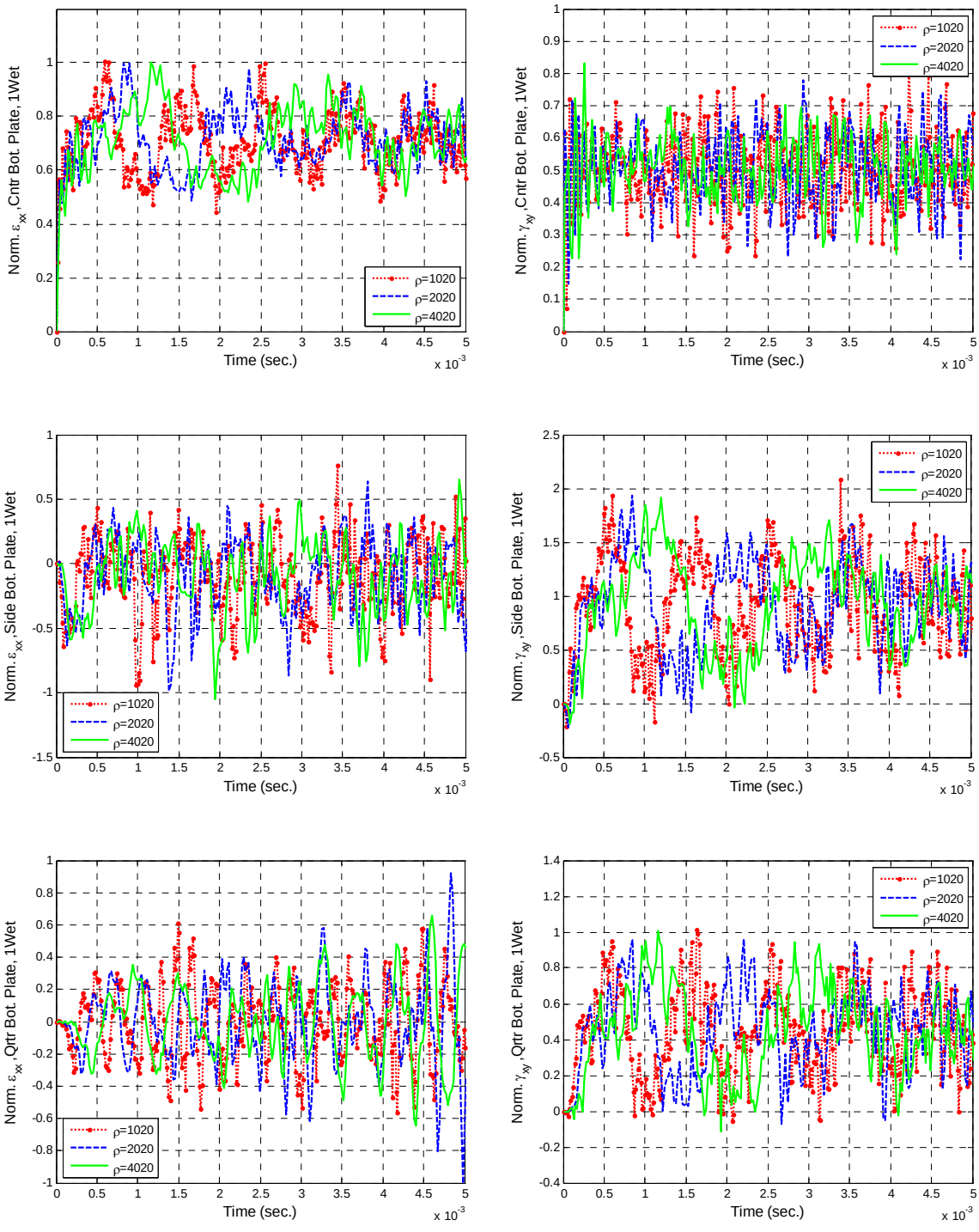

Figure 77. Normal and Shear Strains for Comparison of Differ Density for One-side Wet Structure with Concentrated Force and Clamped Boundary

APPENDIX G: ADDITIONAL FIGURES FOR COMPOSITE ELASTIC MODULUS EFFECTS WITH CONCENTRATED FORCE LOAD AND CLAMPED BOUNDARY

The following use composite density of 2020 kg/m ^{3} and modulus 1.7e ^{10} GPa for normalization in each of the three structures.

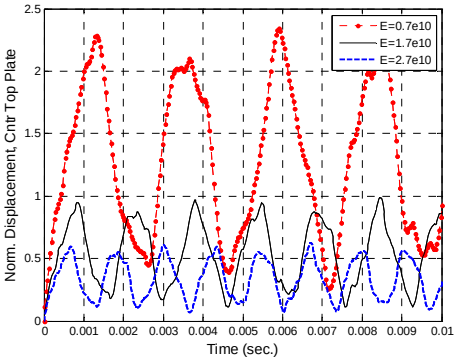

a) Dry Structure

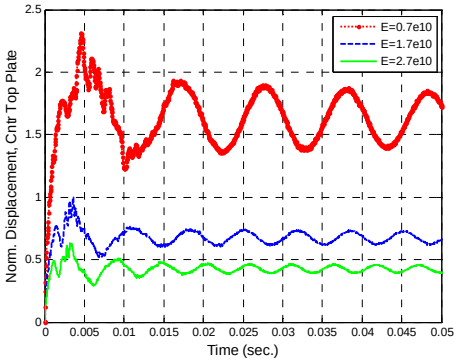

b) Two-sides wet Structure

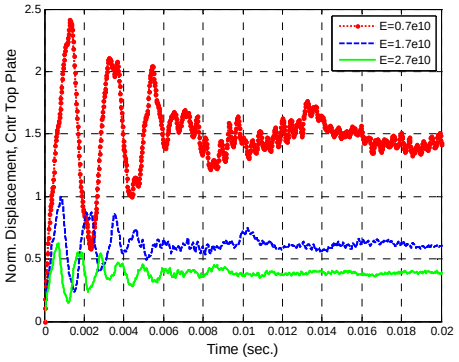

c) One-side Wet Structure

Figure 78. Comparison of Displacement Response for Three Structures Due to Elastic Modulus Effects with Concentrated Force and Clamped Boundary

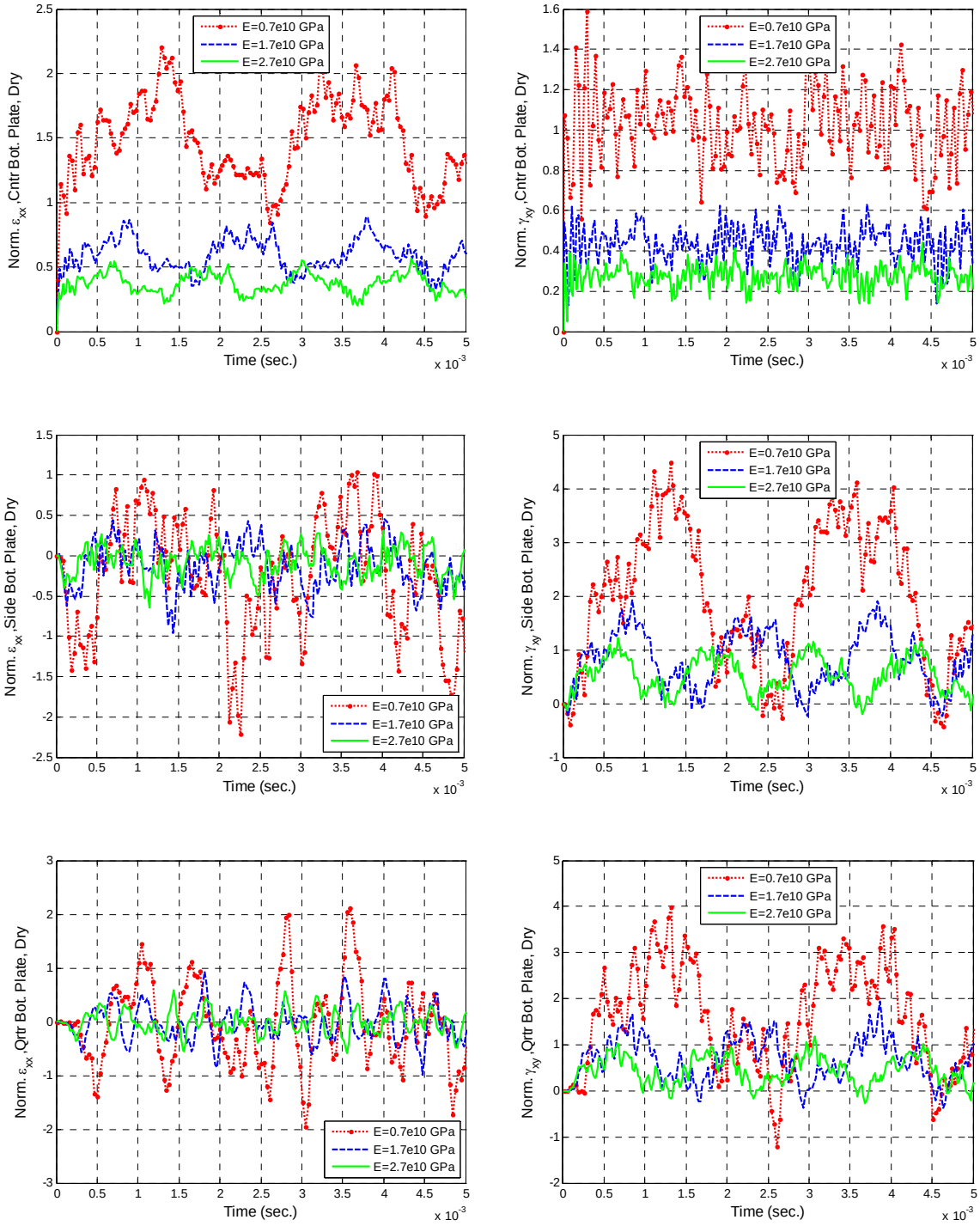

Figure 79. Normal and Shear Strains for Comparison of Differ Elastic Modulus for Dry Structure with Concentrated Force and Clamped Boundary

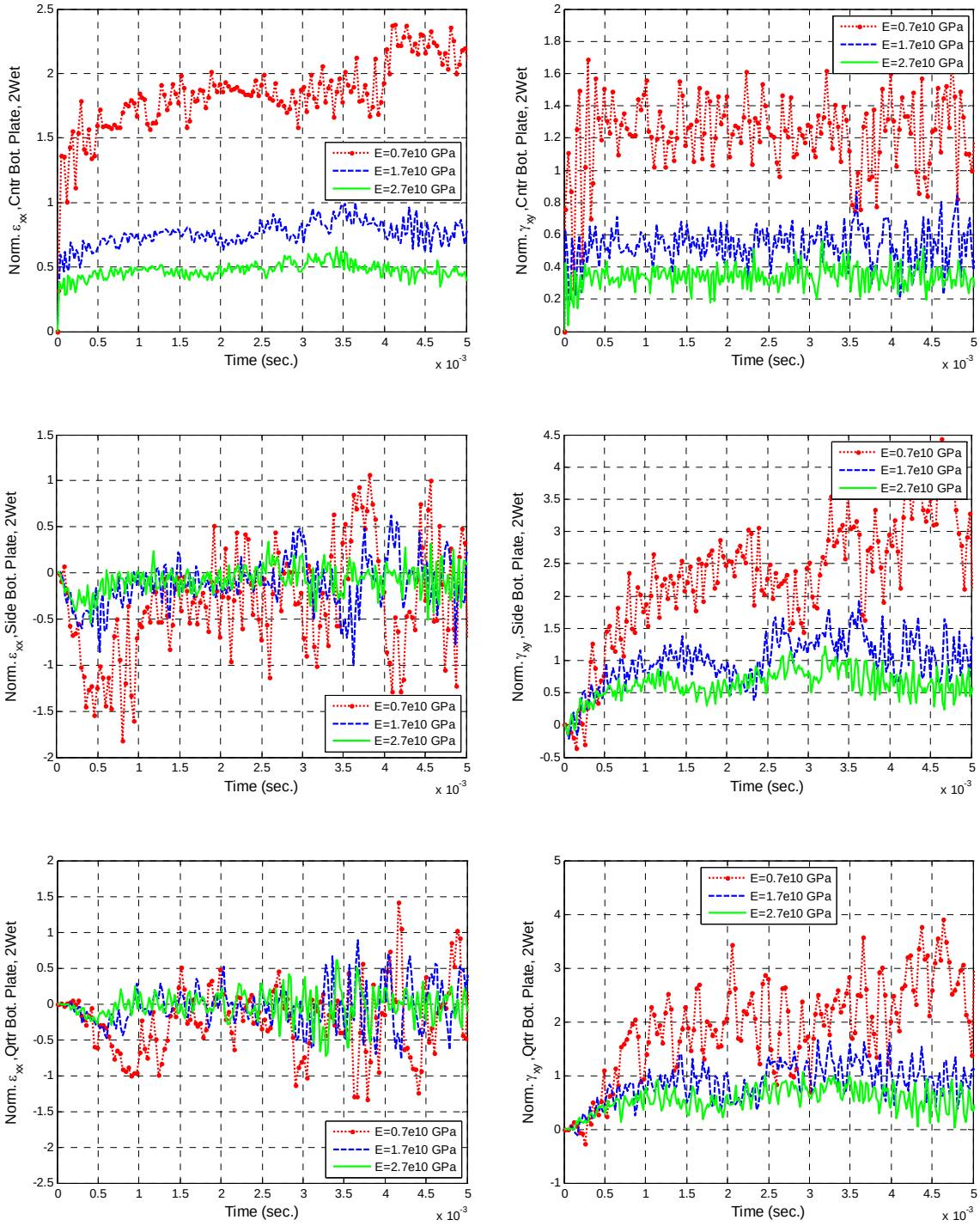

Figure 80. Normal and Shear Strains for Comparison of Differ Elastic Modulus for Two-sides Wet Structure with Concentrated Force and Clamped Boundary

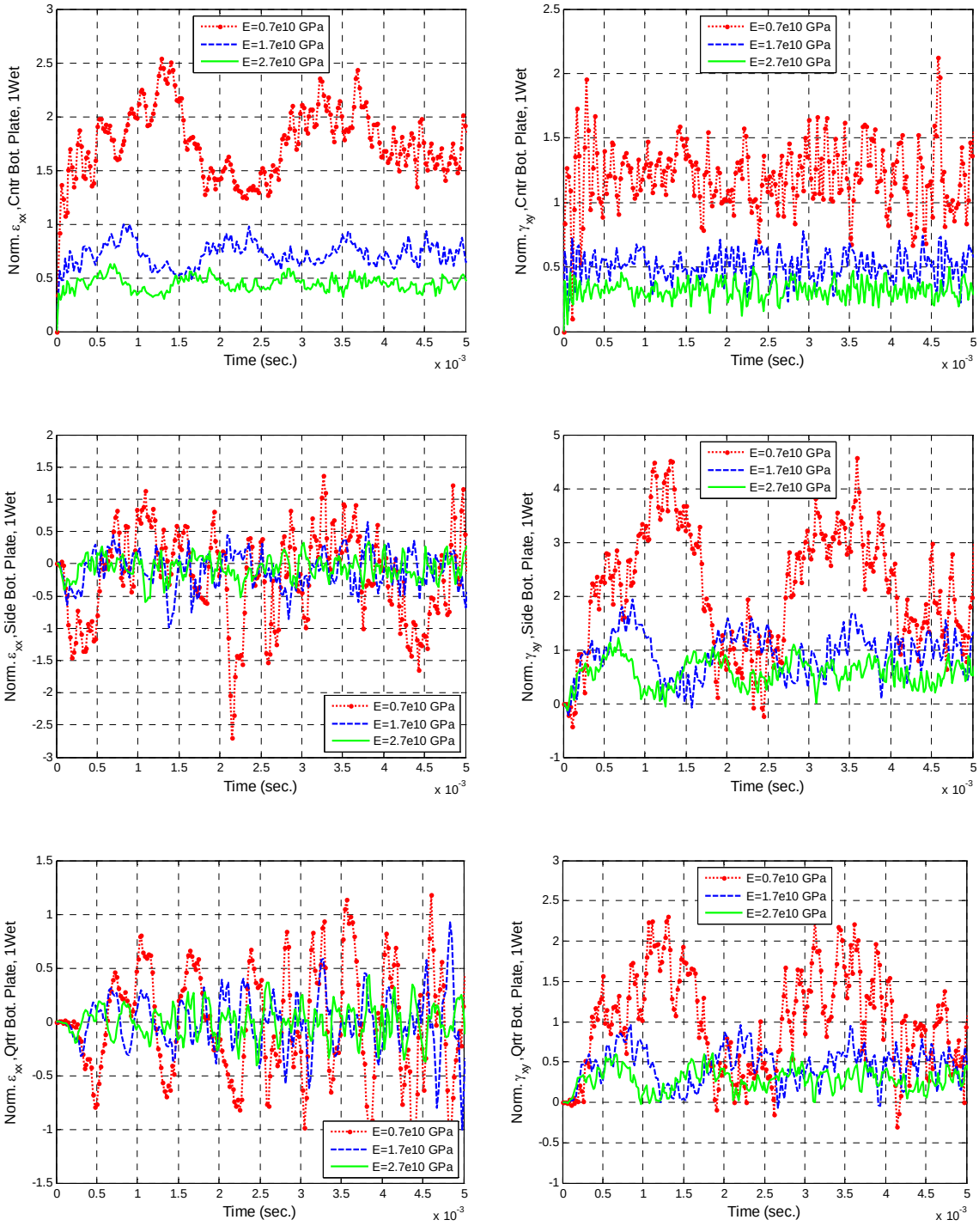

Figure 81. Normal and Shear Strains for Comparison of Differ Elastic Modulus for One-side Wet Structure with Concentrated Force and Clamped Boundary

APPENDIX H: ADDITIONAL FIGURES FOR IMPACTOR SHAPRE EFFECTS WITH CLAMPED BOUNDARY

The following compare circular face to square face impactor, with equal impact area and equal mass, for two-sides and one-side wet structures normalized to respective dry structure.

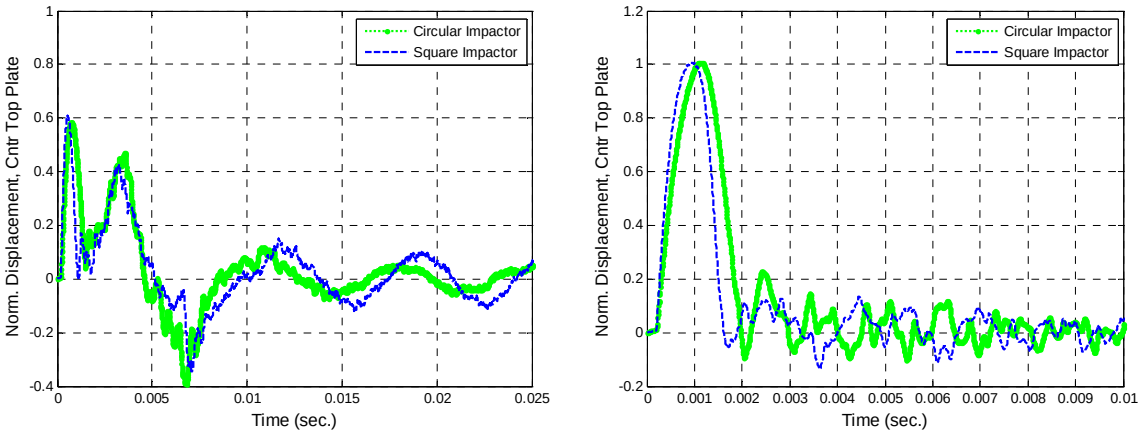

Two-sides Wet One-side Wet

Figure 82. Comparison of Displacement Response for Two-sides and One-side Wet Structures Due to Impactor Shape Effects

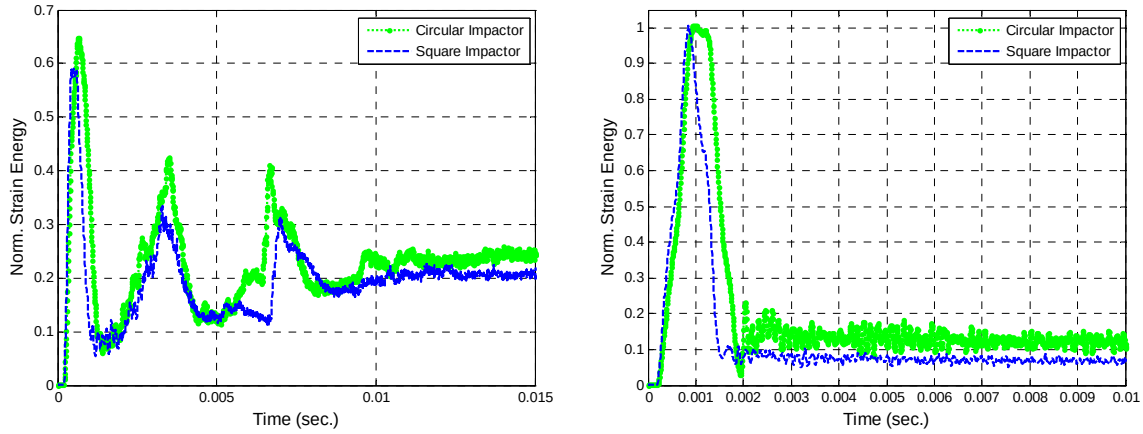

Two-sides Wet One-side Wet

Figure 83. Comparison of Strain Energy Response for Two-sides and One-side Wet Structures Due to Impactor Shape Effects

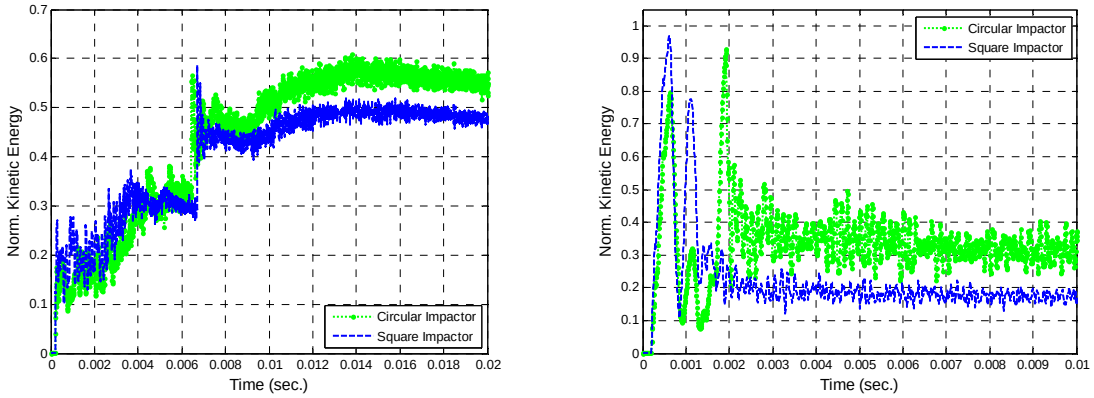

Two-sides Wet One-side Wet

Figure 84. Comparison of Kinetic Energy Response for Two-sides and One-side Wet Structures Due to Impactor Shape Effects

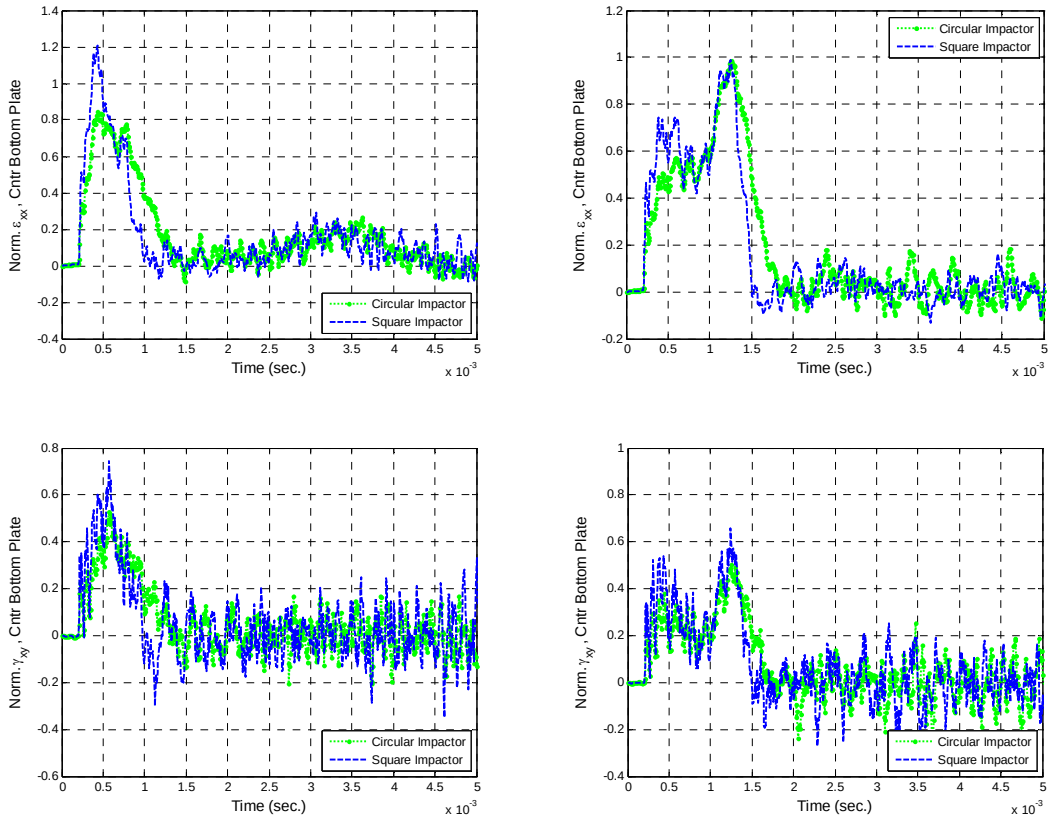

Two-Sides Wet One-side Wet

Figure 85. Normal and Shear Strain Comparison of Different Impactor Shape for

Two-sides and One-side Wet Structure at Center Location

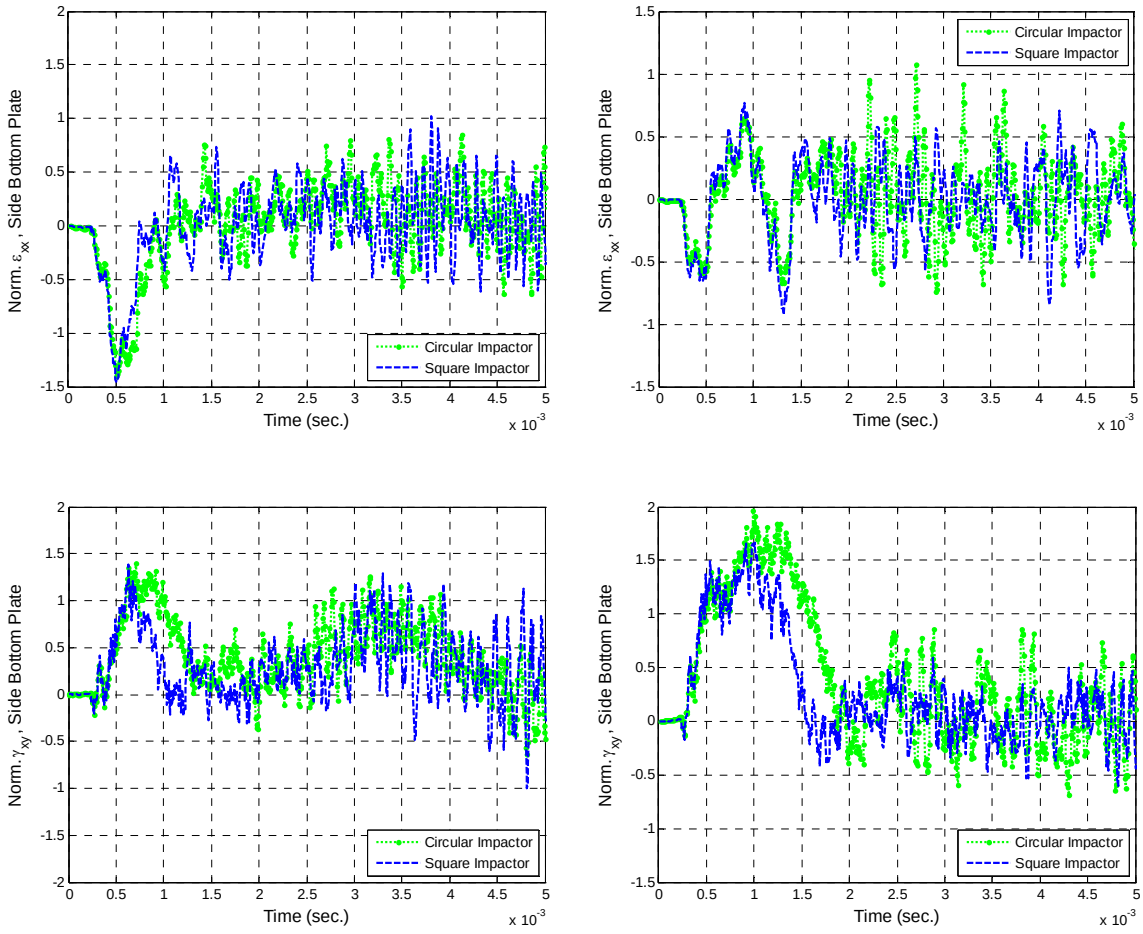

Two-Sides Wet One-side Wet

Figure 86. Normal and Shear Strain Comparison of Different Impactor Shape for Two-sides and One-side Wet Structure at Side Location

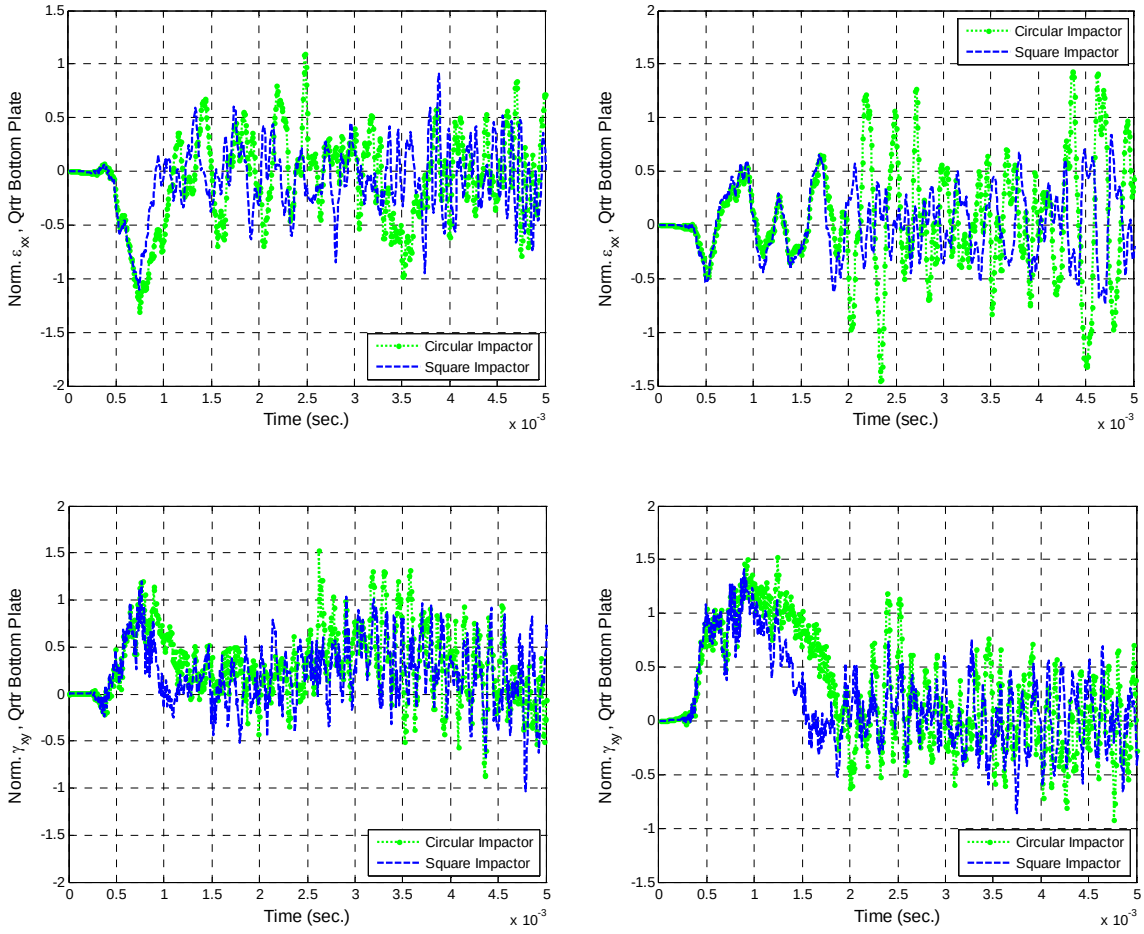

Two-Sides Wet One-side Wet

Figure 87. Normal and Shear Strain Comparison of Different Impactor Shape for Two-sides and One-side Wet Structure at Quarter Location

APPENDIX I: ADDITIONAL FIGURES FOR IMPACT VELOCITY AND SHAPE EFFECTS

The following compare circular face to square face impactor, with equal impact area and equal mass, for different velocities of the three structures, normalized to 1 m/s.

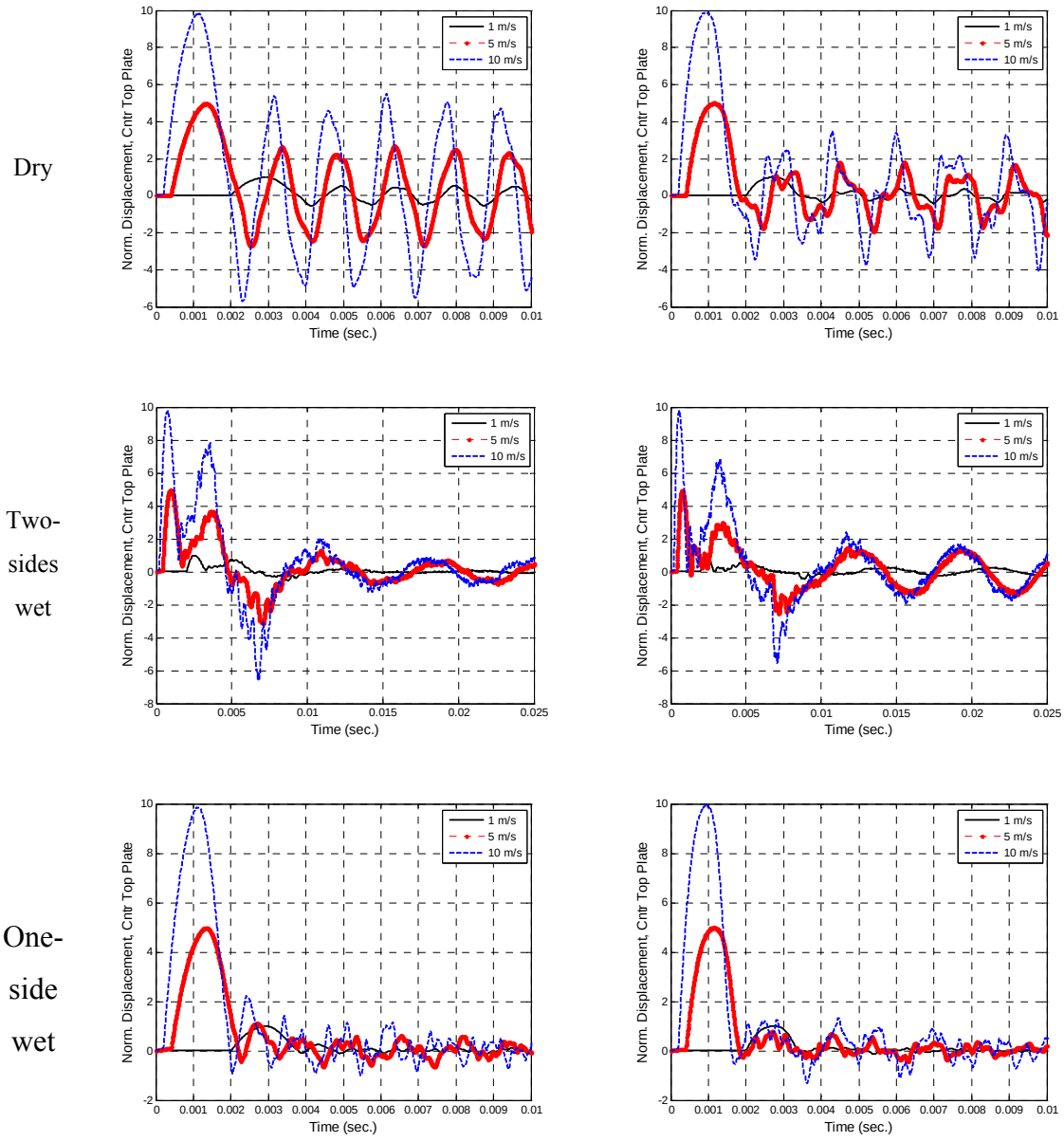

Figure 88. Comparison of Displacement Response for Three Structures Due to Impact Velocity Effects for Circular and Square Faced Impactor

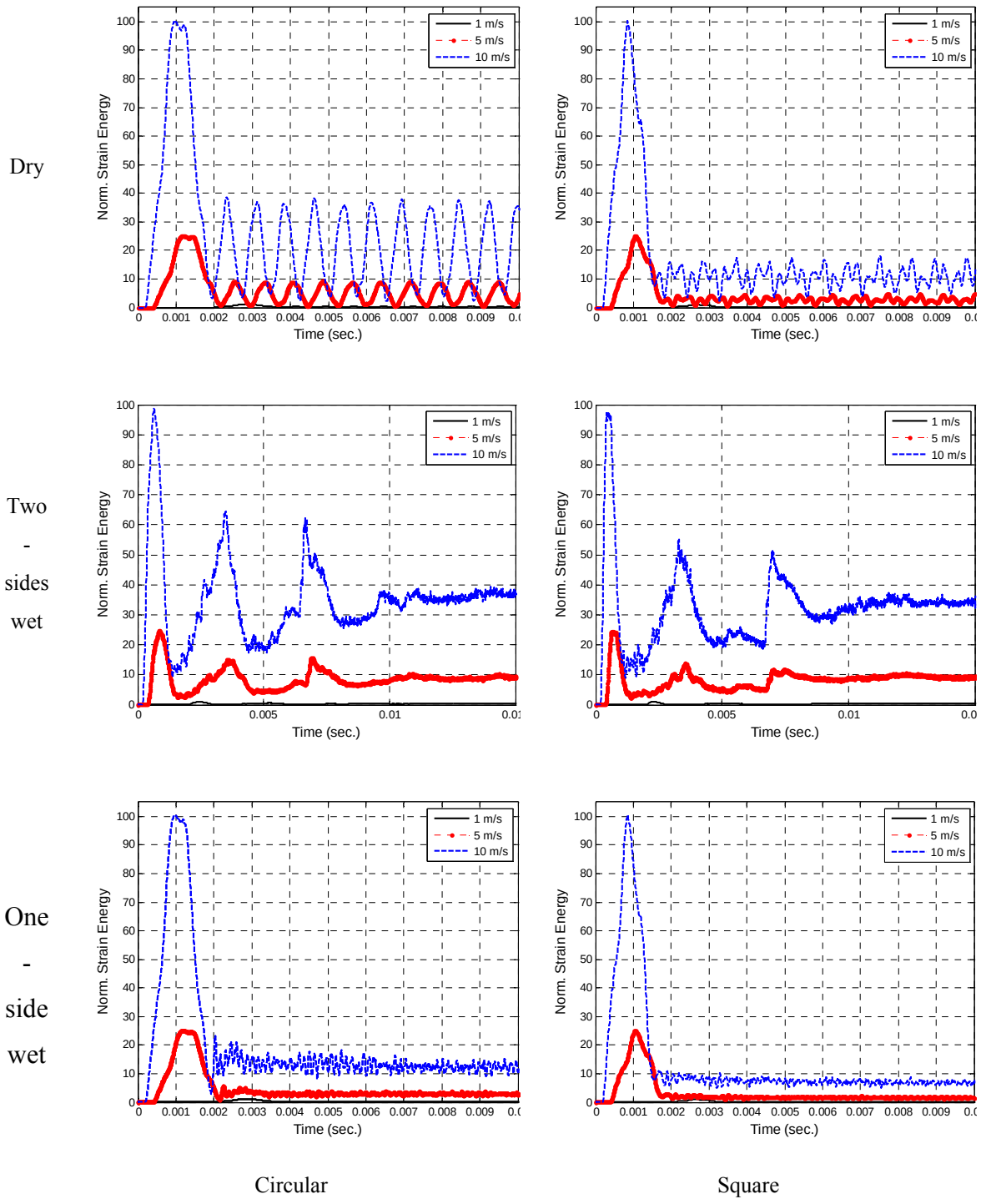

Figure 89. Comparison of Strain Energy Response for Three Structures Due to Impact Velocity Effects for Circular and Square Faced Impactor

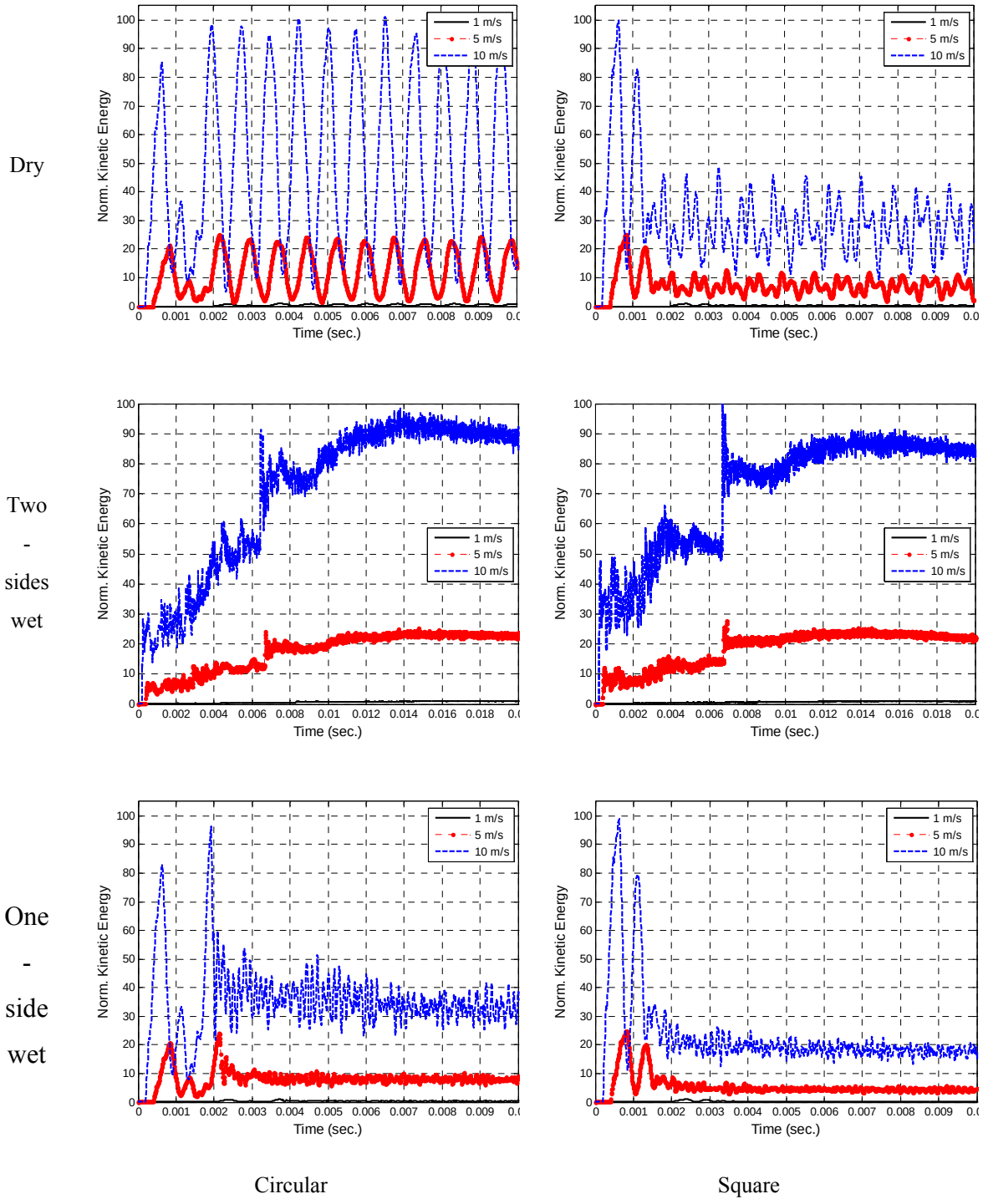

Figure 90. Comparison of Kinetic Energy Response for Three Structures Due to Impact Velocity Effects for Circular and Square Faced Impactor

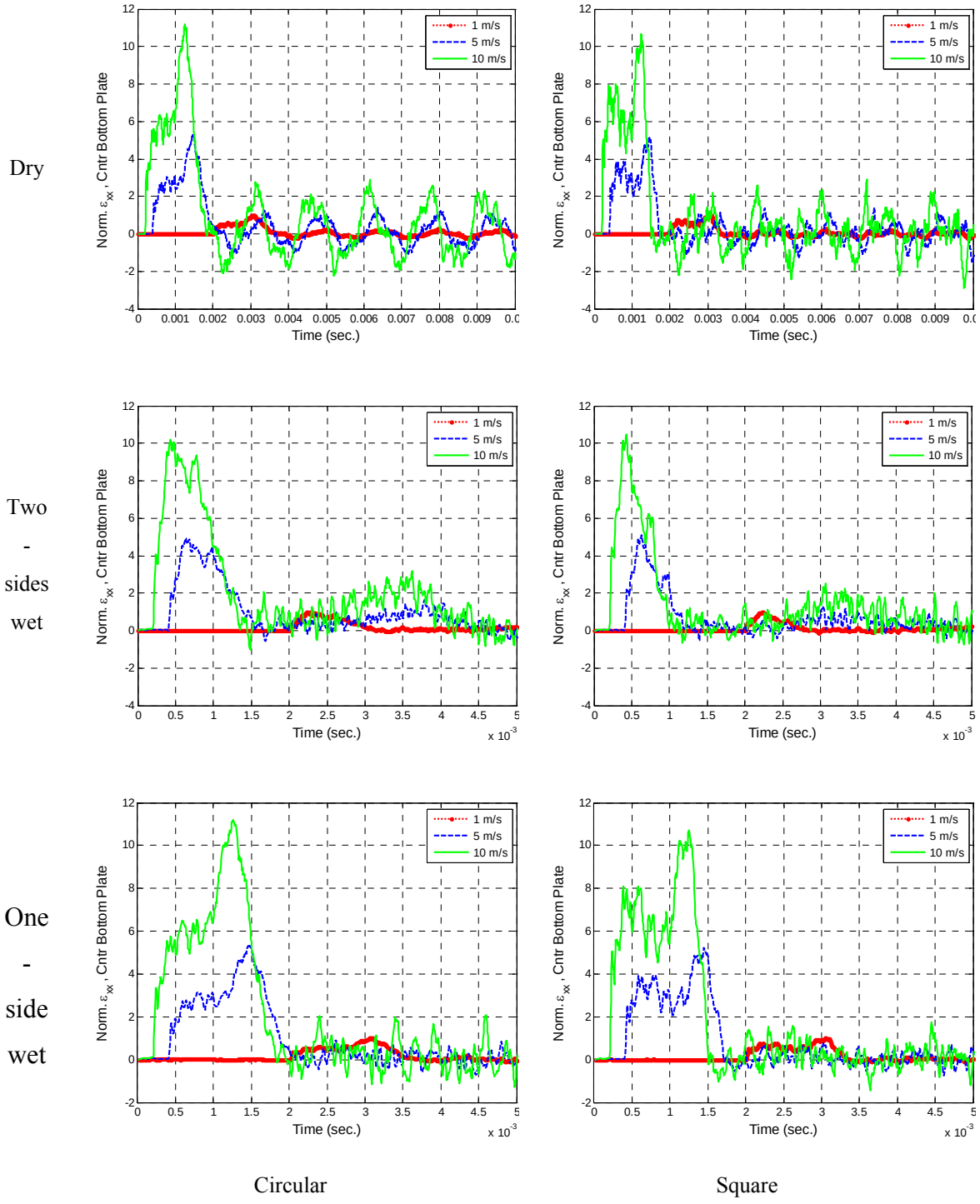

Figure 91. Comparison of Normal Strain at Center Location for Three Structures Due to Impact Velocity Effects for Circular and Square Faced Impactor

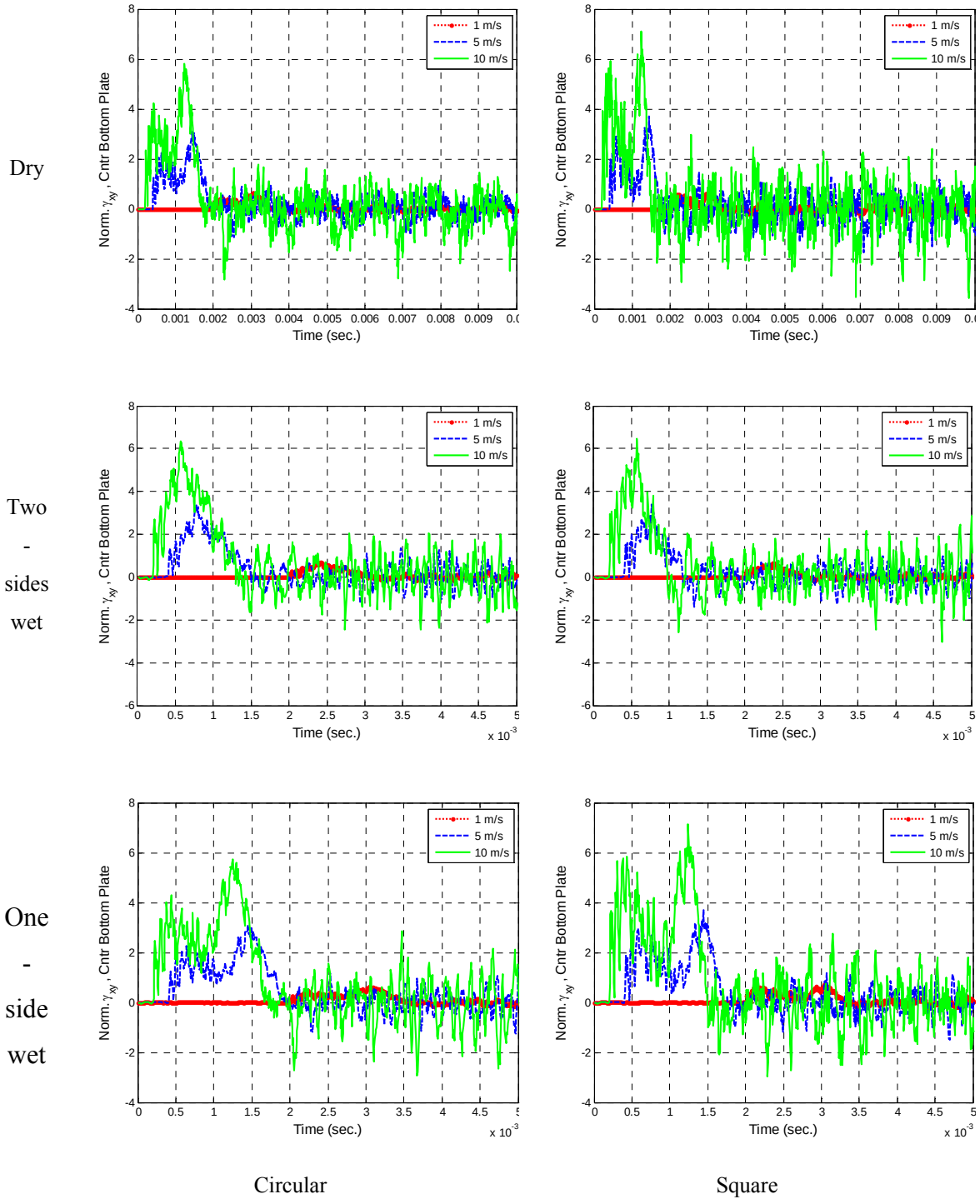

Figure 92. Comparison of Shear Strain at Center Location for Three Structures Due to Impact Velocity Effects for Circular and Square Faced Impactor

THIS PAGE INTENTIONALLY LEFT BLANK

LIST OF REFERENCES

[1] A.P. Mouritz, E. Gellert, P. Burchill, and K. Challis, "Review of advanced composite structures for naval ships and submarines," *Composite Structures*, vol. 53, pp. 21–41, July 2001.

[2] J. Reddy, and A. Miravite, "Practical Analysis of Composite Laminates," CRC Press, Inc., Florida, 1995.

[3] Y.W. Kwon and P.K. Fox, "Underwater shock response of a cylinder subjected to a side on explosion," *Computers and Structures*, 48(4), pp. 637–646, 1993.

[4] Y.K. Kwon, J.K. Bergensen, and Y.S. Shin, "Effect of surface coatings on cylinders exposed to underwater shock," *Journal of Shock and Vibration*, 1(3), pp. 637–646, 1994.

[5] Y.K. Kwon and R.E. Cunningham, "Comparison of USA-DYNA finite element models for a stiffened shell subject to underwater shock," *Computers and Structures*, 66(1), pp. 127–144, 1998.

[6] Y.K. Kwon and P.M. McDermott, "Effects of void growth and nucleation on plastic deformation of plates subjected to fluid-structure interaction," *ASME Journal of Pressure Vessel Technology*, 123, pp. 480–485, November 2001.

[7] P.E. Malone and Y.S. Shin, "Sensitivity analysis of coupled fluid volume to ship shock simulation," *Proceedings of 71st Shock and Vibration Symposium*, Crystal City, VA, 6–9 November 2000.

[8] Y.S. Shin, "Ship shock modeling and simulation for far-field underwater explosion," *Computer & Structure Journal*, Spring 2004.

[9] Y.S. Shin and S.Y. Park, "Ship shock trial simulation of USS John Paul Jones (DDG 53) using LS-DYNA/USA: three dimensional analysis," *70th Shock and Vibration Symposium Proceedings*, Vol. I, November 1999.

[10] Y.S. Shin and N.A. Schneider, "Ship shock trial simulation of USS Winston S. Churchill (DDG81): modeling and simulation strategy and surrounding fluid volume effects," *74th Shock & Vibration Symposium*, San Diego, California, October 27–31, 2003.

[11] E.A. Rasmussen, "Underwater shock testing and analysis of composite cylinders," *Shock and Vibration Symposium*, 1992.

[12] M.P. Rousseau, Y.W. Kwon, and Y.S. Shin, "Modeling the effects of shock on an underwater composite cylinder," *64th Shock & Vibration Symposium*, Ft. Walton Beach, FL, October 1993.

[13] A.P. Mouritz, “The damage to stitched GRP laminated by underwater explosion shock loading”, *Composite Science and Technology*, 55, pp. 365–373, 1995.

[14] A.P. Mouritz, “The effect of underwater explosion shock loading of the flexural properties of GRP laminates,” *Int. J. Impact Engng*, 18(2), pp. 129–139, 1996.

[15] W. McCoy and C.T. Sun, “Fluid-structure interaction analysis of a thick-section composite cylinder subjected to underwater blast loading”, *Composite Structures*, 37(1), pp. 45–55, 1997.

[16] S.W. Gong and K.Y. Lam, “Transient response of stiffened composite submersible hull subjected to underwater explosive shock,” *Composite Structures*, 41(1), pp. 27–37, 1998.

[17] K.Y. Lam, Z. Zong, and Q.X. Wang, “Dynamic response of a laminated pipeline on the seabed subjected to underwater shock,” *Composites Part B: Engineering*, 34, pp. 59–66, 2003.

[18] DYTRAN 2008 r1 User’s Guide, MSC Software Corporation, Santa Ana, CA, 2008.

INITIAL DISTRIBUTION LIST

1. Defense Technical Information Center
   Ft. Belvoir, Virginia

2. Dudley Knox Library
   Naval Postgraduate School
   Monterey, California

3. Graduate School of Engineering and Applied Sciences
   Naval Postgraduate School
   Monterey, California

4. Professor Young W. Kwon
   Naval Postgraduate School
   Monterey, California

5. Engineering and Technology Circular Office, Code 34
   Naval Postgraduate School
   Monterey, California

6. Peter K. Kendall
   Naval Postgraduate School
   Monterey, California